Reactivity of Aluminium chlorofluoride (ACF) towards C−F bond activations and C−F bond formations

Dissertation

zur Erlangung des akademischen Grades

doctor rerum naturalium

(Dr. rer. nat.)

im Fach Chemie

eingereicht an der

Mathematisch-Naturwissenschaftlichen Fakultät

der Humboldt-Universität zu Berlin

von

M.Sc. Maëva-Charlotte KERVAREC

Präsidentin der Humboldt-Universität zu Berlin

Prof. Dr.-Ing. Dr. Sabine Kunst

Dekan der Mathematisch-Naturwissenschaftlichen Fakultät

Prof. Dr. Elmar Kulke

Gutachter:

1. Prof. Dr. Thomas Braun
2. Prof. Dr. Erhard Kemnitz
3. Prof. Dr. Sebastian Riedel

Tag der mündlichen Prüfung: 11 Januar 2021

For my family

Acknowledgment

Firstly, I would like to express my sincere appreciation to my supervisor, Prof. Dr. Thomas Braun, for giving me the chance to complete my Ph.D. thesis in his group. I am very grateful for the continuous support and motivation provided all along this four years journey, which has allowed me to develop my scientific knowledge while also learning how to become independent.

I would also like to thank Prof. Dr. Erhard Kemnitz for always having an open door for discussion on the topics and fruitful advice. Furthermore, I wish to thank all the committee members for their time and support for this final step of my Ph.D. work: Prof. Dr. Sebastian Hasenstab-Riedel for being my external referee, but also for the inspiring collaboration between our two groups; Prof. Dr. Rüdiger Tiemann for finding the time to chair the defense; and a special thanks to Priv.-Doz. Dr. Gudrun Scholz, for the immense guidance in the field of solid state NMR and constant encouragements.

Many thanks to everyone who helped me carry out all the technical analysis for my projects: Mrs. Sigrid Bäßler for the TPD experiment, Dr. Patricia Russo and Dr. Michael Feist for the thermoanalysis measurement, Dr. Thoralf Krahl, and Dr. Mike Ahrens for their help with handling HF and the discussion on the topic, Prof. Dr. Christian Jäger for the valuable time spend performing unique MAS NMR experiments, Kai for the DRIFTS measurement, Ranjit for the surface analysis, Kurt for the in situ gas phase FTIR experiment conducted at the Frei University, Dr. Adam Michalchuk and Dr. Svemir Rudic for the Inelastic Neutron Scattering experiments performed at ISIS in Oxford, and Dr. Andréa Martin for the XRD experiment. A special thanks to the technical analytics of the institute, in particular, the whole NMR service of the institute, the Pinna, Limberg, and Ray lab for the lovely time together.

I thank my fellow colleagues from the Braun group, especially my labmates, for the fun time together; the current Braun Boys, Martin, Nils, Stefan, Simon, Ruben, Konrad; and the Braun Girls, including Silke, Maria, Hui, Dilcan, Domi, Sarah, Yue, Pooja, Liza, Linye; and of course the alumni. I will always remember our time together, sharing beers, barbecues, Christmas parties, and gossip.

I am immensely grateful to the ACF girls, Clara, Bea, Gisa, and Aga, for introducing me to the topic and helping me all along the way. An exceptional thanks to Bea, Cort, Dilcan, Clara, and Pooja, for the strong friendship that we developed and for the support all those years, which I am convinced will continue in the next years.

I could not have finished this Ph.D. without the support from my family, especially my mother, my sister, and my aunts, who visited me regularly and always believed in me. To all my friends who came to see me, in particular, Juliette, Julie, Rémi, and Benjamin, thank you all for the great time spent in Berlin but also in France during my holidays.

Last but not least, I want to thanks my partner, Dr. Andréa Martin, for the incredible last five years together. Nothing would have been possible without you on my side.

« Tout ce qui est impossible reste à accomplir »

Jules Verne

Abstract

The main focus of this thesis lies in the study of the potential of aluminum chlorofluoride (ACF) as a catalyst for the synthesis of fluorinated compounds. In particular, C–F bond activations of various polyfluorinated compounds were studied, showing the efficiency of this solid Lewis acid catalyst for this type of reaction. The potent greenhouse gas 2-chloro-1,1,1,2-tetrafluoropropane was successfully transformed into the dehydrofluorination product 2-chloro-3,3,3-trifluoropropene under mild conditions, without the need of a hydrogen source. Additionally, subsequent hydroarylation or hydrodefluorination reactions were observed by varying the solvent or introducing a hydrogen source. Similarly, transformation of pentafluoropropane isomers, such as 1,1,1,3,3-pentafluoropropane, 1,1,1,2,2- pentafluoropropane and 1,1,1,2,3-pentafluoropropane was also investigated using ACF as a catalyst. It was evidenced that the primary CH_2F group present in 1,1,1,2,3-pentafluoropropane was easily activated without the need for a hydrogen source. In contrast, to activate CF_2 groups, a hydrogen source such as $HSiEt_3$ was required, generating a variety of products, which could be controlled by varying the amount of silane present in the reaction mixture. Consecutive reactions such as Friedel-Crafts or hydroarylation reactions were again observed by using an aromatic solvent such as C_6D_6.

Alternatively, successful hydrofluorination reactions of several substrates were conducted by synthesizing a new material, based on the loading of hydrogen fluoride (HF) at the surface of ACF. This HF-loaded ACF was deeply studied using a wide range of characterization methods. For the bulk, MAS NMR spectroscopy, Fourier Transform Infrared spectroscopy (FTIR), Inelastic Neutron Scattering (INS), Powder X-Ray Diffraction (P-XRD), and thermoanalysis were performed, revealing a slight reorganization of the bulk towards a better-ordered matrix and the formation of polyfluoride structure interacting with the surface of ACF. The BET model was used for the surface area determination, and the pore size analysis was established using the non local density functional theory (NLDFT). Moreover, TEM images and EDX data were recorded to gain a better understanding of the morphology of the material. Finally, various probe molecules were adsorbed at the surface of HF-loaded ACF to determine the acidity of the surface, revealing a significantly reduced Lewis and Brønsted acidity.

Kurzzsusammenfassung

Der Fokus dieser Dissertation lag in der Untersuchung des Potentials von Aluminiumchlorofluorid (ACF) als Katalysator für die Synthese von fluorierten Verbindungen. Insbesondere die C–F-Aktivierung von verschiedenen polyfluorierten Stoffen wurde untersucht, welches die Effizienz des festen Lewis-Säure-Katalysators für diesen Reaktionstyp zeigte. Das potente Treibhausgas 2-Chlor-1,1,1,2-tetrafluorpropan wurde erfolgreich in das dehydrofluorierte Produkt 2-Chlor-3,3,3-trifluorpropen, ohne den Einsatz einer Wasserstoffquelle unter milden Reaktionsbedingungen, überführt. Außerdem wurden konsekutive Hydroarylierungs- oder Hydrodefluorierungsreaktionen beobachtet, indem das Lösungsmittel variiert wurde oder eine Wasserstoffquelle verwendet wurde. Weiterhin wurden Umsetzungen von Pentafluorpropan-Isomeren wie z.B. 1,1,1,3,3-Pentafluorpropan, 1,1,1,2,2-Pentafluorpropan und 1,1,1,2,3-Pentafluorpropan mit ACF als Katalysator untersucht. Es konnte gezeigt werden, dass die Aktivierung der primären CH_2F-Gruppe in 1,1,1,2,3-Pentafluorpropan schnell stattfindet und dabei keine Wasserstoffquelle erfordert. Im Kontrast dazu, wurde für die Aktivierung von CF_2-Gruppen eine Wasserstoffquelle wie etwa $HSiEt_3$ benötigt und resultierte in der Bildung eines Produktgemischs, welches durch die eingesetzte Menge des Silans im Reaktionsgemisch kontrolliert werden konnte. Folgereaktionen, wie z.B. Friedel-Crafts-ähnliche Reaktionen oder Hydroarylierung wurden beobachtet, wenn ein aromatisches Lösungsmittel wie C_6D_6 eingesetzt wurde.

Alternativ wurden Hydrofluorierungsreaktionen von mehreren Substraten durch die Synthese und den Einsatz eines neuen Materials erreicht, welches auf der Immobilisierung von HF auf der Oberfläche von ACF beruht. Dieses HF-beladene ACF wurde unter der Verwendung von vielfältigen Charakterisierungsmethoden umfassend untersucht. Die innere Struktur des Festkörpers, der *bulk*, wurden mit MAS-NMR-Spektroskopie, FTIR, Inelastische Neutronenstreuung, *Powder* XRD und Thermoanalyse analysiert Dadurch konnte gezeigt werden, dass eine geringfügige Reorganisation des *bulks* zu einer besser geordneten Matrix und die Bildung einer mit der ACF-Oberfläche wechselwirkenden Polyfluorid-Struktur vorliegt. Zur Bestimmung der Oberflächengröße wurde das BET-Modell genutzt und zur Analyse der Porengröße wurde die *non local density functional theory* (NLDFT) verwendet. Weiterhin wurden TEM-Bilder aufgenommen und EDX-

Daten gesammelt um ein besseres Verständnis über die Morphologie des Materials zu erhalten. Abschließend wurden verschiedene Probeverbindungen an der Oberfläche des HF-beladenen ACFs adsorbiert um die Azidität der Oberfläche zu bestimmen und es konnte gezeigt werden, dass eine signifikante Reduktion der Lewis- und Brønsted-Azidität vorliegt.

Publications List

[1] M.-C. Kervarec, C. P. Marshall, T. Braun, E. Kemnitz, *J. Fluor. Chem.* 2019, 221, 61–65.

DOI: 10.1016/j.jfluchem.2019.04.001

Selective dehydrofluorination of 2-chloro-1,1,1,2-tetrafluoropropane (HCFC-244bb) to 2-chloro-3,3,3-trifluoropropene (HFO-1233xf) using nanoscopic aluminium fluoride catalysts at mild conditions

[2] M.-C Kervarec, E. Kemnitz, G. Scholz, S. Rudić, T. Braun, C. Jäger, A. A. L. Michalchuk, F. Emmerling, Chem., *A Eur. J.* 2020, 26, 7314–7322.

DOI: 10.1002/chem.202001627

A HF Loaded Lewis-Acidic Aluminium Chlorofluoride for Hydrofluorination Reactions

[3] M.-C. Kervarec, M Ahrens, T. Braun, E. Kemnitz, *manuscript submitted.*

Activation of pentafluoropropane isomers at a nanoscopic aluminum chlorofluoride: hydrodefluorination versus dehydrofluorination

Conference Presentations

09/2016 - 17. Deutscher Fluortag (Schmitten/Taunus, GE)

09/2018 - Summer School 2018 "Catalysis and Energy: from Synthesis to Application" (Gelsenkirchen, GE)

Poster presentation.

09/2018 - 18. Deutscher Fluortag (Schmitten/Taunus, GE)

03/2019 - 52. Jahrestreffen Deutscher Kataliker (Weimar, GE)

Poster presentation.

05/2019 - 2. Kollegseminar des SFB 1349 (Berlin, GE)

Oral presentation.

08/2019 - 19th European Symposium on Fluorine Chemistry (Warsaw, PL)

Poster presentation.

09/2019 - 8. Berliner Chemie Symposium (Berlin, GE)

Poster presentation.

09/2019 - Summer School SFB 1349 (Waren, GE)

Oral presentation.

Table of contents

Chapter 1 Introduction

1- The important role of catalysts

A- Generalities

Jöns Jakob Berzelius was the first to introduce the word "catalysis" in 1835.[1,2] Even though catalytic reactions have been known for centuries, for instance, in the production of alcohol from sugar, Jöns Jakob Berzelius classified them as "the property of exerting on other bodies an action which is very different from chemical affinity. By means of this action, they produce decomposition in bodies and form new compounds into the composition which they do not enter".[2] The International Union of Pure and Applied Chemistry (IUPAC) nowadays describes catalysts as "a substance that increases the rate of a reaction without modifying the overall standard Gibbs energy change in the reaction."[3] Figure **1** represents the typical potential energy diagrams of a catalyzed and uncatalyzed reaction. The activation energy (Ea) required for a reaction to take place is reduced, employing a catalyst, compared to when no catalyst is used, therefore increasing the reaction rate.

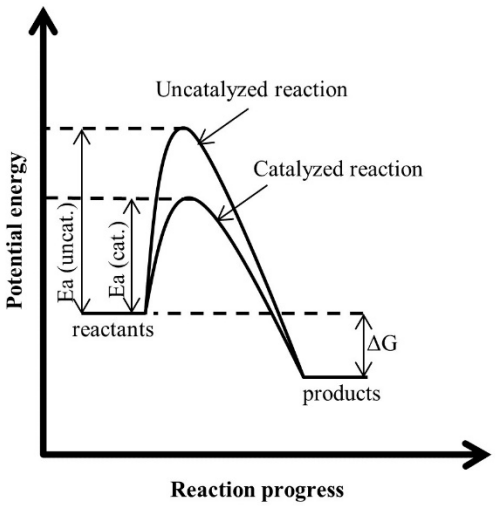

Figure 1. *Potential energy diagrams comparison of a catalyzed and uncatalyzed exothermic reaction. Ea is the activation energy, and ΔG is the Gibbs free energy released.*

Without considering biological systems, two kinds of catalysts can be distinguished: homogeneous and heterogeneous. In homogeneous catalysis, both the catalyst and the

reactants are in the same phase, allowing for a smooth interaction between the substrate and the active sites. In contrast, heterogeneous catalysts are in a different phase as the reactants or the products, which in general enables an easy separation by filtration or decantation of the desired product and the catalyst. The ease of the catalyst recovery stands as an essential factor for the industry, as it enables a simple and straightforward regeneration or recycling of the catalyst. Therefore, heterogeneous catalysts with high activity and selectivity are used in majority by industries for commercial purposes. The drawbacks related to heterogeneous catalysts are the non-uniformity of the distribution and strength of the active sites, as can be seen in Table **1**. However, their high stability represents another appealing advantage, and a considerable amount of studies on the design of new heterogeneous catalysts can be found in the literature.[4–11] Various reaction mechanisms exist, such as the Langmuir-Hinshelwood mechanism, the Eley-Ridea mechanism, or the Mars-Van Krevelen mechanism based on different reactions rate.

Table 1. *Comparison between a heterogeneous and a homogeneous catalyst:*

Aspect	Homogeneous	Heterogeneous
Activity	High	High
Selectivity	High	Low
Recovery	Difficult	Easy
Reaction conditions	Low temperature (>250 °C), low thermal stability	High Temperatures, high thermal stability
Catalyst life	Long	Short
Active site and accessibility	Molecular active site, easily accessible	Not well defined active site, limited accessibility

Many catalytic processes were discovered around the eighteenth century and finally could find industrial applications by the end of the nineteenth century when bulk chemicals were highly demanded during the industrial revolution.[1,12] After the First World War, the well-known Fischer-Tropsch and the Fluid Catalytic Cracking processes were developed, which emphasized the significant importance of catalysts in industrial application.[13–16] Nowadays, around 90% of the industrial processes require the use of a catalyst, such as

polymerizations, production of ammonia and sulfuric acid, or steam reforming of methane to only cite a few examples (Table **2**).[10,17–19]

Table 2. *Examples of some industrial chemical processes using catalysts:*[19]

Chemical processes	Year of discovery	Catalysts used by Industries
Sulfuric acid	1875	Pt, V_2O_5
Nitric acid	1906	Pt/Rh nets
Ammonia synthesis	1908	$Fe/Al_2O_3/K_2O$
Methanol synthesis	1923	Cu/ZnO, ZnO/Cr_2O_3
Cracking of hydrocarbons	1937	Al_2O_3/SiO_2
Alkylation of alkenes	1932	$AlCl_3$
Naphtha reforming	1949	Pt/Al_2O_3

Acid or base catalysts are the most spread catalysts employed by industries, with a wide range of applications in several sectors.[20] In particular, solid acid-base catalysis has considerable advantages due to their low environmental impact and recycling capability compared to liquid acid-base catalysts.[21,22] Furthermore, mostly solid acids catalysts are used by industries when compared to base catalysts, as shown in Table **3**.[17,23]

Table 3. *Survey of catalysts used in industrial processes in 1999 depending on their nature:*[17]

Type of catalysts	Number
Solid acid	103
Solid base	10
Solid acid-base bifunctional catalysts	14

Among the catalysts, solid Lewis acids are of significant relevance.[24,25] Indeed, they are cheap, readily available, very active, and can often be converted to their corresponding

Brönsted acid by hydration or by reaction with protonic species. A short introduction to Lewis acid catalysts is therefore needed and will be the subject of the next section.

B- Lewis acid catalysts

Lewis acids are defined as electron-pair acceptors, according to Gilbert Newton Lewis, and can be applied to a wide variety of elements (Figure **2**).[26,27] Classic C–C bond formation such as Friedel-Crafts reactions or Diels-Alder reactions are, for instance, catalyzed by Lewis acids, such as $AlCl_3$, $TiCl_4$, or $SnCl_4$.[25,28–33]

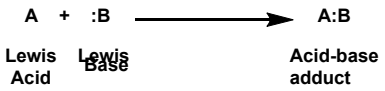

Figure 2. *Lewis acid and base equation.*

SbF_5 is one of the strongest known Lewis acids, and was described by Olah as "by far the strongest Lewis acid known in the condensed phase".[34,35] Indeed, SbF_5 can perform oxidation, fluorination, and Friedel-Crafts type reactions. Moreover, when put together with HF or FSO_3H, a stable super-acid conjugate system is generated.[36–39] Due to its high toxicity and corrosive character, research groups have been attempting to find alternative compounds with improved handling and potentially an even higher Lewis acidity than SbF_5.[40] As a result, Lewis super-acids, such as $B(OTeF_5)_3$ or $Al(OTeF_5)_3$, were found to be interesting compounds. To classify those compounds, a reliable measure of the Lewis acidity was proposed based on the strength of Lewis acids and the binding enthalpy of a fluoride ion F^- with a Lewis acid: the fluoride ion affinity (FIA) (Scheme **1**).[34,36] The FIA was first introduced by Haartz and McDaniel using ion cyclotron resonance spectroscopy to generate data for several compounds, and later, computational methods were found to be a reliable tool for calculating the FIA of a variety of Lewis super-acids.[41]

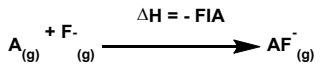

Scheme 1. *The equation for calculating the FIA.*

Lewis acid can also be separated into two groups according to the concept of hard and soft acids and bases (HSAB).[42,43] This principle was introduced by Pearson in 1963 and describes the affinities between acids and bases independently from the atom electronegativity.[44,45] It is stated that hard acids exhibit more affinity for hard bases, as well as soft acids with soft bases.

"Soft" relates to species with a large size that can be strongly polarized. On the contrary, "hard" applies to non-polarizable small species. Moreover, in 1967, Klopman used the molecular orbital theory to quantify Pearson's HSAB principle.[46] He defined the hard-hard interaction as a charge controlled reaction where the reactants have very little electron transfer and, therefore, a large HOMO-LUMO gap. On the other hand, the soft-soft interaction is characterized as a frontier orbital-controlled reaction, in which the energy gap between the two frontier orbitals is small.[42,43,47]

When looking at hard acids, aluminum (III) belongs to this category. Indeed, it forms a strong bond with fluorine-, oxygen- and nitrogen-donor ligands.[48,49] Moreover, aluminum-based compounds are known to be excellent Lewis acids and will be discussed in the next section.

C- Aluminum-based catalysts

Aluminum-based catalysts are widely used by industries.[49] The low cost and natural abundance of aluminum (3rd most abundant element in the Earth's crust, after oxygen and silicon) generate high interest in the development of aluminum-based catalysts. Elemental aluminum (Al(0)) is not stable in nature, and thus can only be found combined with other elements in the form of oxides, hydroxides, and aluminosilicates.[50–52] Bauxite, a sedimental rock with a high aluminum content, was discovered in 1821 in France by the chemist Pierre Bertier and was the first ore used by industry.[53] It consists of a mixture of aluminum hydroxide, oxyhydroxides, iron oxides, and silicates. From bauxite, aluminum oxide (Al_2O_3) can be produced through the Bayer process, developed in 1887.[54–56] Extensively used in industries, aluminum oxide is extremely efficient as a catalyst and deserves a small summary.

i- Aluminum oxide

A broad diversity of aluminum oxide (Al_2O_3) phases is known.[55] Indeed, eight different phases (α, δ, κ, η, χ, ρ, θ, and γ) can be generated starting from the gibbsite ($Al(OH)_3$), boehmite (AlOOH), the diaspore (AlOOH), or the bayerite ($Al(OH)_3$), depending on the applied thermal treatment (Figure **3**). As depicted in Figure **3**, all the transition alumina phases (δ, κ, η, χ, ρ, θ, and γ) will generate the most thermodynamically stable phase, α-Al_2O_3, when the temperature is raised above 1000 °C.

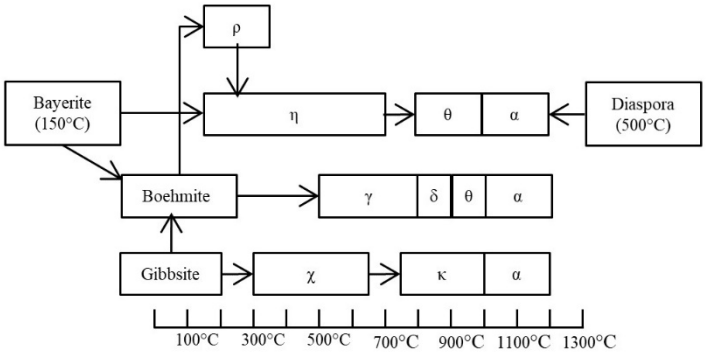

Figure 3. *Phase transformation of Al_2O_3 depending on the temperature.*[55]

The seven transition alumina phase (δ, κ, η, χ, ρ, θ, and γ) can be synthesized in a large variety of sizes and shapes, which influence the properties of the material when used as a catalyst.[51] The large surface area, high Lewis and Brønsted acidity, as well as the thermal stability properties of aluminas, engender a highly suitable catalyst for various industrial processes (Table **4**). Moreover, transition aluminas were found to be interesting materials as supports for catalysts, in particular for hydrogenation, using metals such as palladium, platinum, or nickel (see above, Table **1**).[57]

Table 4. *Examples of industrial processes catalyzed by alumina-based catalysts:*[58]

Catalyst	Reactions
γ-Al_2O_3	Dehydration of alcohols to alkenes Methyl chloride production
SiO_2-Al_2O_3	Catalytic cracking
Co-Mo/γ-Al_2O_3	Hydrogenation of alkenes Hydrodesulfurization
Ni-Mo/γ-Al_2O_3	Hydrogenation of aromatics Hydrodenitrogenation
Cu/ZnO/Al_2O_3	Methanol production Water-gas shift reaction
Fe and promoters/Al_2O_3	Ammonia synthesis (Haber-Bosch)
Cr_2O_3/Al_2O_3	Dehydrogenation of butane

Among all the existing phases, γ-alumina is the most widely used as support for catalysts and as catalyst itself, in particular in the automotive and oil industries, due to its textural and structural properties.[59] γ-Al_2O_3 is usually obtained by decomposition of the boehmite oxyhydroxide or poorly crystallized hydrous oxyhydroxide at a temperature between 400 °C and 500 °C. The structure of γ-Al_2O_3 is generally considered as a cubic defective spinel structure, which is applied to compounds with an AB_2O_4 stoichiometry; however, it is still a matter of controversy.[60–62] Indeed, uncertainty remains regarding the position of the aluminum atoms in the unit cell, and several studies report different results concerning the localizations of the vacancies.[63–66]

ii- Aluminum fluoride

As introduced earlier, aluminum oxides are widely used as heterogeneous catalysts. If oxygen atoms are substituted by fluorine, the Lewis acidity should be enhanced due to the electron-withdrawing characters of fluorine. However, AlF_3 catalysts have shown not to be as efficient as other aluminum halides or other Lewis acid catalysts.[67] As for aluminum oxide, a variety of AlF_3 phase exists in different crystalline structures, all of them consisting

of corner-sharing AlF_6 octahedrons, creating a three-dimensional network. They are called β-AlF_3, η-AlF_3, κ-AlF_3, Θ-AlF_3, and α-AlF_3.

The most stable one, α-AlF_3, has a rhombohedral structure (space group R-3c) at room temperature and is converted into a cubic phase called ht-AlF_3, analogous to ReO_3 at high temperature (Figure **4**). The four other aluminum fluoride phases are not thermodynamically stable. Thus, they irreversibly convert into the α-AlF_3 phase by thermal treatment (Figure **4**).[67]

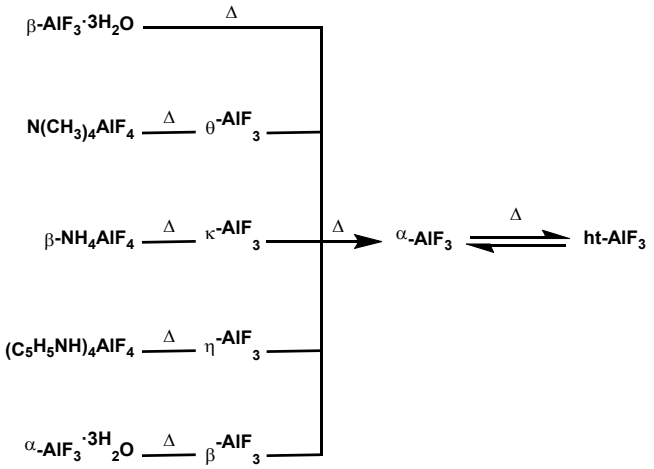

Figure 4. *Different phases of AlF_3. ht = high temperature.*[67]

Interestingly, amorphous phases of AlF_3 were found to be highly catalytically active.[67–69] In 1957, the first amorphous AlF_3 phase was discovered, obtained from the reaction of $Al(CH_3)_3$ with BF_3.[70,71] Later on, using a fluorolytic sol-gel reaction, the amorphous *high surface*-AlF_3 (*HS*-AlF_3) was developed by Kemnitz *et al.*[68] *HS*-AlF_3 was synthesized from the reaction of aluminum isopropylate with anhydrous HF in organic solvents, followed by a post fluorination step with CCl_2F_2 or $CHClF_2$.[72] As indicated in the name, a large surface area is observed, varying from 100 m^2g^{-1} up to 250 m^2g^{-1} depending on the synthesized batch. Furthermore, a large number of very strong acid sites were identified using different probe molecules, e.g., CO or CD_3CN.[68,73] In the case of adsorbed CO, a shift of 95 cm^{-1} was detected for *HS*-AlF_3, which is comparable to the shift observed for SbF_5 (81 cm^{-1}).[74] Various characterizations methods were employed to gain a better understanding of the precursor and the final product of the fluorolytic sol-gel reaction.[75,76] It was found that traces of oxygen atoms remain after the post-fluorination step, which is believed to be

responsible for the structural disorder, and therefore of the high catalytic performance of the catalyst. When exposed to water, weak Brønsted acid sites are created reversibly at the surface of *HS*-AlF_3.

A comparable amorphous AlF_3 material, aluminum chlorofluoride, firstly discovered in 1978 and later patented by DuPont, is the primary focus of this thesis and will be discussed in detail in the next section.

D- Aluminum chlorofluoride (ACF)

Even though DuPont patented the synthesis of aluminum chlorofluoride, the first report of ACF appeared in 1978, when $AlCl_3$ was used as a catalyst in the mechanistic study of the isomerization reaction of $CF_2ClCFCl_2$.[77] After the reaction, a precipitate was observed, which was attributed to the formation of aluminum fluoride by chlorine-fluorine exchange with the substrate. The synthesis of aluminum chlorofluoride was later developed by Krespan and Sievert and patented in 1992.[78,79] It involves the use of a fluorinating agent, such as CCl_3F, which reacts by chlorine–fluorine exchange with $AlCl_3$ (Scheme **2**). Later, Krahl *et al*. carried out further investigations on the synthesis and the structure of ACF and demonstrated that an inert solvent, namely CCl_4, is required during the synthesis due to the extreme exothermic behavior of the reaction.[80,81] Notably, other fluorinating reagents can be used to perform the halogen exchange reaction, such as CCl_2F_2 or $CClF_2$-CCl_2F, and The chlorine-fluorine exchange reaction is possible owing to the formation of the aluminum fluoride phase acting as the driving force of the transformation.

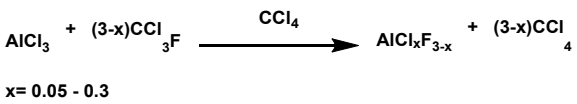

Scheme 2. *Synthesis of ACF.*[79,80]

The presence of chlorine atoms within this "AlF_3 phase" was demonstrated by XANES experiments, and those atoms are responsible for the excellent catalytic activity observed.[80] Various chlorine contents were incorporated into ACF in order to obtain the highest activity, which was shown to be when 12% of chlorine atoms were present in ACF

($AlCl_{0.3}F_{2.7}$). Indeed, ACF exhibits as well an extraordinary acid strength comparable to SbF_5.[78,82–85] Similar to *HS*-AlF_3, this catalyst has a relatively high surface area (>200 m^2g^{-1}) and very strong acid sites, as demonstrated when probe molecules were adsorbed onto its surface.[73,81] Microporosity was detected for ACF, whereas *HS*-AlF_3 is known to be mesoporous.[73,81]

The bulk of ACF has been profoundly investigated using a variety of characterization techniques.[80,81] Solid-state NMR spectroscopy has been proven to be an efficient tool since other characterizations such as infrared spectroscopy or Powder X-ray diffraction were not conclusive due to the amorphous character of ACF. The ^{19}F MAS NMR spectrum of ACF reveals the presence of terminal fluorine atoms in a small amount (>10%), along with fluorine bridging to aluminum atoms, which are also present on the crystalline phase of AlF_3.[80,81] The ^{27}Al MAS NMR spectrum displays a typical shift corresponding to aluminum in octahedral coordination, and the broadness of the signal confirms the high degree of disorder in ACF.[80,81] Since the halogen coordinates aluminum in a six-fold manner, three different types of coordination can occur (Figure **5**). On the one hand, all the fluorine atoms can be bridged to two aluminum atoms, as depicted in Figure **5**a. Additionally, one of the fluorine atoms can be terminal (Figure **5**, b). Alternatively, five fluorines can be bridged to two aluminum atoms and one chlorine to three aluminum atoms in a μ^3 coordination (Figure **5**, c).[81]

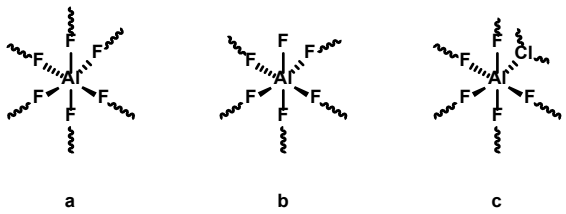

Figure 5. *The proposed structure of elemental arrangements in ACF.*[80]

Temperature Programme Desorption of ammonia (NH_3-TPD) reveals the presence of very strong Lewis acidic sites.[81] Carbon monoxide (CO) and deuterated acetonitrile (CD_3CN) were used as probe molecules to further investigate the nature and strength of the acid sites.[73,81] For both probe molecules, the highest shifts ever reported before were observed, proving the very strong Lewis character of ACF (Table **5**).

Table 5. *Wavenumbers of the (CO) stretching vibration of different adsorbed CO species at ACF and HS-AlF_3:*[73]

Species	CO stretching bands (cm-1)
Gaseous CO	2143
Physisorbed CO	2140-2150
CO at Bronsted acidic centers	2150-2180
CO at weak Lewis acidic centers	2160-2180
CO at medium Lewis acidic centers	2180-2200
CO at strong Lewis acidic centers	2200-2220
CO at very strong Lewis acidic centers	>2220
HS-AlF3	2220, 2179
ACF	2226, 2174

Due to the promising results regarding the catalytic activity of ACF, this catalyst was tested in various reactions, and several studies comparing the reactivity of ACF and SbF_5 towards different substrates revealed considerable advantages in using ACF as a catalyst.[78,82–85] As mentioned earlier, SbF_5 is expensive and toxic, and its use as a catalyst usually gives by-products, lowering the yields of the reactions.

A considerable amount of isomerization reactions of a variety of substrates such as fluorocarbons, fluoroepoxides, fluorocyclopropanes as well as halopolyfluoroalkanes were tested in the 90s using ACF as the catalyst (Scheme **3**).[78,84] The isomerization of 1,2-dibromo-hexafluoropropane into 2,2-dibromo-hexafluoropropane was used to test the Lewis acidity of the catalyst since this reaction can only be performed at room temperature by a very strong Lewis acid (Scheme **3**, up).[86] In this reaction, ACF shows extraordinary activity, reaching more than 90% conversion at room temperature after 2 hours (Scheme **3**, up).[80,87] Whereas using SbF_5, 80 °C was needed to reach the same conversion, and in the case of $AlCl_3$ as the catalyst, no conversion was observed in the same conditions.[87]

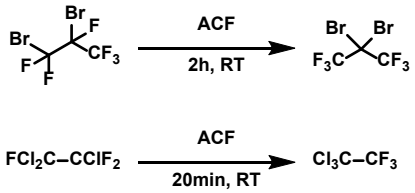

Scheme 3. *Selected isomerization reactions performed using ACF as the catalyst.*[80]

ACF was initially used as a catalyst for the production of polyfluorides and chlorofluoropropanes by the addition of various fluorinated or chlorinated substrates to tetrafluoroethene (TFE). The products are commonly used as a solvent or cleaning agents.[79,82,85,88,89] Successful addition reactions, as well as fluoroolefin condensations, were performed under mild conditions, which resulted in a broad scope of application (Scheme **4**).

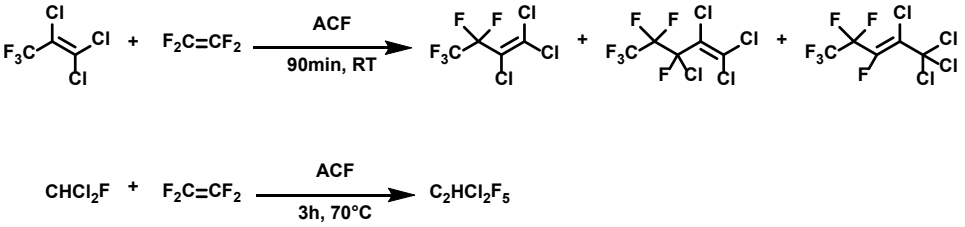

Scheme 4. *Selected addition reactions performed using ACF as the catalyst.*[79,88]

Later on, in 2011, hydrogen-deuterium (H/D) exchange reactions under mild conditions were observed using ACF as a catalyst, which usually requires harsh conditions, such as the use of a precious transition-metal, high temperature, or long reaction time.[90] Only 40 °C were required to generate hydrogen-deuterium exchange reactions with benzene and various cycloalkanes with the use of ACF as the catalyst (Scheme **5**). Furthermore, reasonable deuterium incorporation was obtained after only 22 hours of reaction time.

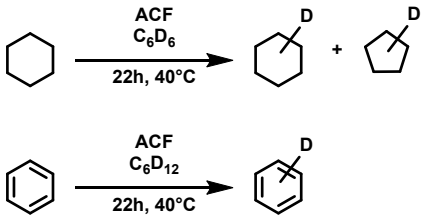

Scheme 5. *Selected H/D exchange reactions performed using ACF as the catalyst.*[90]

Furthermore, in a recent study, when arenes and olefins were mixed in the presence of ACF, the corresponding hydroarylation products were formed under mild conditions with high conversions for a variety of substrates (Scheme **6**).[91] It has been shown that ACF can trigger the formation of the Markovnikov hydroarylation product when deuterated benzene was used in the presence of ethylene, propylene, or 1-hexene. Moreover, when 3,3,3-trifluoropropene was used as the substrate, the anti-Markovnikov addition product was formed.[91]

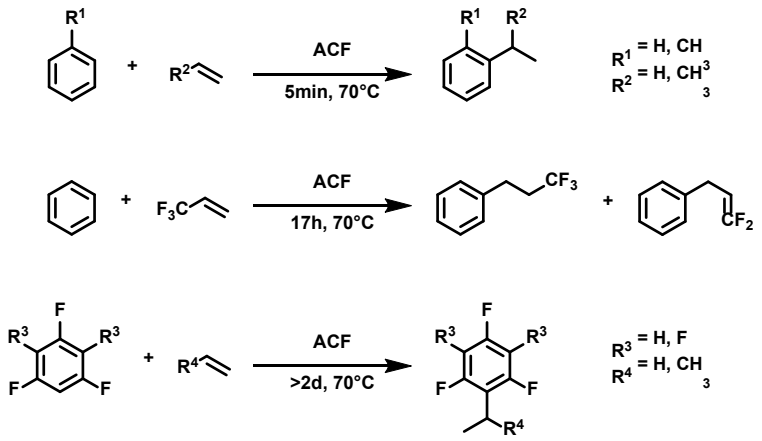

Scheme 6. *Selected hydroarylation reactions performed using ACF as the catalyst.*[91]

Another challenging reaction known is the carbon–halogen bond activation. Indeed, the energy dissociation of such bonds is considerably high, especially for C–F bonds (480 kJ/mol).[92] Thus, due to the exceptional catalytic properties of ACF, C–Cl, and C–F bond activation reactions were recently intensively studied using ACF as a catalyst.[93–97] For example, chlorinated and fluorinated methanes were activated in the presence of a hydrogen source via hydrodehalogenation (Scheme **7**).[94,95] The selectivities obtained were shown to be dependent on the additional hydrogen sources used.

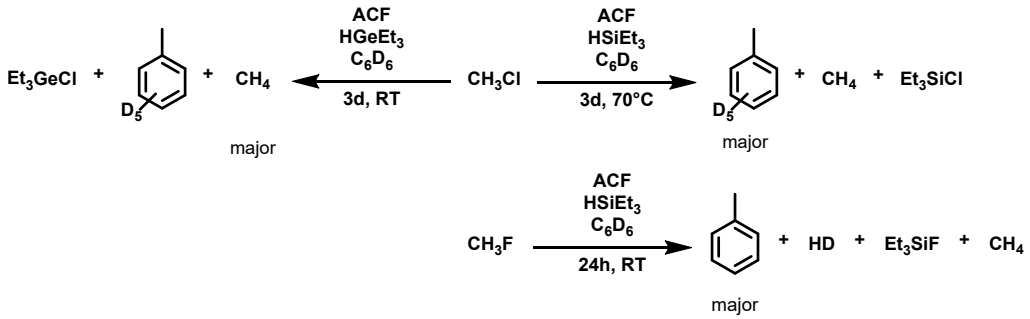

Scheme 7. *Selected C–Cl and C–F bond activation reactions in halomethanes performed using ACF as the catalyst.*[93–95]

Moreover, fluoropentane was tested in similar conditions, in the presence of silane or germane as a hydrogen source, using a modified ACF as the catalyst (Scheme **8**).[96] Again, depending on the hydrogen source used, the generation of different products was observed.

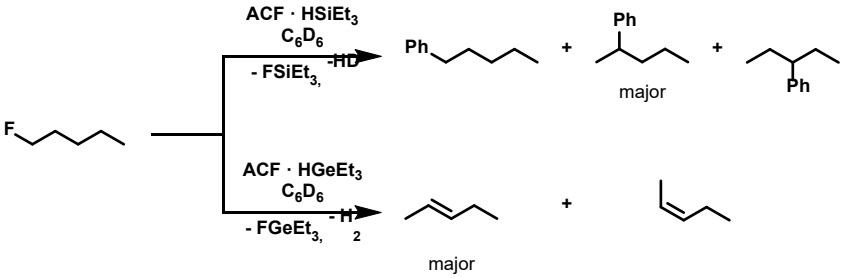

Scheme 8. *C–F bond activation reaction in fluoropentane using Et_3SiH or Et_3GeH as a hydrogen source, performed using ACF as the catalyst.*[96]

Most of the reactions mentioned above can be performed under mild conditions, reaching satisfying yield, making ACF an attractive candidate for the activation of a large variety of substrates, not tested yet.

2- Fluorinated organic compounds

A- Generalities

Fluorine-containing molecules can be found in everyday life through a variety of applications, such as drugs, crop protection, or fire extinguishants, only to cite a few examples [98,99,108,109,100–107]. Since the discovery and isolation of the fluorine atom by Henri Moissan in 1886, obtained by the electrolysis of a solution of KHF_2 dissolved in HF, using an irradiated platinum electrode at low temperature, the fluorine chemistry field has widely expanded.[110–113] However, substantial work on fluorine chemistry only started in the middle of the 20th century, with the Manhattan project and the development of Freons.[114–116] This development in fluorine chemistry led to a variety of application fields, such as material science, with the invention of Teflon in 1938, or the development of drugs in the pharmaceutical field and herbicides in the agrochemical field.[117–123] One of the first major discoveries in the pharmaceutical field was evidenced in a study on the influence of the incorporation of a halogen atom in the drug 9α-cortisones, responsible for glucocorticoid activity (Scheme **9**).[124] In this study, it was shown that when a fluorine atom was substituted to a hydrogen atom, the activity of the cortisone acetate outpaced by a factor of 10 the parent hormone.

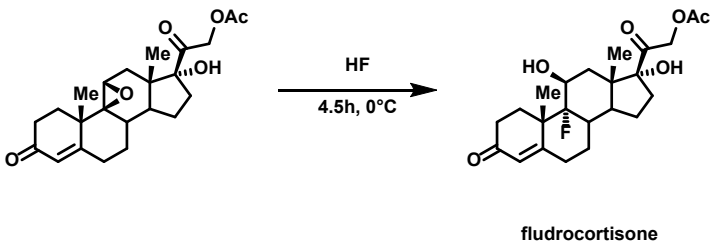

Scheme 9. *Synthesis of the fludrocortisone.*

Fluorine is not only used by pharmaceuticals in drug development; it is as well applied to medicine itself.[125–128] Indeed, the short-lived ^{18}F radioisotope was introducing to biologically active molecules such as 2-deoxy-2-^{18}F-fluoro-β-D-glucose (^{18}F-FDG), a compound commonly employs in *Positron Emission Tomography* (PET) for the early detection of tumors and the assessment of response to cancer therapy.[129–131]

Since those early findings, industries have increased their use of fluorinated molecules, and the research is concentrating on the easiest way to synthesize them.[98,105,132] In 2018, the

global demand for fluorochemicals reached 3.8 million metric tons and will continue to rise, according to an industrial report released by the Freedonia group.[133] Among various applications, the production of refrigerants is a considerable sector within the global fluorochemical market.

As mentioned earlier, refrigerants appeared in the 30s with the development of Freons by General Motors Corporation and have led to years of research on fluorocarbons.[98,102,134] Indeed, Freon 12 (CF_2Cl_2) was the first commercialized organic fluoride, owing to its significant advantageous refrigerant properties, that allowed the widespread use of refrigerators and air conditioners at that time.[116,135,136] Later on, it was found that those chlorofluorocarbons (CFCs) refrigerants were responsible for the depletion of the ozone layer in the stratosphere.[137–141] This finding resulted in the development of alternatives to CFCs, such as hydrochlorofluorocarbons (HCFCs) and hydrofluorocarbons (HFCs), which will be discussed in detail later on.[142–144]

As a consequence of the development of CFCs, polytetrafluoroethylene (PTFE) and polychlorotrifluoroethylene (PCTFE) were discovered in 1938.[134,136,145–147] PTFE or Teflon is produced by the polymerization of monomers of tetrafluoroethylene (TFE) (Scheme **10**, bottom). Initially, TFE was obtained by the combination of chloroform ($CHCl_3$) and HF, heated above 600 °C (Scheme **10** top and middle), followed by its polymerization in the presence of a radical initiator (Scheme **10**, bottom). Those fluoropolymers are extensively used nowadays, as thermoplastics, coatings, elastomers, and are present in our everyday life, in kitchenware and wire insulation.[102,103,118]

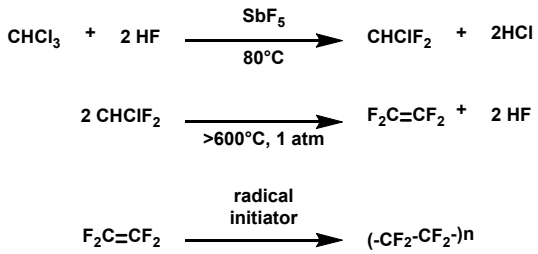

Scheme 10. *Production of Teflon (PTFE) from chloroform.*

Another important field influenced by the use of fluorine concerns the agrochemical sector: around 40% of the produced compounds are fluorine-containing molecules, with the most

common applications being herbicides and insecticides.[118,148–151] For instance, cyfluthrin, launched in the 80s, differs from its predecessor, the cypermethrin, by the presence of an additional fluorine atom, which resulted not only in a considerably increased performance in the rate for the control of cotton pests but also with an application in household insecticide (Figure **6**).[152] When more fluorine was added to this moiety (CF_3 group instead of a chlorine atom), this new insecticide, the λ-cyhalothrin, was also able to reduce the phytophagous mites.[152]

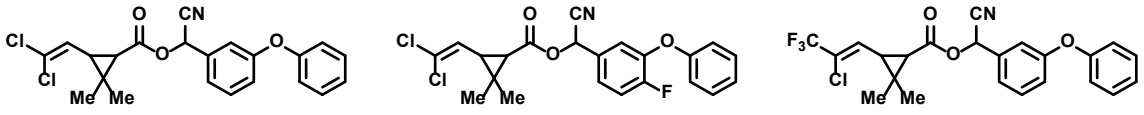

Figure 6. *Various herbicides with different fluorine content.*

As described, the interest in fluorinated compounds arises from the enhanced properties observed compare to the non-fluorinated one. Hence, a better understanding of the fluorine properties must be explained.

B- Properties induced by fluorine

Fluorine can be found in nature in the form of calcium fluorspar (CaF_2), cryolite (Na_3AlF_6), or fluorapatite ($Ca_5(PO_4)_3F$). It is ranked as the 13th most abundant element in the earth's crust; however, very little natural organic compounds have been identified to date.[153] Since the discovery of elemental fluorine, the estimated annual production of F_2 reached 28 000 tons in 2013.[118]

To explain this enormous interest in fluorine chemistry, some properties induced when fluorine is present in a compound need to be reviewed. Indeed, a change in the polarity, biological activity, but also in the thermal stability, is generally observed in fluorinated molecules compared to the non-fluorinated ones.[99,103,154] For instance, when the fluorine content is increased in olefinic polymers, their chemical and flame resistance increases, as well as their melting point, whereas the friction coefficient decreases.[102]

Those enhanced properties arise from the uniqueness of fluorine. Fluorine is the most reactive halogen, but also the smallest ones: the Van der Waals radius of fluorine can be compared to hydrogen (Table **6**).[92,155,156] Thus, a simple substitution between those two atoms can occur without any steric hindrance.[92,98,122,149,157] This substitution was studied to mimic hydrogen in bioactive molecules, and it was shown that microorganisms often do not distinguish when fluorine is replacing hydrogen.[106,157,158]

Table 6. *Properties of different elements:*[155]

Aspect	F	Cl	Br	I	H
Van der Waals radius (Å)	1.47	1.75	1.85	1.98	1.20
Electronegativity (Paulus)	4.0	3.2	3.0	2.7	2.2
Atomic polarizability	0.5	2.2	3.1	4.7	
Electron affinity (kcal/mol)	79.5	83.3	72.6	70.6	17.42
Ionization potential (kcal/mol)	401.8	299.9	272.4	242.2	313.9
C–X bond energy (kcal/mol)	108	84	70	56	105

Moreover, being the most electronegative element according to the Pauling electronegativity scale (4.0), fluorine possesses a high negative inductive ability (-*I*), which can affect the electron density of adjacent functional groups and therefore modify their acidity as illustrated in Table **7**.[92,159,160] This change in pK_a can strongly affect the pharmacokinetic properties of a molecule, such as the oral bioavailability, necessary for good absorption of the drug by the systemic circulation.[161]

Table 7. *pKa value of some selected acids:*[162,163]

Acid	pK_a	Acid	pK_a
CH_3COOH	4.76	CF_3COOH	0.52
CH_3CH_2OH	15.9	CF_3CH_2OH	12.4
C_6H_6COOH	4.21	C_6F_6COOH	1.75
C_6H_6OH	10.0	C_6F_6OH	5.5

Due to the high electronegativity of fluorine, when combined with other atoms, such as carbon, significantly strong bonds are formed.[92] Thus, the bond dissociation energy of a C–F bond is the highest one within the carbon–halogen bond (see above, Table **6**). The high electronegativity of the fluorine induces an electrostatic attraction, resulting in a highly polarized bond, presenting a strong dipole moment (μ = 1.41D) and a low lying C−F σ^* orbital, which can interact via hyperconjugation with a vicinal C−H bond.[92] This hyper conjugative interaction favorises a *gauche* conformation in fluoroalkyl groups, which is an interesting approach in the alteration of the conformation of a molecule (Scheme **11**).[99,164–167]

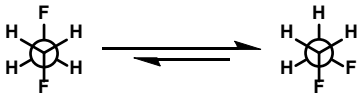

Scheme 11. *The gauche preference for 1,2-difluoroethane.*[165]

As a consequence of this electrostatic attraction induced by fluorine, a shortening of the bond is observed, which is even more pronounced when the fluorine content is increased.[92,168] For instance, in tetrafluoromethane, the C–F bond length is equal to 1.32 Å, whereas, in fluoromethane, the C–F bond length reaches 1.39 Å.[168] The polarization of the C–F bond can also influence the geometry of the molecules, depending on the number of fluorine atoms present.[92]

To obtain those fluorinated compounds with enhanced properties, one primary synthetic approach involves the derivatization of readily fluorinated building blocks using, for

instance, a catalytic process. On the other hand, using fluorinating reagents, direct fluorination of a variety of molecules can be produced. Those synthetic approaches towards fluorinated organic compounds will be discussed in the next section.

C- C−F bond activation

In order to break the C–F bonds, various strategies can be employed.[169–171] With the use of a transition metal, a reductive heterolysis of the C−F bond can take place by oxidative addition of the C−F bond to an electron-rich metal center (Scheme **12**, up). Low-valent metals can alternatively induce a homolytic splitting of the C−F bond via a single-electron transfer process (Scheme **12**, middle).[170,172–180] Besides those strategies, a heterolytic fluoride abstraction will be possible in the presence of a strong fluorophilic Lewis acid (Scheme **12**, bottom).[169,181,182]

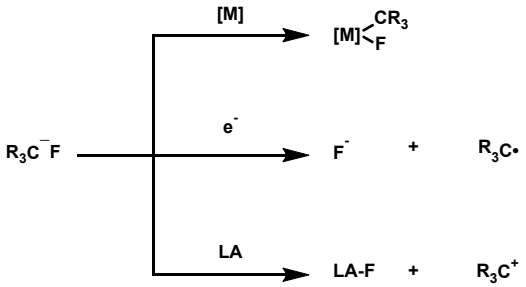

Scheme 12. *Selected strategies for the activation of C–F bonds.*
[M]: electron-rich metal; e⁻: low valent metal; LA: Lewis acid.[169]

i- Hydrodefluorination

The replacement of a fluorine atom by hydrogen in organic molecules is the easiest approach to access building blocks via derivatization.[183] Therefore, H_2 could be employed; however, it leads to the formation of HF in the reaction mixture, which remains a significant drawback. As an alternative to H_2, other hydrogen sources such as silanes with formula R_3SiH where R= alkyl or aryl can be used, generating the corresponding fluorosilane, which is thermodynamically stable (Scheme **13**).[184–186]

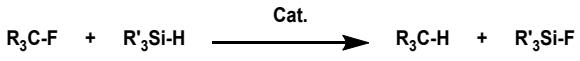

Scheme 13. *Hydrodefluorination reaction using silane as a hydrogen source.*

Several working groups reported the hydrodefluorination of aliphatic C(sp^3)–F bonds under mild conditions via the abstraction of fluoride by electrophilic silylium-species.[185–187] Following those discoveries, various catalysts were investigated in combination with a hydrogen source (Scheme **14**).[181,188–190] For instance, the hydrodefluorination of a trifluoromethyl group in perfluorinated arenes was possible in the presence of $AlCl_3$ and Et_3SiH as a hydrogen source (Scheme **14** top).[191] Besides, aluminum and boron-based catalysts, such as aluminum ions (R_2Al^+) and $B(C_6F_5)_3$, were shown to be efficient in the activation of C(sp^3)-F under mild conditions (Scheme **14** middle and bottom).[181,188,190,192–194]

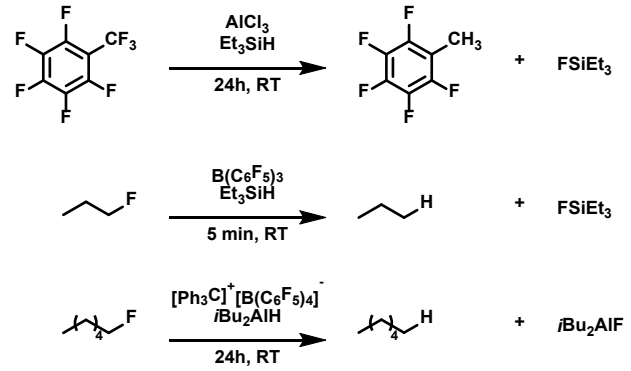

Scheme 14. *Selected hydrodefluorination reactions using $HSiEt_3$.*[195]

Moreover, when main group Lewis acids are used as catalysts, consecutive functionalization of the C–F bond could occur, due to the formation of carbenium species as intermediates.[186,187,196–200] Therefore, using a nucleophile or an aromatic solvent will lead to subsequent C–Nucleophile or C–C bond formation reactions.[169]

Mechanistically, in the presence of silylium-ions (Si^+X^-), a cleavage of the C−F bond can occur by abstraction of a fluoride, generating the corresponding carbenium ion and a fluorosilane (Scheme **15**).[185] By the subsequent reaction of the carbenium ion with a triorganosilane, a C−H bond can be generated, together with the regeneration of the catalyst Si^+X^-.

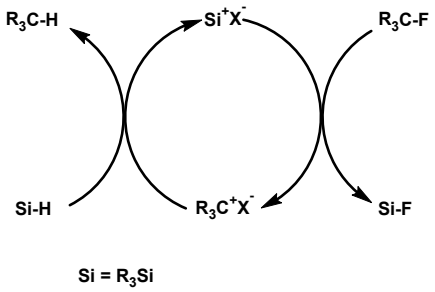

Scheme 15. *Proposed mechanism in the hydrodefluorination of C(sp^3)–F bonds using silylium-ion as the catalyst.*[185]

ii- Dehydrofluorination

Alternatively, through the elimination of HF, a C=C bond can be formed from a C–F bond and C–H bond. Indeed, the alpha carbon bearing the halogen is electropositive due to the electronegativity of the fluorine; therefore, fluorophilic Lewis acid catalysts can abstract fluorine from a C–F bond, as shown previously (Scheme **12**). In comparison to hydrodefluorination, dehydrofluorination usually requires harsh conditions to eliminate HF and form a double bond.

Several patents describe the preparation of hydrofluoroolefins via dehydrofluorination, starting from fluoroalkanes.[201–208] For instance, in 1996, the group of Takita investigated the catalytic dehydrofluorination of CF_3CH_3 into $CF_2{=}CH_2$, using various metal phosphates, and showed the efficiency of $Mg_2P_2O_7$ to selectively form $CF_2{=}CH_2$ at 500 °C.[201] The mechanism involved in this reaction was proven to take place via a heterolytic cleavage of the C–F bond (Scheme **16**). Even though the dissociation energy of a C–H bond is lower than for a C–F bond (410 kJ/mol vs. 517 kJ/mol), the strong interaction of the acidic sites of the catalyst and the electronegative fluorine pre-value leading to an abstraction of the fluorine and the formation of carbenium-ion like species.[201,203,209]

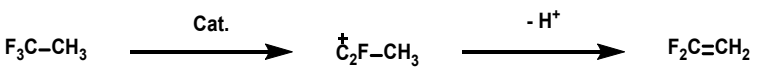

Scheme 16. *Dehydrofluorination of CF_3CH_3.*[203]

Aluminum-based catalysts have been commonly used for dehydrofluorination reactions of alkanes. Thus, in 1952, du Pont de Nemours and Co. published a patent describing the use

of aluminum sulfate ($Al_2(SO_4)_3$) as an efficient catalyst in the dehydrofluorination of 1,1-difluoroethane.[210] The temperature was set between 250 °C and 400 °C, while a specific rate of 1,1-difluoroethane was passed through the reactor. However, only a low yield of the corresponding olefin was obtained. Later on, in 1964, a patent developed by Phillips Petroleum Co. describes the use of fluorinated alumina in the dehydrofluorination reaction of difluoroethane.[211] In this instance, high conversion was obtained at elevated temperatures. Moreover, multiple fluorinated alkanes were tested, showing the considerable potential of fluorinated alumina-based catalysts.[212]

Teinz *et al.* recently investigated the dehydrohalogenation of 3-chloro-1,1,1,3-tetrafluorobutane using AlF_3 and a variety of other catalysts.[213] Reaching full conversion and full selectivity towards dehydrofluorination, the strong Lewis acid AlF_3 was, therefore, further used as a dehydrofluorinating catalyst.[214–218] For instance, γ-AlF_3 was modified by a variety of metal oxides and tested in the dehydrofluorination of CF_3CFH_2.[219] The fluorinated NiO/Al_2O_3 was found to be the catalyst exhibiting the highest catalytic activity at different temperatures.

D- C−F bond formation

Another possible approach to synthesize fluorinated compounds requires the use of fluorinating agents. A variety of reagents exists and can be divided into two categories: electrophilic or nucleophilic reagents.[122,220–222]

Among the electrophilic fluorinating agents, elemental fluorine needs to be considered, since a formal transfer of F^+ to an electron-rich site can take place.[223–226] However, considering its high reactivity and toxicity, further electrophilic reagents were developed, such as O-F or N-F-based reagents (Figure **7**).[227–234]

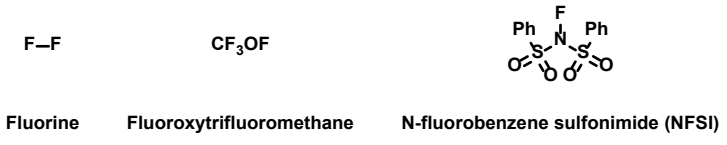

Figure 7. *Selected electrophilic fluorinating reagents.*

Alternatively, the use of nucleophilic reagents turns out to be another useful strategy to achieve fluorination of organic molecules.[222,235–239] The release of a fluoride ion using fluoride salts such as KF, AgF, CsF, or tetra-n-butylammonium fluoride (TBAF) allows a straightforward and economic fluorination process.[237,238,240–243] However, in protic solvents, the fluoride is strongly solvated, resulting in a poor nucleophile character.[122] Thus, fluoride forms tight ion pairs in aprotic solvents, which also diminishes the nucleophilicity of the fluoride ion.[244] Therefore, new reagents were developed with higher nucleophilicity, such as diethylaminosulfur trifluoride (DAST) and derivatives (Figure **8**).[122,236,245–249] Moreover, superacids, such as HF-SbF_5, were recently used in fluorination reactions, showing satisfying efficiency.[250]

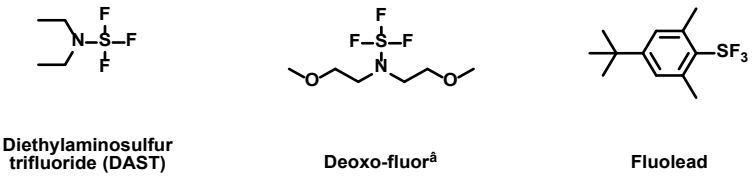

Figure 8. *Selected nucleophilic fluorinating reagents.*

On the other hand, HF based reagents were shown to be efficient in the fluorination of organic compounds. It is a very inexpensive source of fluoride, which is used as a precursor in most of the known fluorinated compounds, although great care needs to be taking into account when using HF, due to its high toxicity and corrosive character.

HF was first observed in 1771 by Wilhelm Scheele, who used CaF_2 together with sulphuric acid and observed etching of glass (Scheme **17**).[98] HF was further used by industries in the development of inert Freons refrigerants.[98]

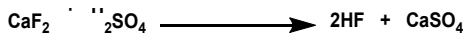

Scheme 17. *Production of HF.*

Anhydrous HF is a very strong acid, having a relatively strong intermolecular H---F hydrogen bond. It is commonly used by industries, mostly in halogen exchange reactions, production of fluorinated carbons, but also of elemental fluorine.[251] In comparison, aqueous HF is a very weak acid and a weak nucleophile due to a strong ion pair or proton

transfer between water molecules and fluoride ion. It is, therefore, easier to handle, but weaker than anhydrous HF in fluorination reactions. However, it is still used by industries as a cleaning agent for cast metals or in the etching of silicon for photovoltaic applications.

Due to the difficult handling conditions of pure HF, and the diminished nucleophilicity of fluoride in protic solvents, the combination of HF with a Lewis base was developed.[252,253] Hirschman presented in 1955 the tetrahydrofuran-hydrogen fluoride system and its application as a reagent.[254] This work was followed by many researchers that reported stable solutions of HF with amines, amides, carbamic acids and esters, trialkyl phosphines, and alcohols.[252] They all have the drawback of being limited to specific fluorinations of organic compounds. Later in the 70s, Olah and his group introduced the famous Olah's reagent: pyridinium poly(hydrogen fluoride) consisting of 30% pyridine and 70% hydrogen fluoride, which showed good efficiency towards a variety of substrates (Table **8**).[255,256]

Table 8. *Selected fluorination reaction using Olah's reagent:*

Substrate	Product	Yield (%)
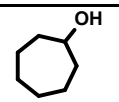	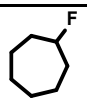	84
		80
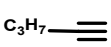		70

Later on, another HF source emerged, $Et_3N{\cdot}3HF$, less corrosive than anhydrous HF or Olah's reagent, and showed good reactivity towards nucleophilic substitution with halides, ring-opening of epoxides, and halofluorinations (Scheme **18**).[252] By using $Et_3N{\cdot}HF$, the reaction can be carried out in standard glass vessels without the release of toxic HF.

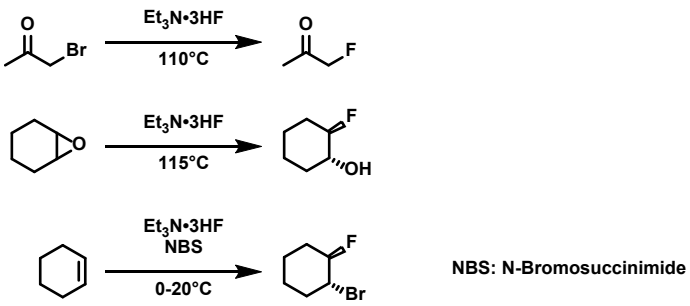

Scheme 18. *Selected reactions performed using $Et_3N{\cdot}3HF$.*

One of the most recent HF-based fluorinating reagents is the 1,3-dimethyl-3,4,5,6-tetrahydro-2(1H)-pyrimidinone-HF (DMPU-HF) complex, developed by Hammond and Xu.[257] DMPU exhibits lower basicity, as well as a better hydrogen bond basicity compared to pyridine or trimethylamine, resulting in a more stable and less basic complex with HF (Table **9**).[258] The hydrogen bond basicity (pK_{BHX}) is defined as a scale measuring the basicity towards HX, where X stands for 4-FC_6H_4OH as reference.[259]

Table 9. *Comparison between pyridine, triethylamine, and DMPU:*[258]

Base	pK_{BHX}	pK_{aH}	Nucleophilicity
Pyridine	1.86	5.2	++
Triethylamine	1.98	10.2	+++
DMPU	2.82	<0	+

pK_{BHX}: Hydrogen bond basicity ($pK_{BHX} = -\log_{10}K_{BHX} = +\log_{10}K$)
pK_{aH}: basicity

Very recently, Hammond developed a novel solid anhydrous HF equivalent, efficient in the hydrofluorination reactions of alkenes, in the ring-opening of aziridines, and in fluoro-Prins reactions under mild condition.[260] This solid was prepared by mixing HF gas with an anion exchange resin (Scheme **19**). Compared to the HF-based reagents described before, this polymer-supported HF reagent has the advantage to be easily separated from the reaction mixture and reusable, but also, its synthesis is straightforward and inexpensive. Finally, it was shown in the reactivity study that it could be used for flow fluorination and multiple other fluorination reactions.

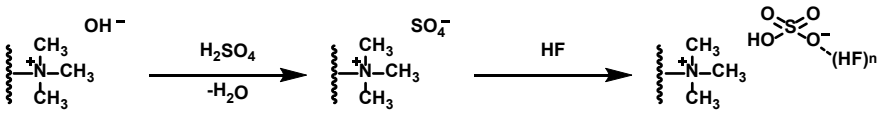

Scheme 19. *Preparation of the polymer-supported HF reagent.*[260]

Since hydrofluorination using HF-based reagents is an interesting approach to produce fluorinated compounds, this thesis will describe a new material for showing efficiency in those reactions.

Chapter 2 Aim and Objectives

Due to the rising demands for fluorinated compounds and the considerable potential of ACF as a catalyst in carbon-halogen bond activation, this thesis will focus on the use of ACF as a catalyst in the synthesis of various fluorinated molecules via two different approaches. The first approach will address dehydrofluorination reactions under mild conditions of compounds with a high ozone depletion potential, such as hydrochlorofluorocarbons (HCFCs) and hydrofluorocarbons (HFCs). Up to date, ACF was scarcely tested in the dehydrohalogenation of polyfluorinated compounds. Thus, one of the aims of this thesis will be the activation of various substrates, using this unique catalyst. To achieve the activation of polyfluorinated compounds, a hydrogen source such as $HSiEt_3$ will also be employed to observe hydrodehalogenation of the substrates, in addition to the dehydrohalogenation products generated without the silane. The potentiality in forming Friedel-Crafts products from those HCFCs and HFCs in the presence of an aromatic solvent such as C_6D_6 will also be a matter of investigation.

The second approach in the synthesis of fluorinated compounds will involve the development and the study of a modified ACF, loaded with HF, and its application in hydrofluorination reactions. In the first place, various synthesis conditions will be used to obtain the best performing material in hydrofluorination reactions. Secondly, several characterization methods will be used to understand the modification in the bulk and at the surface induced by the loading of ACF with HF. Among those characterizations, MAS NMR spectroscopy, Inelastic Neutron Spectroscopy, and adsorption of probe molecules at the surface of the materials, such as acetonitrile or pyridine, will be of great significance and will be presented in details. Finally, several substrates will be tested, such as alkynes, alkenes, ynamides, aziridines, and epoxides, to establish the potential of HF-loaded ACF in hydrofluorination reactions.

Chapter 3 C–F bond activation of polyfluorinated molecules using ACF as a catalyst

1- Introduction

Hydrochlorofluorocarbons (HCFCs) and hydrofluorocarbons (HFCs) are extensively used in everyday life, mainly as refrigerants due to their low toxicity and extraordinary properties.[131,261,262] HCFCs and HFCs were thought to be a good replacement for chlorofluorocarbons (CFCs) because of their similar physicochemical properties and the presence of hydrogen atoms, resulting in their decomposition in the lower atmosphere.[137,138,263] Thus, the transport of chlorine to the stratosphere from the troposphere (for HCFCs) is greatly reduced. CFCs are indeed ozone depletion substances (ODS) and were therefore highly restricted by the Montreal protocol since 1987.[140,264–266] Even though some HCFCs exhibit a low ozone depletion potential (ODP) (for example, HCFC-22 has an ODP = 0.034) and HFCs have an ODP value of zero, both are still known to be potent greenhouse gases because of their high global warming potential (GWP).[143,267,268] Therefore, in 1992, HCFCs were also banned by the Copenhagen amendment of the Montreal protocol, followed in 2016 by the Kigali amendment phasing down the use of HFCs as well.[264,269–273] The fourth generation of refrigerants recommended by the Montreal Protocol is based on unsaturated HFCs: hydrofluoroolefins (HFOs).[139,274–276] HFOs exhibit a negligible GWP and a zero ODP, which makes them highly valuable and thus applicable as heat transfer media or foaming and blowing agents, for instance.[276,277] In particular, HFO-1234yf (2,3,3,3-tetrafluoropropene) and HFO-1134ze (1,3,3,3-tetrafluoropropene) are nowadays of high importance due to their low toxicity compared to others. Thus, many patents, as well as publications, are reporting their synthesis and their reactivity.[274,277–281] Those reports are mainly based on the use of chromia-based catalysts or metal-halogen supported catalysts using HFCs or HCFCs as starting compounds. However, harsh conditions are needed to synthesize HFOs. Undeniably, C–F bonds in HFCs are challenging to activate, and the high dissociation energy can be usually overcome by the generation of Al–F or Si–F bonds being thermodynamically more favored.[83,169,282,283]

Among the HCFCs, HCFC-244bb (2-chloro-1,1,1,2-tetrafluoropropane) is an interesting precursor in the preparation of olefins.[274,284,285] Via dehydrofluorination, HFO-1233xf (2-chloro-3,3,3-trifluoropropene) can be obtained, and via dehydrochlorination, the target molecule HFO-1234yf is formed (Scheme **20**). The group of Teinz and the group of Mao carried out detailed investigations on the two different pathways that can occur on the activation of HCFC-244bb.[214,286] Testing different conditions and catalysts, Teinz *et al.* evidenced that using fluorinated-chromia or *HS*-AlF_3 as catalysts, dehydrofluorination occurred, whereas when using SrClF or BaClF, dehydrochlorination was observed.[214] As mentioned already in the introduction, the difference in selectivity can be explained by the HSAB theory. Therefore, it is in good agreement that using an Al–based catalyst, dehydrofluorination will occur, whereas when a Ba–based catalyst is employed, dehydrochlorination is favored.[213,214] Moreover, the reaction pathway between the HFOs and HCFC-244bb, as well as the HFC-245cb (1,1,1,2,2-pentafluoropropane), was studied, revealing the influence of the catalyst used in the product formation and the establishment of a temperature-sensitive equilibrium between HFO-1234yf and HFC-245cb (Scheme **21**).

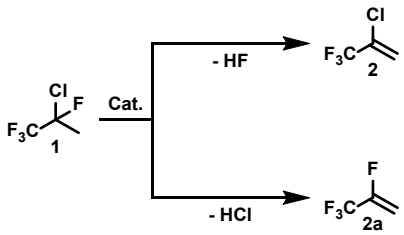

Scheme 20. *Dehydrohalogenation of HCFC-244bb.*

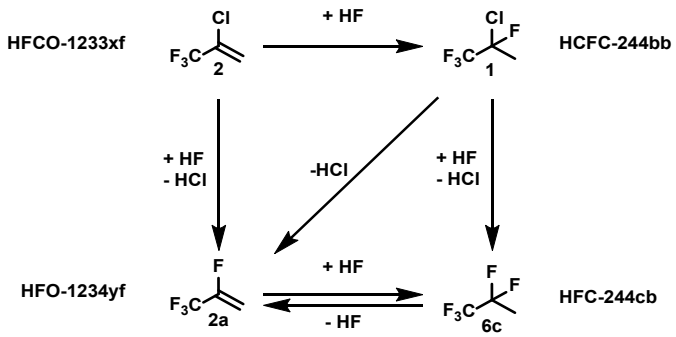

Scheme 21. *Possible reaction pathways of HCFC-244bb to access HFOs and HFCs.*

HFCs can also be considered as interesting starting compounds in the synthesis of HFOs, although their activation requires harsh conditions.[205,282,287] Numerous patents described the conversion of different HFC-245 isomers (pentafluoropropane isomers) to access HFO-1234yf or HFO-1234ze at elevated temperature (>250 °C) using a variety of solid acid catalysts.[206–208,216,217,280,288–290] The vapor-phase dehydrofluorination from HFC-245 isomers to the corresponding hydrofluoroolefin is indeed the most common route used by industries to prepare HFO-1234ze since high yields are obtained.[207]

As described previously, ACF is a strong Lewis acid that exhibits excellent reactivity towards carbon-halogen bond activation.[93–97] Within the scope of this thesis, it was therefore of interest to study the reactivity of HCFC-244bb and HCF-245 isomers using ACF as a catalyst, together with the use of a hydrogen source such as silane in order to form the thermodynamically stable Si–F bond. It was suggested by Ahrens *et al.* and Meißner *et al.* that when silanes or germanes were put in contact with ACF, the formation of surface-bound species with a silylium or germylium–ion–like character might be formed at the Lewis acidic sites.[96,291] Pulse thermal analysis (Pulse TA) evidenced the interaction of $HSiEt_3$ with the surface of ACF, with a high surface coverage of about 0.13 mol%.[291] Solid-state NMR spectroscopy and the ^{19}F spin-echo measurements evidenced the disappearance of the terminal-fluorine atoms, usually present at the surface of ACF. Those terminal-fluorine atoms are revealed by a signal at about δ = -200 ppm. Immobilized species were detected using ^{1}H-^{13}C CP MAS NMR spectroscopy for germanes and $^{29}Si\{^{1}H\}$ CP MAS NMR spectroscopy for silanes.

Moreover, ACF is also known to perform Friedel-Crafts type reactions as well as hydroarylation reactions when C_6D_6 is present as the solvent, as described earlier.[91,93,94,97] Friedel-Crafts reactions play an important role in many industrial processes and are, therefore, highly relevant. Discovered in 1887 by Charles Friedel and James Mason Crafts, Friedel-Crafts alkylation consists of the replacement of a C–H aromatic ring by an alkyl group from an alkyl halide, usually in the presence of a Lewis acid, e.g., $AlCl_3$ or BF_3 (Scheme **22**). A study showed that by modifying the Lewis acid catalyst, as well as the amount of the substrate used, or the temperature, $AlCl_3$ was found to be the most active catalyst.[30]

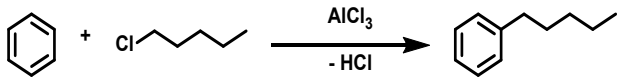

Scheme 22. *Friedel-Crafts reactions catalyzed by $AlCl_3$.*

Therefore, in the following section, C_6D_6, as well as C_6D_{12}, were employed as solvents to observe the plausible corresponding Friedel-Crafts and hydroarylation products formation.

2- Activation of 2-chloro-1,1,1,2-tetrafluoropropane - (HCFC-244bb)

A- Without the presence of a hydrogen source

When 2-chloro-1,1,1,2-tetrafluoropropane (HCFC-244bb, **1**) was treated with ACF in C_6D_{12} as a solvent, the formation of 2-chloro-3,3,3-trifluoropropene (HFO-1233xf, **2**) was observed with a conversion of 61% after 7 days (Scheme **23**, top; Table **10**, entry 1).

Treatment of **1** in C_6D_6 gave the dehydrofluorination product **2,** together with the additional hydroarylation product $CF_3CClDCH_2C_6D_5$ (**3**) (Scheme **23**, bottom). Those two products were detected in a ratio of 1:1, reaching 55% conversion after 7 days (Table **10**, entry 2). In a recent report on the hydroarylation of olefins using ACF, fluorinated olefins were also found to undergo hydroarylation, which is in good agreement with the observation made here with HCFC-244bb.[91]

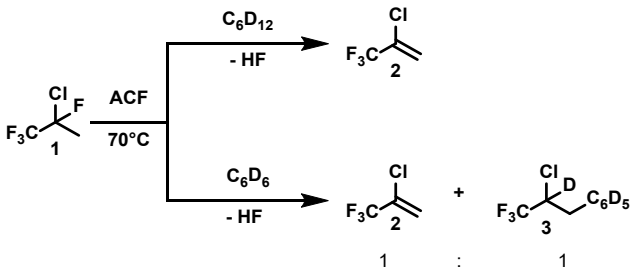

Scheme 23. *Reactivity of HCFC-244bb (**1**) using ACF as a catalyst in C_6D_{12} (top) and C_6D_6 (bottom).*

Since the formation of **3** presumably results from a subsequent activation of the double bond at HFO-1233xf (**2**) with benzene, an independent reaction was performed (Scheme **24**; Table **10**, entry 3). The formation of the hydroarylation product **3** was observed, with 90% conversion after 7 days, which confirms the suggested pathway through the hydroarylation reaction of **2** (Table **10**, entry 3).

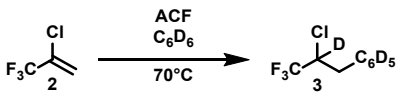

Scheme 24. *Reactivity of HFO-1233xf (**2**) using ACF as a catalyst in C_6D_6.*

Table 10. *Conversion and TON of **1** and **2** in different solvents using ACF as a catalyst:*

Entry	Substrate	Solvent	Products	t [days]	Conversion [%]	TON
1	**1**	C_6D_{12}	**2**	7	61	5
2	**1**	C_6D_6	**3** and **2** (1:1)	7	55	5
3	**2**	C_6D_6	**3**	1	59	6

Remarkably, no activation of the C–Cl bond was detected at HCFC-244bb (**1**), even though ACF revealed in previous studies the ability to activate chlorinated methane in the presence of silane or germane as hydrogen sources.[94,95] Moreover, it was also reported that when both fluorine and chlorine are present in the substrates, e.g., $CHCl_2F$, dismutation reactions followed by hydrodechlorination were observed to give CH_2Cl_2 and CH_2F_2 as major products.[95] However, in the case of HCFC-244bb (**1**), no isomerization product could be detected.

The results obtained for the activation of HCFC-244bb (**1**) are furthermore in good agreement with a report on the activation of 3-chloro-1,1,1-3-tetrafluorobutane, using different fluoride-based metal catalysts such as AlF_3, CaF_2, or BaF_2 (see above).[213] It was shown that the conversion, as well as the selectivity, can be entirely contrastive depending on the catalyst used, emphasizing the critical role of the metal-halogen affinity in the product selectivity. Since the formation of AlF_3 is strongly favored over the formation of $AlCl_3$, the fluorine atom in the substrate will selectively interact with the aluminum acidic sites of AlF_3.

In the case of HCFC-244bb (**1**), its activation at ACF is exceptional, since no usage of a hydrogen source was needed. Indeed, most of the C–F bond reactions using ACF as a catalyst require an additional hydrogen source such as silane or germane in the reaction mixture, causing an additional separation step to isolate the products.[93,96,97] Moreover, dehydrofluorination reactions usually require elevated temperatures, whereas, with ACF, only 70 °C was needed to observe the almost full conversion of HCFC-244bb (**1**) to HFO-1233xf (**2**).[201,215,292] In contrast, in the dehydrohalogenation of 3-chloro-1,1,1,3-tetrafluorobutane reported by Teinz *et al.*, the temperature was set to 200 °C.[213]

Furthermore, the research group of Lu investigated as well the dehydrohalogenation of HCFC-244bb (**1**) with temperatures set above 350 °C for all their reactions.[286]

Mechanistically, the catalyst can abstract the fluorine on the CFCl group generating a carbenium-like species at the surface of the catalyst (Scheme **25**). After an HF-elimination step, HFO-1233xf (**2**) is released, and the catalyst regenerated.

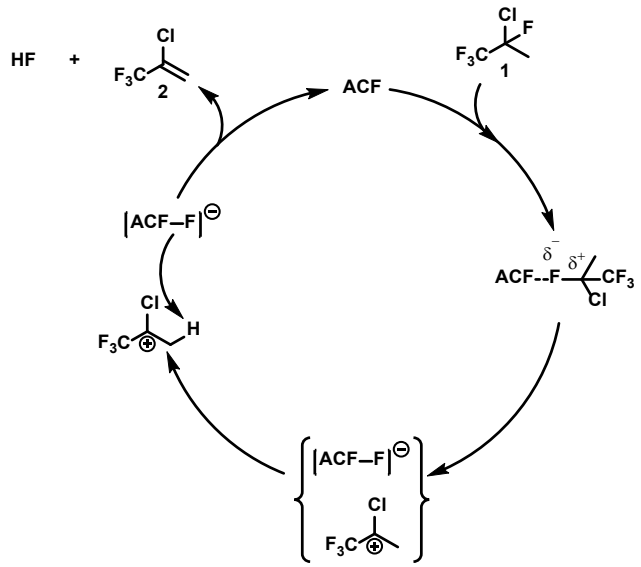

Scheme 25. *Proposed catalytic cycle of the activation of HCFC-244bb (**1**) in C_6D_{12}.*

When C_6D_6 is present as a solvent, a subsequent hydroarylation at the double bond at **2** takes place to form the corresponding hydroarylation product, as proven independently. Different pathways are conceivable: after the initial formation of **2**, the CF_3 group can undergo a subtraction of a fluoride by the Lewis acid sites at the surface of the catalyst, followed by an electrophilic attack at the aromatic solvent, forming a zwitterionic Wheeland-like intermediate (Scheme **26**). The migration of the deuterium, together with the attack of the fluoride, finally gives the hydroarylation product **3** and regenerates the catalyst (Scheme **26**, middle). Another possibility is the release of DF from the Wheeland-like intermediate, to form $F_2C{=}CCl\text{-}CH_2C_6D_5$, which can then further react with the formed DF to give the final hydroarylation product **3** (Scheme **26**, left). However, since no observation of the intermediate $F_2C{=}CCl\text{-}CH_2C_6D_5$ was possible at any reaction time, it is more likely that the deuterium will migrate from the Wheeland-like intermediate to generate the final product **3**.

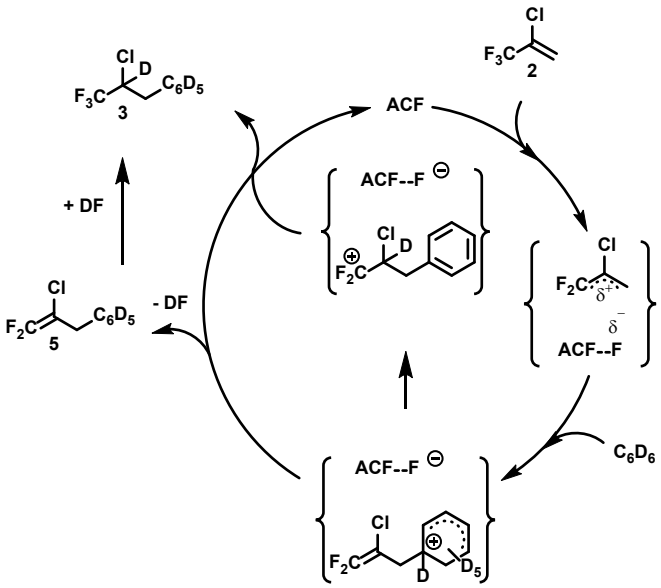

Scheme 26. *Proposed catalytic cycle of the activation of HCFC-244bb (**1**) in C_6D_6.*

A recent study revealed the very similar behavior of ACF and *HS*-AlF_3.[73] Both catalysts are very strong Lewis acids, with a similar surface area. As one of the main differences among them is their porosity; in some cases, diverse reactivity can be expected. Since *HS*-AlF_3 is a mesoporous catalyst, larger substrates which cannot be activated by ACF for sterical reasons could be activated at *HS*-AlF_3. Besides, higher conversions could be expected at *H*S-AlF_3 due to the easier availability of the acidic sites for larger substrates. Indeed, *HS*-AlF_3 has bigger pores (90 Å), which allow the substrate to enter the pores slightly faster and more efficiently than on ACF, which has smaller pores (>15 Å) (Table **11**).

Since a reasonable conversion was achieved at ACF in the activation of HCFC-244bb (**1**), the reactivity of *HS*-AlF_3 was tested as well. Under the same conditions, identical products as when ACF was used as a catalyst were observed. However, their selectivity differs. When C_6D_6 was used as the solvent, a ratio of 10:1 was found between the HFO-1233xf (**2**) and the hydroarylation product (**3**), respectively, in the case of *HS*-AlF_3, whereas a ratio of 1:1 was obtained using ACF. As mentioned before, ACF is prone to form hydroarylation products, whereas this finding was never evidenced at *HS*-AlF_3. In C_6D_{12}, HFO-1233xf (**2**) was selectively formed, with 78% conversion (Table **11**).

Table 11. *Comparison between ACF and HS-AlF_3:*[73]

	ACF	*HS*-AlF_3
Surface area by BET (m^2/g)	334	240
Pore size (Å)	10	90
Conversion of 1 in C_6D_6 (%)	55	67
Conversion of 1 in C_6D_{12} (%)	61	78

B- In the presence of a hydrogen source

As mentioned before, various C–F bond activation reactions at ACF are reported using a hydrogen source.[93,96,97] Therefore, it was of interest for an accurate comparison to observe the impact of the hydrogen source in the activation of HCFC-244bb (**1**). Scheme **27** shows the three conditions discussed with $HSiEt_3$ as a hydrogen source in combination with C_6D_6 or C_6D_{12}.

In the presence of a solvent such as C_6D_{12}, dehydrofluorination occurred to give the HFO-1233xf (**2**) and the allylic hydrodefluorination product 2-chloro-1,1difluoropropane (**4**) in a 4:1 ratio (Scheme **27**, top; Table **12** entry 1). The conversion significantly improves to 78% when compared to the reaction without silane, confirming the ability of silane to promote C–F bond activation reactions. The generation of **4** could be caused by a subsequent hydrodefluorination of **2** formed *in situ*. Independent reactions will be described later to demonstrate the formation of **4**.

When the aromatic solvent C_6D_6 was used instead of C_6D_{12}, in the presence of silane, both the Friedel-Crafts ($CF_2CClCH_2C_6D_5$, **5**) and the hydroarylation (**3**) products were generated, resulting from the electrophile attack of the double bond from the HFO-1233xf (**2**) after C−F bond cleavage (Scheme **27**, middle). Noticeably, **2** is also present in the reaction mixture, and the three products obtained are in a 1:1:4 ratio, the major product being the Friedel-Crafts one (Scheme **27**, middle; Table **12**, entry 2). As expected, the presence of C_6D_6 induces the formation of the hydroarylation product **3**, which was already observed when no silane was present in the reaction mixture.

In neat $HSiEt_3$, the reaction is similar to the one performed in pure C_6D_{12} when no hydrogen source was introduced (Scheme **1**, top and Scheme **27**, bottom). Indeed, the HCFC-244bb (**1**) is selectively converted at 45% into HFO-1233xf (**2**) using ACF as a catalyst, and $FSiEt_3$ is released in the reaction mixture (Table **12**, entry 3). Surprisingly, an increase in the conversion was not observed in this condition; on the contrary, the conversion dropped from 61% to 45% (Table **11**, entry 2 and Table **12**, entry 3). Similar results were observed in a study on the activation of fluoromethanes.[93] For the latter, an increase of the conversion was observed when the amount of the hydrogen source was increased, and a solvent was present, whereas, when the reactions were performed in neat silane, a drop in the conversion was observed.[93] It is conceivable that the acidic sites of ACF are blocked by the large excess of $HSiEt_3$, preventing the adsorption of substrates at the surface of the catalyst.[96,291]

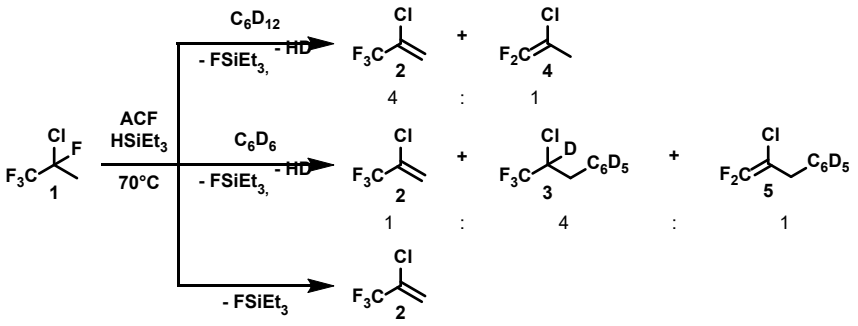

Scheme 27. *Reactivity of HCFC-244bb (**1**) using ACF as a catalyst in the presence of $HSiEt_3$ and solvents (C_6D_6 or C_6D_{12}).*

Table 12. *Conversion and TON of **1** in different solvents in the presence of $HSiEt_3$ using ACF as the catalyst:*

Entry	Substrate	Solvent	Products	t [days]	Conversion [%]	TON
1	**1**	C_6D_{12}	**2** and **4** (4:1)	7	78	7
2	**1**	C_6D_6	**2**, **5** and **3** (1:1:4)	7	48	4
3	**1**	-	**2**	7	45	4

For an accurate understanding of the generation of the products **4** and **5**, independent reactions were performed: **2** was put into contact with ACF in the presence of $HSiEt_3$ and C_6D_{12} or C_6D_6 as solvents as well as in neat $HSiEt_3$ (Scheme **28**).

When C_6D_{12} was used as the solvent, activation of the CF_3 group could be observed via an allylic hydrodefluorination, producing 2-chloro-1,1-difluoropropene (**4**) (Scheme **28**, top; Table **13**, entry 1). Noticeably, when **2** was treated in silane and benzene, the Friedel-Crafts product **5** was detected, together with the release of HD and $FSiEt_3$ (Scheme **28**, middle; Table **13**, entry 2). Interestingly, no observation of the hydroarylation product **3** was possible, even though it is the main product observed when starting from **1** (Scheme **28** middle, see above, Scheme **27**). This observation can come from the fact that the activation of the CF_3 group takes place substantially faster than the competitive hydroarylation reaction. Finally, in neat $HSiEt_3$, the formation of **4** could be observed, as also observed in C_6D_{12} and $HSiEt_3$ (Scheme **28**, top and bottom; Table **13**, entry 3). Again, a lower conversion was observed when the reaction was performed in neat silane, suggesting a likely blocking of the acidic sites by the presence of a large excess of silane in the reaction mixture. When the tetrafluoropropene analog of **2**, HFO-1234yf (**6**), was activated by ACF, the corresponding product derivated from the allylic monohydrodefluorination was also generated (Scheme **29**).[97]

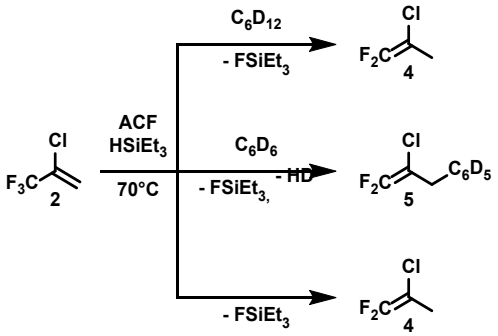

Scheme 28. *Reactivity of HFO-1234xf (**2**) using ACF as a catalyst in the presence of $HSiEt_3$ and solvents (C_6D_6 or C_6D_{12} or neat $HSiEt_3$).*

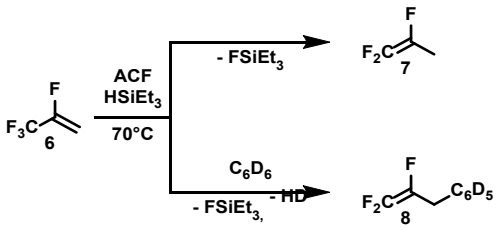

Scheme 29. *Reactivity of HFO-1233yf (**6**) using ACF as a catalyst in the presence of neat $HSiEt_3$ (top) or in combination with C_6D_6 (bottom).*[97]

It appears that by using $HSiEt_3$, the consecutive reaction of **2** towards the monoallylic hydrodefluorination and Friedel-Crafts products can be observed, depending on the conditions. To note, for the three conditions described ($HSiEt_3$ and C_6D_{12}, $HSiEt_3$ and C_6D_6, and neat $HSiEt_3$), the conversion of **2** into its different products exceeded 70% after 24 hours at room temperature, revealing the reactive character of **2** using ACF as the catalyst in the presence of silane (Table **13**).

Table 13. *Conversion and TON of **2** in different solvents in the presence of $HSiEt_3$ using ACF as the catalyst:*

Entry	Substrate	Solvent	Products	t [days]	Conversion [%]	TON
1	**2**	C_6D_{12}	**4**	1	76	8
2	**2**	C_6D_6	**5**	1	76	8
3	**2**	-	**4**	1	78	8

The mechanism involved when $HSiEt_3$ is present in the reaction mixture resembles the one described before on the activation of HCFC-244bb (**1**) in C_6D_6 (see above). After the first C–F bond activation generating HFO-1233xf (**2**), followed by the abstraction of a fluoride from the CF_3 group of the latter, two pathways can be distinguished depending on the reaction conditions: in the presence of silane, fluorosilane, and the corresponding allylic monohydrodefluorination product **4** can be producing, together with the regeneration of the catalyst (Scheme **30**, left). When benzene is present, the same mechanism as when no hydrogen source was present is likely to occur (Scheme **30**, right). However, the release of DF led to the formation of fluorosilane and HD (Scheme **26** and **30**, right).

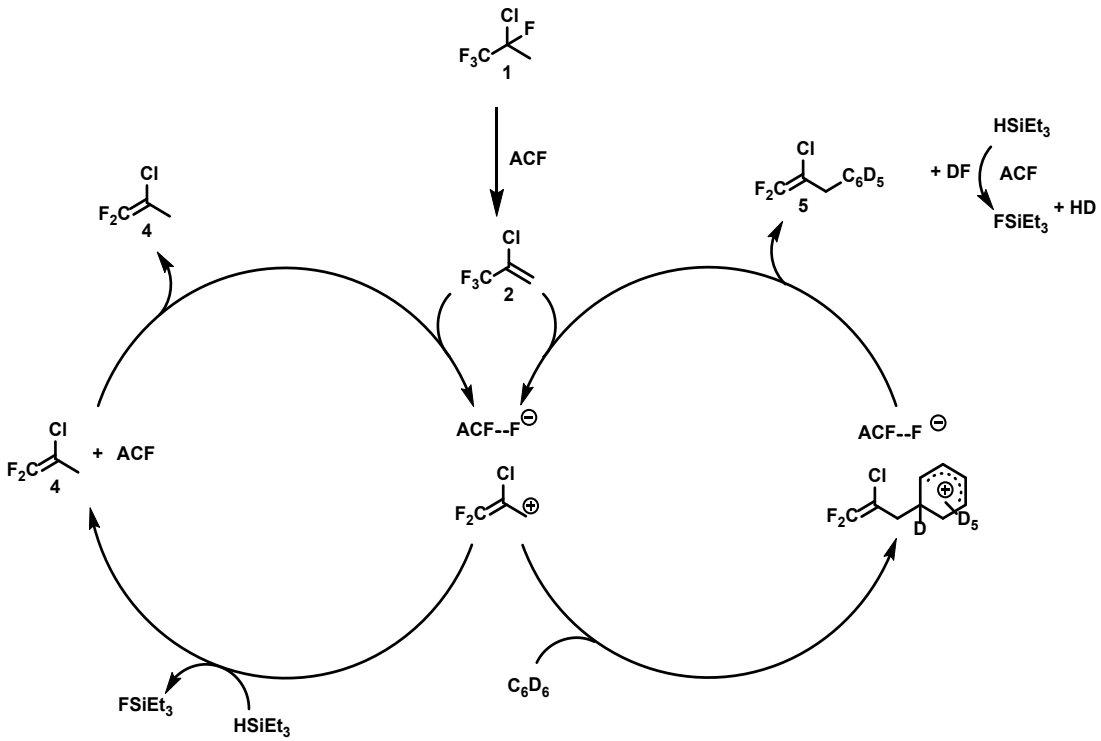

Scheme 30. *Proposed catalytic cycle of the activation of HCFC-244bb (**1**) in the presence of $HSiEt_3$ (left) or in C_6D_6 (right).*

Nevertheless, an alternative mechanism needs to be considered, according to the independent reaction starting from **2**. Indeed, the primary formation of silylium-ion-like species can be initiated by an interaction between ACF and $HSiEt_3$ (Scheme **31**). The polarization of the Si–H bond, as the proton from the $HSiEt_3$, interacts with the Lewis acidic sites at the surface of the catalyst, which can lead to the generation of silylium-like species.[93,291] This initial step would be followed by a subsequent C–F bond activation to form $FSiEt_3$ and the corresponding carbenium-like species. On the catalyst, a surface-bound hydride can, therefore, further react with this carbenium-like species to generate **4**. In the presence of C_6D_6, the Friedel-Crafts product **5** can as well be generated from the carbenium-like species as already described in the study on the activation of HFO-1234yf (**6**).[97] This conceivable mechanism was previously reported by the Braun and Kemnitz groups in the study on the activation of fluoromethanes at room temperature using silane as a hydrogen source.[93]

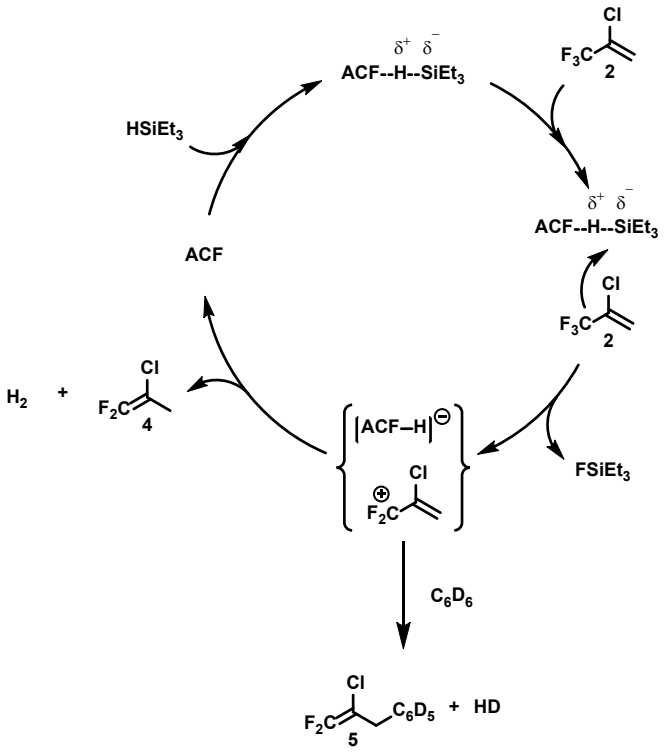

Scheme 31. *Proposed catalytic cycle of the activation of HFO-1233xf (**2**) in the presence of silylium-ion like species at the surface of ACF.*

C- Using $AlCl_3$ as a catalyst

In the presence of $AlCl_3$ as a catalyst, HCFC-244bb (**1**) could furthermore be activated under mild conditions. However, in this case, no dehydrofluorination products were observed. Instead, only the chlorine-fluorine exchange product **9** was generated, as shown in Scheme **32** and Tables **14** and **15**.

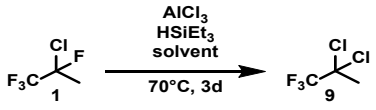

Scheme 32. *Reactivity of HCFC-244bb (**1**) using $AlCl_3$ as a catalyst, with and without the presence of $HSiEt_3$ and different solvent (C_6D_6, C_6D_{12}, or neat $HSiEt_3$).*

$AlCl_3$ is well known to perform halogen exchange reactions.[87,293,294] Indeed, chlorofluoromethanes and ethanes can undergo chlorine-fluorine exchange when they are in contact with $AlCl_3$.[295,296] Similarly, benzotrifluoride can be fully converted into benzotrichloride.[192] The generation of **9** via chlorine-fluorine exchange with the catalyst ($AlCl_3$) is therefore rational.

Table 14. *Conversion and TON of **1** in the presence of $HSiEt_3$ in different conditions using $AlCl_3$ as the catalyst:*

Entry	Substrate	Solvent	Products	t [days]	Conversion [%]	TON
1	**1**	C_6D_{12}	**9**	3	73	0.9
2	**1**	C_6D_6	**9**	3	99	1.2
3	**1**	-	**9**	3	84	1

Table 15. *Conversion and TON of **1** in different solvents using $AlCl_3$ as the catalyst:*

Entry	Substrate	Solvent	Products	t [days]	Conversion [%]	TON
1	**1**	C_6D_{12}	**9**	3	82	1
2	**1**	C_6D_6	**9**	3	99	1.2

D- Small summary

All those results demonstrated the remarkable character of ACF in the activation of C–F bonds, which could be achieved under mild condition, as compared to the literature, where elevated temperatures are needed.[86,297–300] Moreover, C–F bond activations at ACF are usually performed using a hydrogen source, which was not necessary in the case of HCFC-244bb (**1**), reducing the cost, and the reactions step to recover the final product.[93,96,97] This study demonstrated the importance of the conditions used to control the product selectivity. Indeed, the variation of the solvent for an aromatic one allows subsequent reactivity of the HFO-1233xf (**2**) towards Friedel-Craft and hydrorylation product formation, always under mild conditions.

Furthermore, by introducing a hydrogen source in the system, diverse reaction mechanisms could be proposed and are supported by independent reactions. Indeed, the silylium-ion formation at the surface of ACF when silane is present in the reaction mixture was demonstrated before and is further evidenced in this study. As shown, distinct reactivity was observed depending on when $HSiEt_3$ was present or not in the reaction mixture. It appears that the likely existence of silylium-ion induces activation of the CF_3 group via a single allylic monohydrodefluorination, whereas when no hydrogen source is introduced, the CF_3 group remained untouched.

No activation of the C–Cl bond was observed in any experiment performed with ACF, which indicates a high affinity of the catalyst to fluorine. Therefore, more substrates containing C–F bonds could be considered as candidates for testing the extensive potential of ACF in the cleavage of C–F bonds.

3- Activation of pentafluoropropane - (HFC-245) isomers

A- Activation of 1,1,1,2,3-pentafluoropropane - HFC-245eb

i- Without the presence of a hydrogen source

When 1,1,1,2,3-pentafluoropropane (HFC-245eb, **10a**) was treated with ACF in different solvents (C_6D_6 or C_6D_{12}) at 70 °C, the activation of the CH_2F group was observed (Scheme **33**). A different reactivity was found, depending on the solvent used. In C_6D_{12}, the formation of HFO-1234yf (**6**) was observed, together with 1,1,1,2,2-pentafluoropropane (HFC-245cb, **10c**) in a 1:2 ratio respectively, reaching almost full conversion after 7 days (Scheme **33**, top; Table **16**, entry 1). An equilibrium between these two products (**6** and **10c**) when HF is present in the reaction mixture was previously described in the literature by the group of Kemnitz.[214] They demonstrated that when starting from HFO-1233xf (**2**), depending on the catalyst used and in the presence of HF, HFO-1234yf (**6**) can be generated, which further reacts to produce HFC-245cb (**10c**) (see above, Scheme **21**).

Besides, when C_6D_6 was used as a solvent instead of C_6D_{12}, **6** is generated as major compound together with traces of the Friedel-Crafts CF_3-CHF-$CH_2C_6D_5$ (**11**) and the hydroarylation CF_3-CDF-$CH_2C_6D_5$ (**12**) products. (Scheme **33**, bottom; Table **16**, entry 2). In C_6D_6, the conversion did not exceed 22% after 7 days at 70 °C. This significant difference in conversion, depending on which solvent was used, can possibly arise from an interaction of benzene with the surface of ACF, blocking the acidic sites of the catalyst, as described earlier. A recent study using a Pulse TA experiment and ^{1}H MAS NMR spectroscopy suggested a strong interaction when benzene was put into contact with ACF.[95] This strong interaction can, therefore, hinder the adsorption of other substrates, resulting in a decrease in the conversion.

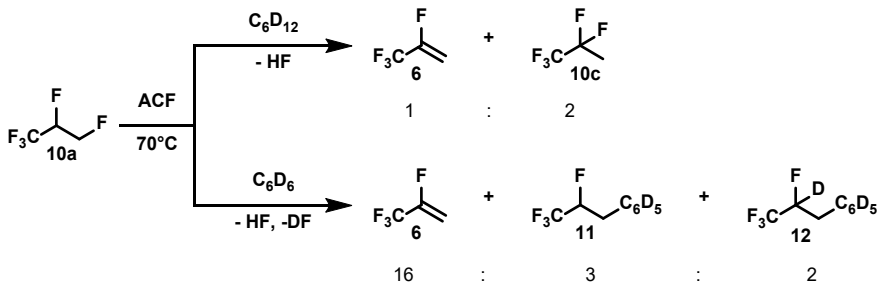

Scheme 33. *Reactivity of HFC-245eb (**10a**) using ACF as a catalyst in C_6D_{12} (top) or C_6D_6 (bottom).*

Table 16. *Conversion and TON of* ***10a*** *in different solvents using ACF as a catalyst:*

Entry	Substrate	Solvent	Products	t [days]	Conversion [%]
1	**10a**	C_6D_{12}	**6** and **10a** (1:2)	7	99
2	**10a**	C_6D_6	**6**, **11** and **12** (16:3:2)	7	22

The performance of ACF as a catalyst in the dehydrofluorination of HFC-245eb (**10a**) is astonishing since it is successfully achieved at very mild conditions as compared to the literature.[206,207] Indeed, with the use of chromia-based catalysts, the reaction temperature required to activate **10a** is set above 200 °C according to published patents.[206,207]

Mechanistically, in a similar way as previously described in the activation of HCFC-244bb (**1**), the surface of ACF can abstract a fluorine from the CH_2F group. Indeed the C−F bond present in the CH_2F group is weaker than the secondary C–F bond in the CHF group, therefore easier to activate by the catalyst (Scheme **34**). Thus, a carbenium-like species and a surface-fluoride can be generated. In the presence of C_6D_{12}, the olefin HFO-1234yf (**6**) is produced via HF elimination. This released HF can re-attack the double bond formed, generating the isomer HFC-245cb (**10c**) (Scheme **34,** left). In the presence of C_6D_6, the hydroarylation product **12** can be produced from **6** (Scheme **34**, left top). Simultaneously, the aromatic solvent can attack the initial carbenium-like species to generate a zwitterionic Wheeland-like intermediate, which subsequently gives the Friedel-Crafts product **11** and DF, thus allowing the catalyst to regenerate itself (Scheme **34**, right).

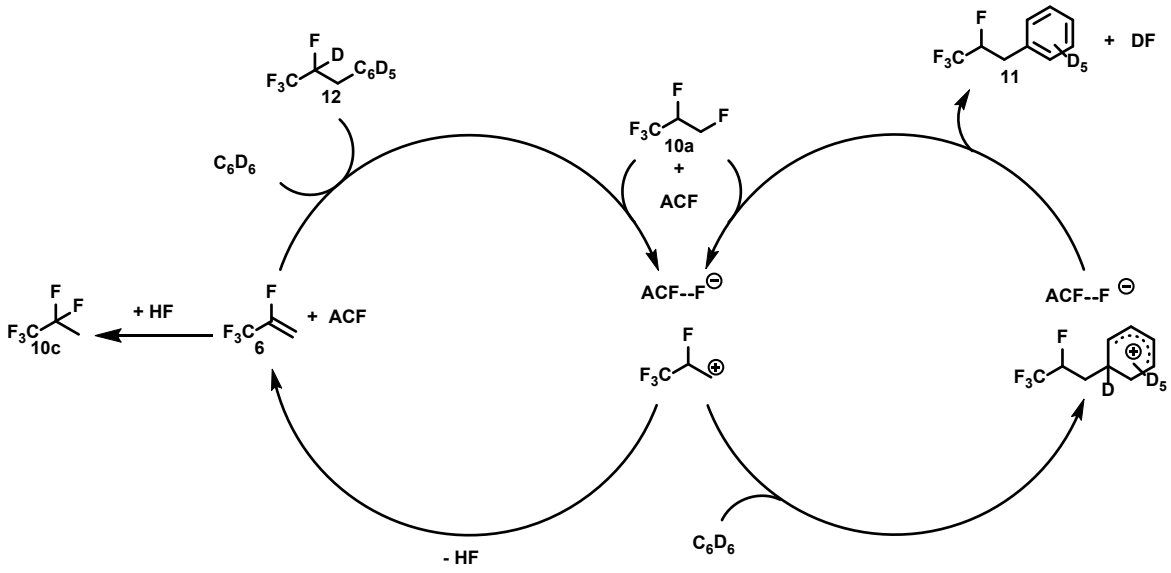

Scheme 34. *Proposed catalytic cycle of the activation of HFC-245eb (**10a**).*

ii- In the presence of a hydrogen source

As detailed previously, the conditions were modified in order to observe different reactivity or selectivity when a hydrogen source was introduced. When C_6D_{12} was used as a solvent, together with $HSiEt_3$, the same products were generated, like those obtained in the reactions without the hydrogen source, with additional traces of 1,1,2-trifluoropropene (**7**) (Scheme **35**, top). Noticeably, a change in the product ratio was observed, compared to the reaction performed without silane. Indeed, a ratio of 3:1 was observed for HFO-1234yf (**6**) and HFC-245cb (**10c**), respectively, when $HSiEt_3$ was present in the reaction mixture, whereas a ratio of 1:2 was obtained when no hydrogen source was present (Table **7** and **8**, entry 1). It can be conceivable that less HF is produced in the reaction containing $HSiEt_3$ since an alternative mechanism pathway can be considered where $FSiEt_3$ and H_2 are produced instead of HF, which hinders the formation of **10c** via refluorination and gives a higher selectivity towards the olefin **6** (see below). [86,96,301]

Similarly, in C_6D_6, the same products (**6**, **11**, **12**) as when no hydrogen source was present are generated, with the additional formation of the Friedel-Crafts CF_2=CF-$CH_2C_6D_5$ product (**8**) observed only in traces (Scheme **35**, middle). The selectivity remains the same as in neat C_6D_6; however, a considerable increase in conversion was observed from 22% to 99% when silane is present in the reaction mixture (Table **16** and **17**, entry 2). This increase

can arise from the presence of silane, which can now as well interact with the surface of the catalyst and form silylium-ion like species in a competing pathway, allowing more substrate to convert (see above).

Treatment of HFC-245eb (**10a**) in neat silane, gave **6**, **10c** and 1,1,2-trifluoropropene **7** once again, together with 1,1,1,2-tetrafluoropropane (**13**), 1,1-difluoropropene (**14**) and 1,1,1-trifluoropropane (**15**) (Scheme **35**, bottom). The compound **15** was generated in majority, via consecutive reactivity which will be described later; however, various intermediates are still present in considerable amounts.

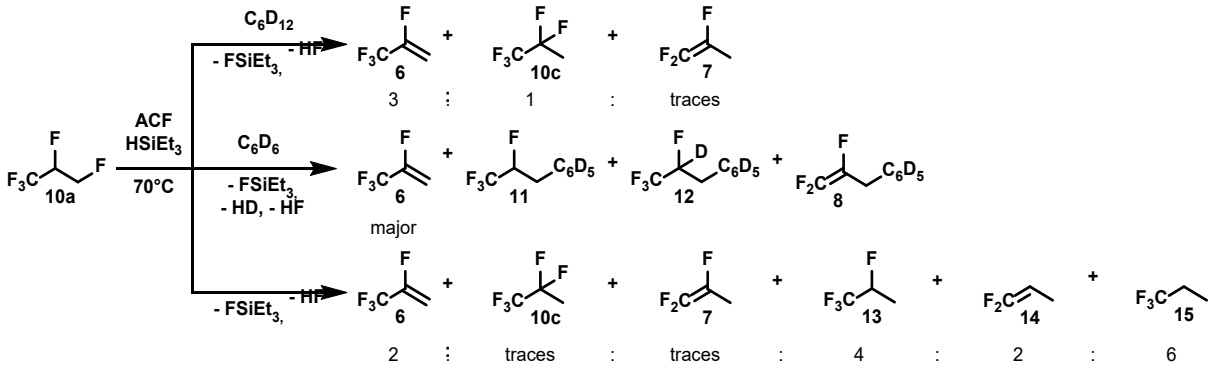

Scheme 35. *Reactivity of HFC-245eb (**10a**) using ACF as a catalyst in the presence of $HSiEt_3$ and solvents (C_6D_6 or C_6D_{12}).*

Table 17. *Conversion and TONs of **10a** in different solvents in the presence of $HSiEt_3$ using ACF as the catalyst:*

Entry	Substrate	Solvent	Products	t [days]	Conversion [%]	TON
1	**10a**	C_6D_{12}	**6**, **10c** and **7** (3:1:t)	7	99	4
2	**10a**	C_6D_6	**6** (major), **8, 11** and **12**	7	99	4
3	**10a**	-	**6**, **10c**, **7, 13**, **14** and **15** (2:t:t:4:2:6)	7	99	4

t: traces

Note that in all cases (C_6D_6 and $HSiEt_3$, C_6D_{12}, and $HSiEt_3$ or in neat $HSiEt_3$), the conversion reaches over 99% after 7 days at 70 °C, which highlights the significant role of the hydrogen source (Table **17**). Those improved conversions can result from an interaction

of the silane with the surface of ACF, involving different C–F bond activation as compared with the reaction without any silane. Indeed as mentioned already, the formation of silylium-like-species is highly likely, which can initiate the C–F bond activation at the primary carbon in **10a** (Scheme **36**). Thus, the corresponding carbenium-like species, $FSiEt_3$ and a surface-bound hydride, can be generated, followed by the formation of **13** via hydrodefluorination or **6** via dehydrofluorination. Moreover, the CF_3 group in **6** can further be activated in the presence of silylium-ion like species, yielding once more a surface hydride and the corresponding carbenium-like species. Via allylic hydrodefuorination, **7** can subsequently be generated, as it was observed previously at ACF, in the activation study of tetrafluoropropenes.[97] Alternatively, since **10a** could be activated without the presence of silane, the formation of the products **6**, **10c**, **11**, and **12** can be directly initiated by ACF, via abstraction of a fluoride from the CH_2F group at the surface of the catalyst. The corresponding carbenium-ion generated could therefore react with silane, yielding the hydrodefluorination products, or via dehydrofluorination, HF and $HSiEt_3$ can form $FSiEt_3$ and H_2. Additionally, in the presence of C_6D_6, Friedel-Crafts-like reactions can occur with any carbenium-like species intermediate present in the reaction mixture.

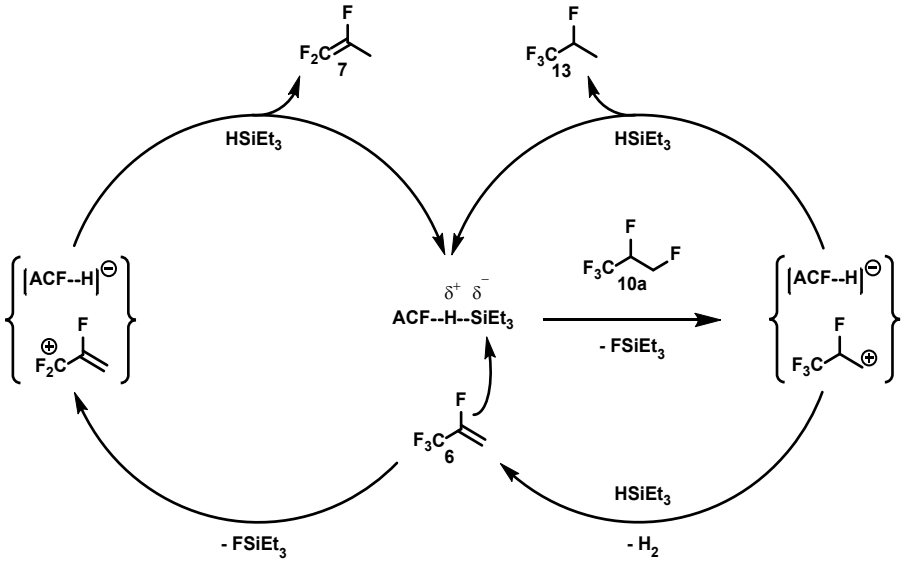

Scheme 36. *Proposed catalytic cycle in the activation of HFC-245eb (**10a**) in the presence of silylium-ion like species at the surface of ACF.*

iii- Independent reactions

As various reaction steps are involved in the formation of the products described above, such as dehydrofluorination, hydrodefluorination, hydrofluorination, allylic hydrodefluorination, hydroarylation, and Friedel-Crafts like reactions, independent reactions were performed to elucidate the reaction patterns and the transformation between certain products (Scheme **37**).

The activation of **13** using ACF as the catalyst in C_6D_{12} combined with $HSiEt_3$ or in neat $HSiEt_3$, led to the formation of **14** and **15** (Scheme **37**, top and bottom). In the presence of C_6D_6 and $HSiEt_3$, **16**, **14,** and the Friedel-Crafts product (CF_2=CH-$CH_2C_6D_5$) **17** were generated (Scheme **37**, middle). In the absence of silane and in C_6D_{12}, the selective formation of **16** was observed, whereas, in C_6D_6, **16** was once again generated together with the corresponding Friedel-Crafts and hydroarylation products, both found in traces. (Scheme **37**).

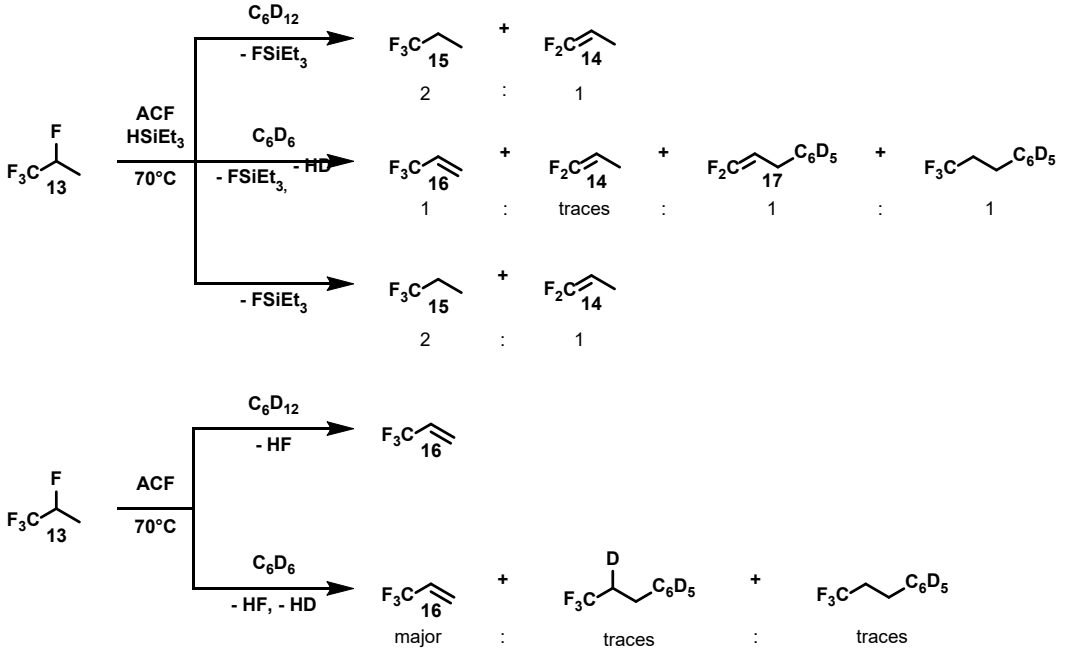

Scheme 37. *Reactivity of 7 using ACF as a catalyst in the presence of $HSiEt_3$ and solvents (C_6D_6 or C_6D_{12}, top) or in solvent only (bottom).*

Additionally, **16** was as well tested in the presence of ACF and $HSiEt_3$ in both solvents (C_6D_6 and C_6D_{12}) (Scheme **38**). In C_6D_{12} and $HSiEt_3$, **14** was generated as the main compound via allylic hydrodefluorination, together with **15** and traces of 2-chloro-1,1,1-trifluoropropene (**18**) (Scheme **38**, top). The chlorinated product **18** can arise from the

formation of HCl if the substrate is fluorinating ACF. Note that for the synthesis of ACF, $AlCl_3$ is fluorinated using fluorinated reagents.[80,81]. In the presence of C_6D_6, **14**, **15**, and traces of the corresponding Friedel-Crafts product CF_2=CH-$CH_2C_6D_5$ **17**, were produced from **16** (Scheme **38**, middle). To establish the formation of **15** in those reactions, the substrate **14** was as well tested in an independent reaction, using ACF as a catalyst and in the presence of HF (Scheme **38**, bottom). In those conditions, **15** was generated in traces via hydrofluorination. Consistent with this, when **15** was tested as a substrate, the formation of **14** was detected (Scheme **38**, bottom). Therefore, an equilibrium can be assumed between **14** and **15**, which depends on the amount of HF present in the reaction mixture.

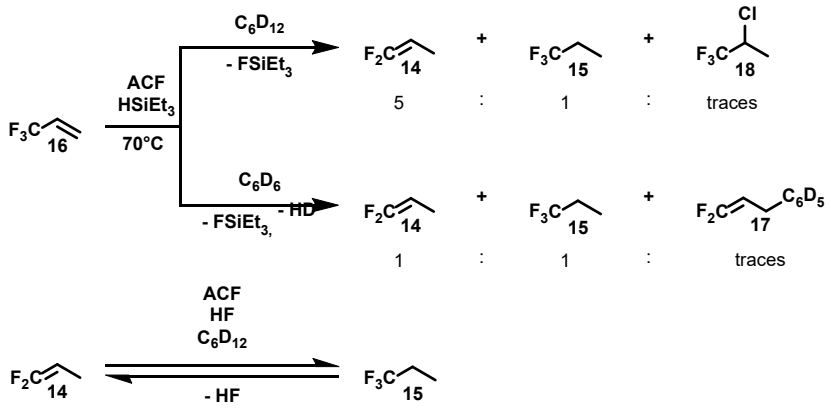

Scheme 38. *Reactivity of **16**, **15**, and **14** using ACF as a catalyst in the presence of $HSiEt_3$ or HF and solvents (C_6D_6 or C_6D_{12}).*

From the independent reactions, it could be shown that starting from 1,1,1,2-tetrafluoropropane **13**, three consecutive C–F bond activation steps can occur in a specific way, as shown in the summary depicted in Scheme **39**.

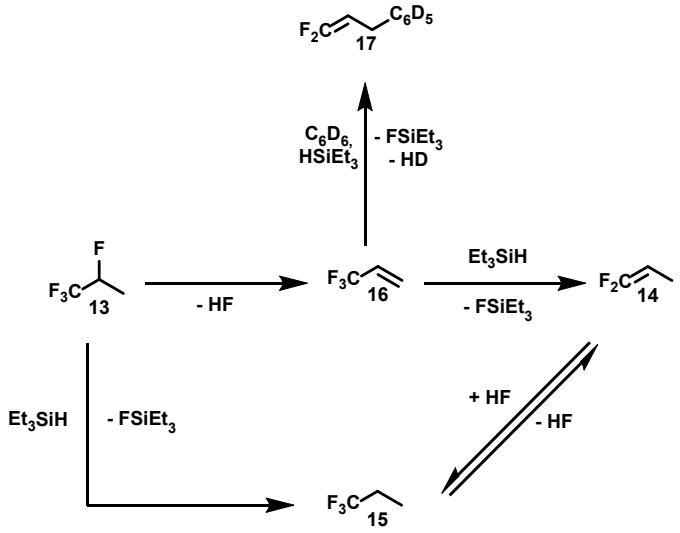

Scheme 39. *Proposed reaction pathway between **13**, **14**, **15**, **16**, and **17** in the presence of ACF as a catalyst.*

iv- Reaction pathway starting from HFC-245eb (10a)

Considering all these results from the independent reactions, a general reaction pathway starting from **10a**, which illustrates the generation of each product observed, can be proposed (Scheme **40**). Since the products resulting from the activation of **10a** observed in C_6D_6 or C_6D_{12} and silane were the same as when no hydrogen source was present, the mechanism is believed to be similar (see above, Scheme **34**). Moreover, the additional presence in traces of **7** in C_6D_{12} and **8** in C_6D_6 results from the further activation of HFO-1234yf (**6**), which was proven in a recent study.[97] This reaction from HFO-1234yf (**6**) to **7** and **8** was repeated independently under the same conditions as used for the activation of HFC-245eb (**10a**), confirming their generation. Besides, via dehydrofluorination, an equilibrium can be formed between HFC-245eb (**10a**) and HFO-1234yf (**6**). The latter can further react via HF addition to give the HFC-245cb (**10c**). In the presence of C_6D_6, HFO-1234yf (**6**) can be transformed into the corresponding hydroarylation product **12**. The Friedel Crafts product **11** can alternatively be directly generated from HFC-245eb (**10a**) when silane is present or in the same way as described before when no silane was used (see above, Scheme **24**).

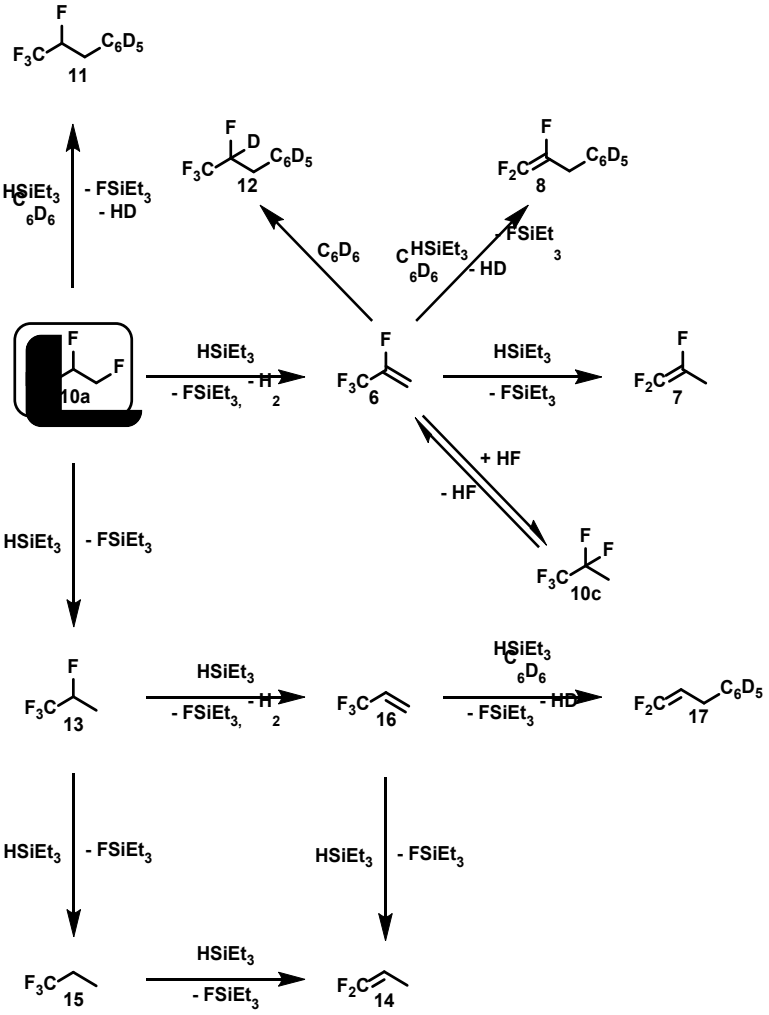

Scheme 40. *Proposed summary of all the plausible reaction pathways in the activation of HFC-245eb* ***(10a)****.*

B- Activation of 1,1,1,3,3-pentafluoropropane - HFC-245fa

1,1,1,3,3-pentafluoropropane (HFC-245fa, **10b**), an isomer of HFC-245eb (**10a**), was also tested under the same conditions as **10a**, to further elucidate conceivable reaction pathways and to understand potential similarities in their reactivity. However, no activation was observed without the use of $HSiEt_3$ as a hydrogen source. Thus, the following sub-section will only display the results obtained in the presence of $HSiEt_3$.

Interestingly, when **10b** was treated with 0.5 equivalents of $HSiEt_3$ with respect to the substrate and ACF as a catalyst at 70 °C, the selective formation of the 3,3,3,1-tetrafluoropropene (HFO-1234ze) isomers E (**19a**) and Z (**19b**) was observed in a 10:1 ratio, respectively (Scheme **41**). This observation is remarkable since the formation of HFO-1234ze (**19a** and **19b**) usually requires elevated temperatures and the presence of chromia-based catalysts.[208,217,287,290,302]

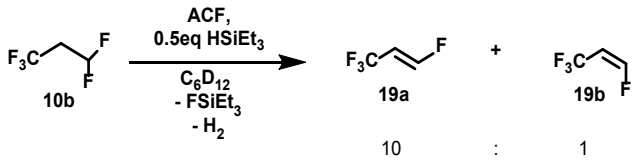

Scheme 41. *Reactivity of HFC-245fa (**10b**) using ACF as a catalyst in the presence of 0.5eq of $HSiEt_3$ in C_6D_{12}.*

A similar mechanism as the one proposed in the activation of **10a** in the presence of silane is likely to take place starting from **10b** (Scheme **42**). Indeed, silylium-like species are believed to be involved in the C–F bond activation steps at ACF, since no activation was observed in the absence of silane. Two pathways can be plausible: the silylium-ion like species can induce an initial C–F bond activation at **10b**, producing fluorosilane and the corresponding carbenium-like species. The latter can thus produce **19** and H_2, together with the regeneration of the catalyst. Alternatively, the surface of the catalyst can abstract a fluoride at the CHF_2 group, leading to the carbenium-like species, which by HF elimination can generate **19**. HF can, therefore, further react with $HSiEt_3$, yielding $FSiEt_3$, and H_2.

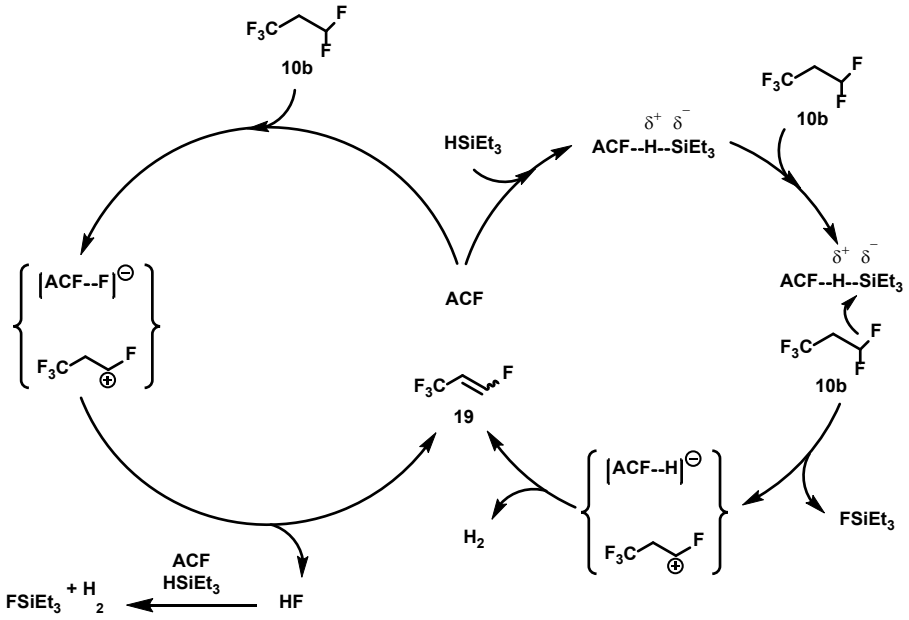

Scheme 42. *Proposed catalytic cycle in the activation of HFC-245fa* ***10b****.*

As mentioned earlier, the Meissner *et al.* previously studied the activation of the tetrafluoropropenes HFO-1234yf (**6**) and HFO-1234ze (**19**) using ACF as a catalyst and a hydrogen source.[97] In the case of HFO-1234ze (**19**), they demonstrated the formation of 1,1-difluoropropene (**14**) and 1,1,1-trifluoropropane (**15**) in neat silane, whereas, in C_6D_6, the Friedel-Crafts products CF_2=CH-$CH_2C_6D_5$ (**17**) and CF_3–CH=CHC_6D_5 (**20**) as well as the hydroarylation product CF_3-CHD-$CH_2C_6D_5$ were observed.[97] Therefore, it was of interest to increase the amount of silane present in the activation of HFC-245fa (**10b**) to study the potential subsequent reactivity of HFO-1234ze (**19**) and compare the results with the one reported on the activation of HFO-1234ze (**19**).[97]

In the presence of 1 equivalent of $HSiEt_3$, starting from HFC-245fa (**10b**), further reactivity was indeed observed (Scheme **43**). In C_6D_{12}, the products **16**, **14,** and **15** were generated (Scheme **43,** top; Table **18**, entry 1). As demonstrated earlier in the study of the activation of HFC-245eb (**10a**), all three products are related to each other, and their interconversion was proven independently (Scheme **39**). When C_6D_6 was used as a solvent, the same products as in C_6D_{12} were formed (**16**, **14**, and **15**), together with the Friedel-Crafts products **17** and **20**, both which were also observed in the activation of HFO-1234ze (**19**) (Scheme **43,** top; Table **18**, entry 1).[97]

In neat silane, **15** and **14** were generated in a 4:1 ratio, respectively (Scheme **43**, bottom). This result is consistent with the previously published report on the activation of HFO-1234ze (**19**) in neat silane; however, the two products **14** and **15** were observed in a different ratio (0.8:1) (Scheme **43**, bottom; Table **18** entry 3).[97] The presence of HF, which is released in the activation of HFC-245fa (**10b**), is likely to be responsible for this difference observed in selectivity since it can induce a hydrofluorination form **14** to **15**, as shown in the study of independent reactions (see above, Scheme **39**).

Noticeably, in neat silane, no formation of **16** could be detected, whereas when less silane was present in combination with a solvent, this product could be observed (Scheme **43**). A reason for this observation could arise from the large amount of silylium-like species generated in excess of silane, which could contribute to increasing the rate of the reaction from **10b** to **15** as compared to the reaction performed in a limited amount of silane.

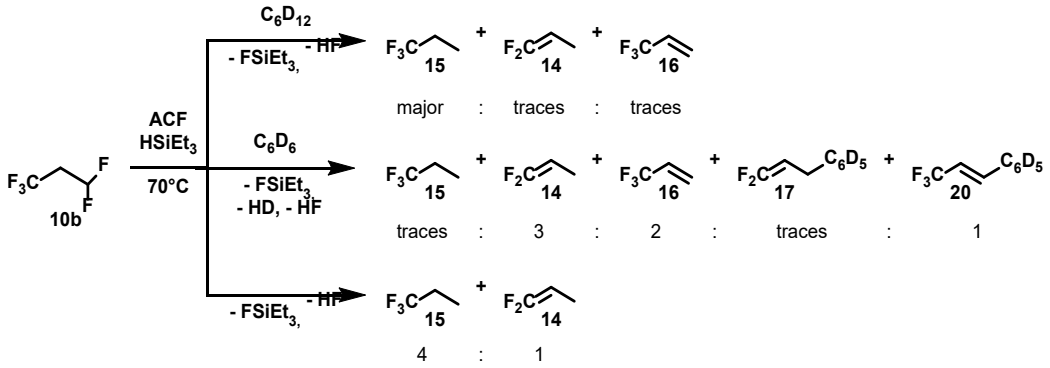

Scheme 43. *Reactivity of HFC-245fa (**10b**) using ACF as a catalyst in the presence of $HSiEt_3$ and solvents (C_6D_6 or C_6D_{12}).*

Table 18. *Conversion and TON of **10b** in different solvents in the presence of $HSiEt_3$ using ACF as the catalyst:*

Entry	Substrate	Solvent	Products	t [days]	Conversion [%]	TON
1	**10b**	C_6D_{12}	**16**, **14** and **15** (major)	7	92	5
2	**10b**	C_6D_6	**16**, **14**, **15**, **17** and **20** (2:3:t:t:1)	7	95	5
3	**10b**	-	**14** and **15** (1:4)	7	86	5

For all conditions (C_6D_6 and $HSiEt_3$, C_6D_{12} and $HSiEt_3$, or in neat $HSiEt_3$), by monitoring the reactions by ^{19}F NMR spectroscopy, it was possible to observe the early generation of HFO-1234ze (**19a** and **19b**) after 24 hours of reaction time at 70 °C. After 3 days, its transformation into the different products mentioned before was detected. Besides, the continuous formation of $FSiEt_3$ was observed for all reactions, which underlines the crucial role of the hydrogen source at each reaction stage.

Overall, a reactivity pathway can be proposed starting from **10b**, which includes several consecutive C–F bond activation steps (Scheme **44**). Via dehydrofluorination, **19**, is generated as described above. Subsequent activation of the CF_3 group at **19** can lead to the formation of the intermediate (not observed) 1,1,3-trifluoropropene, which in the presence of benzene, can undergo a Friedel-Crafts type reaction generating **17**. Alternatively, via hydrodefluorination, 1,1,3-trifluoropropene can lead to **14**. Moreover, **19** can also via HF addition regenerate **10b**, which, via hydrodefluorination give the intermediate 1,1,1,3-tetrafluoropropane. This intermediate can either produce **15** via a second hydrodefluorination reaction or **16** via dehydrofluorination. Thus, **16** can in the presence of C_6D_6 from the Friedel-Crafts product **17**, or via hydrodefluorination, yield to **14** as shown by the independent reaction (see above). Finally, **20** can be generated directly from **10b** via Friedel-Crafts type reaction followed by an HF elimination.

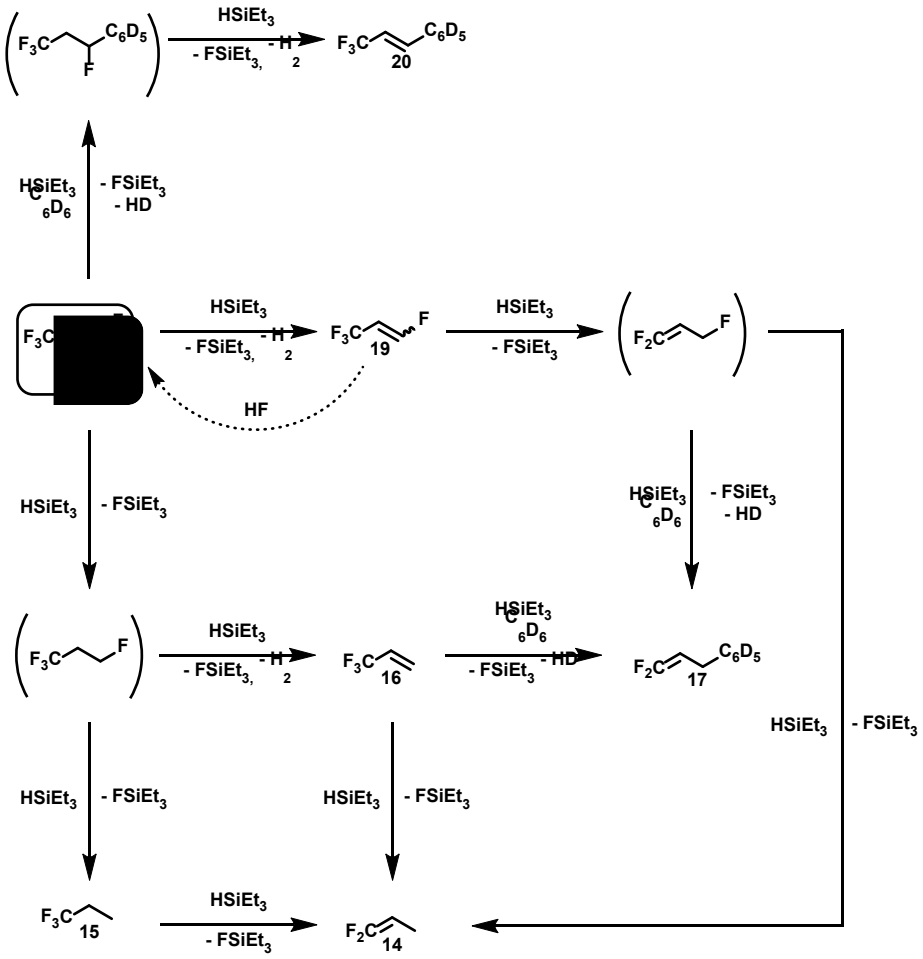

Scheme 44. *Proposed summary of all the plausible reaction pathways in the activation of HFC-245fa (**10b**). The parentheses represent key intermediates, which were not observed.*

C- Activation of 1,1,1,2,2-pentafluoropropane - HFC-245cb

As for HFC-245fa (**10b**), the isomeric 1,1,1,2,2-pentafluoropropane (HFC-245cb, **10c**) could not be activated without the presence of a hydrogen source. Moreover, in general, only low conversions were obtained, although $HSiEt_3$ was used (Table **19**). HFC-245cb (**10c**) is known to be a very stable compound that requires elevated temperatures to be activated.[280] Furthermore, an equilibrium with HFO-1234yf (**6**) is initiated, as described previously.[214]

Treatment of **10c** in silane and C_6D_{12} at 70 °C gave the allylic monohydrodefluorination product 1,1,2-trifluoropropene (**7**) and **14** in a 1:1 ratio with 38% conversion (Scheme **45**, up; Table **19**, entry 1). This observation is consistent with the equilibrium existing between **10c** and **6** since the latter is known to generate **7** when it is in the presence of silane and ACF (see above).[97] In the presence of C_6D_6 and $HSiEt_3$, the corresponding Friedel-Crafts products of **8** and **20** were observed, and the conversion reached only 18% (Scheme **45**, middle; Table **19**, entry 2). In that case, the benzene might interact with the surface of the catalyst and block some acidic sites, which would explain the lower conversion when compared to the reaction performed in C_6D_{12}.

When the reaction was executed in neat silane, the same products obtained in C_6D_{12} and $HSiEt_3$ were generated (**7** and **14**) (Scheme **45**, bottom). The only difference between those two conditions can be seen in the conversion. Indeed, in neat silane, the conversion did not exceed 10%, whereas, in C_6D_{12}, it reached 38% (Table **19**, entries 1 and 3). Again, as it was described before, $HSiEt_3$ can, in the same way as benzene, block the access to some acidic sites, resulting in a lower conversion compared to when a smaller amount of silane is used.

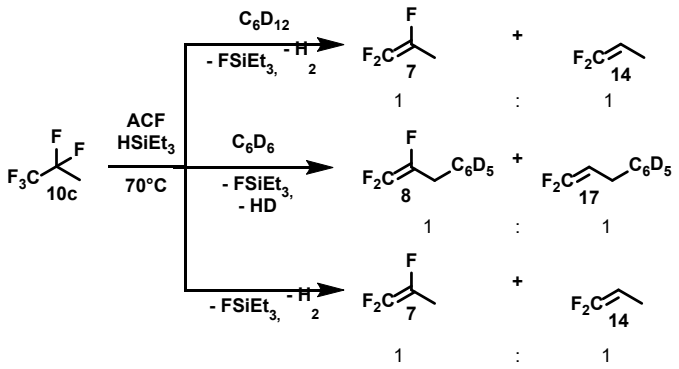

Scheme 45. *Reactivity of HFC-245cb (**10c**) using and ACF as a catalyst in the presence of $HSiEt_3$ and solvents (C_6D_6 or C_6D_{12}).*

Table 19. *Conversion and TON of **10c** in different solvents in the presence of $HSiEt_3$ using ACF as the catalyst:*

Entry	Substrate	Solvent	Products	t [days]	Conversion [%]	TON
1	**10c**	C_6D_{12}	**7** and **14** (1:1)	7	38	1
2	**10c**	C_6D_6	**8** and **17** (1:1)	7	18	1
3	**10c**	-	**7** and **14** (1:1)	7	10	0.4

Mechanistically, in the same way as for the initial activation of **10b,** via the formation of surface silylium-ion like species, **6** will be initially generated, together with $FSiEt_3$ and H_2. Thus, a general reaction pathway can be proposed (Scheme **46**). Via an allylic monohydrodefluorination, **7** can be formed, as it was observed in the study on the activation of HFO-1234yf (**6**).[97] Similarly, in the presence of C_6D_6, **6** can generate the corresponding Friedel-Crafts product **8**. Moreover, to rationalize the presence of **14** and **17**, it is possible that as for the other two HFC-245 isomers studied before, HFC-245cb (**10c**) could via a hydrodefluorination form the intermediate **13**. This intermediate can further react as it has been described earlier, to give **16**, which can also react to generate **14**, or in the presence of C_6D_6, the Friedel Crafts product **17**.

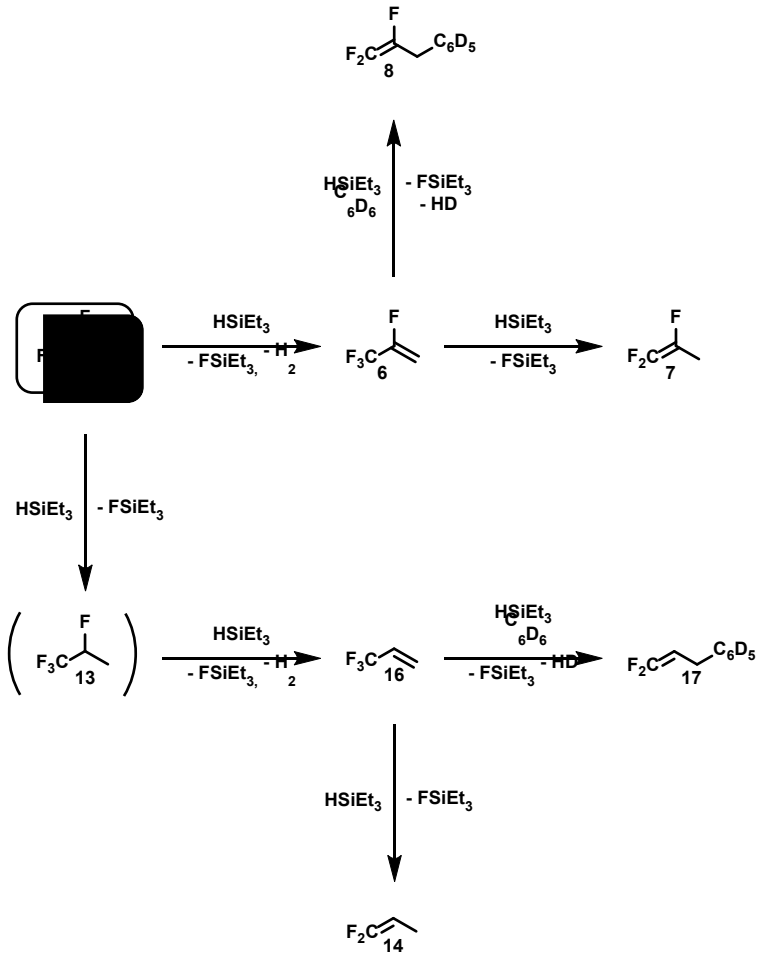

Scheme 46. *Proposed summary of all the plausible reaction pathways in the activation of HFC-245cb (**10c**). The parentheses represent key intermediates, which were not observed.*

D- Small summary

Overall, a variety of polyfluorinated compounds could be easily activated by ACF via dehydrofluorination and hydrodefluorination reactions under mild conditions. The three HFC-245 isomers (**10a**, **10b**, and **10c**) were found to be reactive in that order:

HFC-245eb (**10a**) > HFC-245fa (**10b**) > HFC-245cb (**10c**)

Due to the strong polarization of the C–F bond, the bond strength becomes more challenging to break, as the fluorination degree at the carbon increases, as revealed by the bond dissociation energy (BDE) values of fluoromethanes.[283] Indeed, the BDE increases with the content of fluorine attached to a carbon atom (Table **20**).[283]

Table 20. *Bond dissociation energy (BDE) of fluoromethanes:*

Compound	BDE (kcal/mol)
CH_3F	109
CH_2F_2	122
CHF_3	128
CF_4	129.7

Hence, it is more difficult to break a C–F bond in a trifluoromethyl group than in a difluoromethyl one or a monofluoromethyl group, a principle which was evidenced once more in this study of three hydrofluorocarbons isomers.

In HFC-245eb (**10a**), the primary C−F bond in the CH_2F group was easily activated without the need for a hydrogen source. However, in the presence of a silane, further reactivity could be observed, yielding to the formation of subsequent defluorination products. On the other hand, the study on HFC-245fa (**10b**) and HFC-245cb (**10c**) (CHF_2 and CF_2 groups) revealed the need for a hydrogen source to promote the activation of at least one C−F bond through the formation of the thermodynamically stable Si−F bond. Moreover, the primary C−F bond at the CHF_2 group in HFC-245fa (**10b**) was found to be more reactive than the secondary C−F bond at the CF_2 group in HFC-245cb (**10c**). All those results are in good agreement with a study on fluoromethanes using ACF as a catalyst.[93] Indeed, higher yields were obtained for the activation of CH_3F than for CH_2F_2 or CHF_3, confirming the order of reactivity observed with the HFC-245 isomers.

For **10a** and **10b**, when only a limited amount of silane was present in the reaction mixture, dehydrofluorination products were shown to be favored, whereas, in excess of silane, hydrodefluorination products were generated in majority. In contrast, for **10c**, both dehydrofluorination and hydrodefluorination pathways compete with each other, independently from the amount present of the hydrogen source. Besides, by using an aromatic solvent such as C_6D_6, several Friedel-Crafts type reaction take place, generating a variety of Friedel-Crafts products.

Chapter 4 Loading of HF at the surface of ACF for hydrofluorination reactions

1- Introduction

Fluorination reactions are of high interest nowadays, due to the enhanced properties induced by the incorporation of a fluorine atom into a molecule.[122,303] As described in the introduction, various fluorinating reagents can be used to fluorinate a large scope of substrates. Among them, HF-based reagents are widely used due to their low prices and simple handling.[256,257,304,305] Often combined with transition metal complexes, such as iridium, palladium, or gold, pyridinium poly(hydrogen fluoride), triethylamine-HF ($Et_3N{\cdot}3HF$), and DMPU-HF have shown to be efficient in hydrofluorination reactions of alkenes and alkynes.[305–308] In particular, gold-catalyzed hydrofluorination reactions have been deeply studied in the past years after the pioneering work of Sadighi, who reported in 2007 the first gold-carbene complex efficient in the hydrofluorination of alkynes, when combined with $Et_3N{\cdot}3HF$ and acidic additives.[309] Later on, several research groups followed the work of Sadighi and continued to develop gold-complexes to use in combination with HF-sources in hydrofluorination reactions (Scheme **47**).[257,310–314]

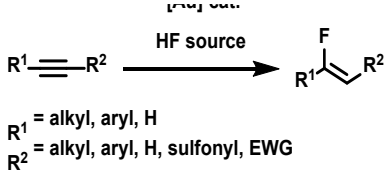

Scheme 47. *Gold-catalyzed hydrofluorination reactions of alkynes.*

Recently, Fustero *et al.* developed the selective synthesis of (E)-β-fluorovinyl sulfones with the use of a copper-based catalyst combined with $Et_3N{\cdot}3HF$. Those fluorovinyl sulfones compounds are attractive fluorinated building blocks that can undergo various processes.[315] Additionally, α-vinylfluoride thioethers were synthesized by O'Hagan using a Lewis acid and $Et_3N{\cdot}3HF$ (Scheme **48**).[316] It was proposed that the Lewis acid increases the acidity of the HF-source, which can lead to the protonation of the substrate, followed by a fluoride attack to give the final product.[316]

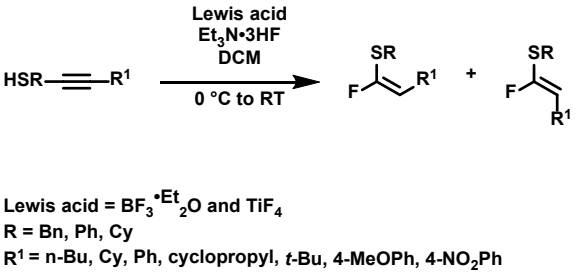

Scheme 48. *Hydrofluorination reactions of alkenyl sulfides.*[316]

Another interesting system based on super acidity was applied to hydrofluorination reactions. The superacid HF/SbF_5 was able to hydrofluorinate aminoalkynes, ynamides as well as unsaturated amines.[317] Thibaudeau *et al.* evidenced the formation of β-fluoroamines, using the HF/SbF_5 system, via the formation of a superelectrophilic dication intermediate, which can be conveniently fluorinated by the solvated fluorine in the polymeric anion in $Sb_nF_{5n+1}^-$ (Scheme **49**).[318]

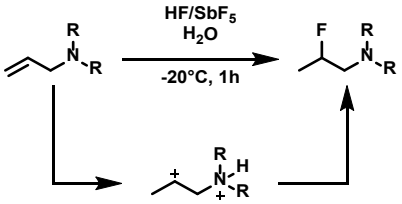

Scheme 49. *Hydrofluorination of N-allylpiperidine using the HF/SbF_5 system.*[318]

Non-functionalized alkenes were as well successfully tested in hydrofluorination reactions by using the highly acidic hydrogen bond acceptor $KHSO_4$-13HF.[319] Later on, HSO_4^- was fixed on an ion exchange resin and further complexed with HF, creating a solid anhydrous HF equivalent, which was able to perform a variety of hydrofluorination reactions (see above, Chapter 1).[320]

HF itself is also used in many synthetics procedures. For instance, the sol-gel route to obtain *HS*-AlF_3 consists of a two-step synthesis, involving the use of HF. In the first step, aluminum alkoxide is fluorinated using a solution of HF dissolved in isopropanol or diethyl ether under anhydrous conditions (Scheme **50**).[68] The second step involves the post fluorination of the synthesized precursor, at 350 °C using a fluorinating agent such as

CCl_2F_2 (Scheme **50**, top). In a mechanistic study of the synthesis of *HS*-AlF_3, various fluorinated reagents were tested in the post fluorination step, such as diluted gaseous HF at 100 °C or 200 °C (Scheme **50**, bottom).[75] However, low catalytic activity and low surface area were detected for the observed material compared to *HS*-AlF_3 synthesized traditionally. Photoacoustic FTIR of adsorbed pyridine of *HS*-AlF_3 and aluminum alkoxide fluoride treated with HF, as well as *HS*-AlF_3 exposed to HF, were recorded, and the latter two did not exhibit the band at 1453 cm^{-1}, representative for the Lewis acidic sites.[75] The study revealed a reduced acidity when the precursor was post-fluorinated by HF, suggesting a blocking of the acidic sites by HF. Nevertheless, the high acidity observed in *HS*-AlF_3 could be recovered upon heat treatment in the presence of CCl_2F_2 or $CHClF_2$, resulting in complete desorption of the HF at the Lewis acidic sites. The same tendency was observed when water was adsorbed onto the surface of *HS*-AlF_3.[321] Indeed, water does not destroy the bulk of *HS*-AlF_3 but remains only at the surface without diffusing into the solid. This observation contrasts with the similar material aluminum chlorofluoride, for which adsorption of water at the surface leads to immediate hydrolysis of the Al–Cl bond and loss of catalytic activity irreversibly.[81]

Scheme 50. *Synthesis of AlF_3 using CCl_2F_2 (top) or HF (bottom) as fluorinating reagents for the post fluorination step.*[68,75]

Moreover, in 2007, the group of Harrison studied the adsorption of HF on β-AlF_3 surfaces using Density Functional Theory (DFT).[322] This investigation revealed the formation of FHF^- species at high coverage, whereas, at low coverage, the formation of hydrogen bonds to neighboring dandling fluorine ions occurred. However, to the best of our knowledge, no experimental studies were performed on the adsorption of HF on aluminum fluoride, except the one mentioned above by Kemnitz *et al.*[75]

Nevertheless, the loading of ACF with particular substrates is of recent interest, since the development of bifunctional materials can give rise to enhanced properties and, thus, to a

broader reactivity.[93,96] Previously, successful loading of hydrogen sources such as triethylsilane or triethylgermane was achieved at ACF.[93–96,291] Different characterization methods were used to study the interaction of the substrates with the surface, such as MAS NMR spectroscopy, Pulse TA, and Temperature Program Desorption (TPD).[93,96,291] Those technics revealed different interactions depending on the hydrogen source immobilized at the surface of ACF. In the case of silane, as it was described earlier, silylium-like species could be generated at the surface of ACF.[93,96,291] In contrast, for immobilized germanes at the surface of ACF, two distinct types of surface-bonded germane species were distinguished.[96] Those results are in good agreement with the distinct reactivity observed for both materials, as described in the introduction.[94–96]

In diverse C–F bond reactions using ACF as a catalyst, the formation of HF could be observed. For instance, when 1-fluoropentane was combined with ACF and C_6D_{12}, traces of 2-fluoropentane and 3-fluoropentane were detected, indicating a possible refluorination reaction of the 2-pentene formed via HF-elimination.[96] Moreover, in the previous section on the activation of C–F bonds at ACF, dehydrofluorination products, as well as HF release, was evidenced. In some cases, this released HF could generate an equilibrium between hydrofluorination and dehydrofluorination products.[86] The presence of HF in the reaction mixture can not only induce a reaction with the substrates, but an interaction with the surface of ACF could also take place as it was earlier indicated for *HS*-AlF_3.[75]

Consequently, it was of interest to investigate the interaction between the surface of ACF and HF, intending to test this material in hydrofluorination reactions. The following section will describe the synthesis and characteristics of HF-loaded ACF using a broad range of characterization techniques, as well as its reactivity towards several substrates.

2- Synthesis and characterization

A- Synthesis

A defined amount of freshly synthesized ACF was transferred into a PTFE inliner. A second PTFE inliner was loaded with a drying agent, hexafluoronickelate (K_2NiF_6, KNF). Both inliners were connected together using Teflon wire and connections. Outside the glovebox, the HF bottle was linked to the inliner containing K_2NiF_6 (Figure **9**, connection A), followed by the inliner containing ACF (Figure **9**, connection B). The exit wire after the inliner containing ACF was attached to a suction pump (Figure **9**, connection C). For a picture of the experimental setup, see Annex **S1**. In a flow of an argon stream, HF was condensed onto the drying agent, leaving the inliner containing ACF closed (Scheme **51**, left). A deep red solution was observed, and after 30 minutes, the freshly dried HF was condensed onto a defined amount of ACF for another 30 minutes (Scheme **51**, middle). Afterward, a vacuum was applied for 15 minutes to remove the excess of HF, which has not interacted with the surface of ACF (Scheme **51**, right). The material was weighed before and after the loading with HF, leading to an increase of 8% in weight after loading. A slight color change was observed after the loading of HF, giving a brown-yellow fine powder.

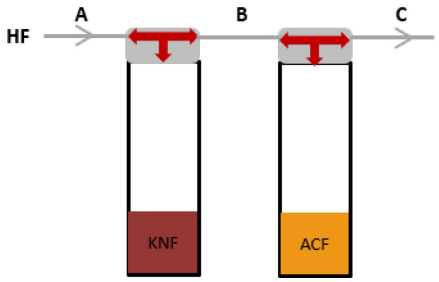

Figure 9. *Experimental setup for the HF-loading onto ACF.*

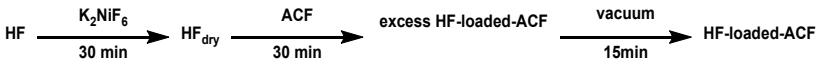

Scheme 51. *Synthesis of HF-loaded ACF.*

B- Characterization – bulk and thermal behavior

i- MAS NMR spectroscopy

a- ^{27}Al MAS NMR spectroscopy

Figure **10** displays the ^{27}Al MAS NMR spectra recorded for the pure ACF and HF-loaded ACF (batch A). Both samples exhibit a signal at δ = -16 ppm. The signal position at this chemical shift is typical for ACF containing mainly AlF_6 units and a few $AlCl_xF_{6-x}$ units.[80] Noticeably, the signal belonging to HF-loaded ACF appears more narrow compared to the one of ACF, featuring a decreased line-width of about 250 Hz, which suggests a slightly better-ordered aluminum fluoride matrix, resulting from the HF-loading.

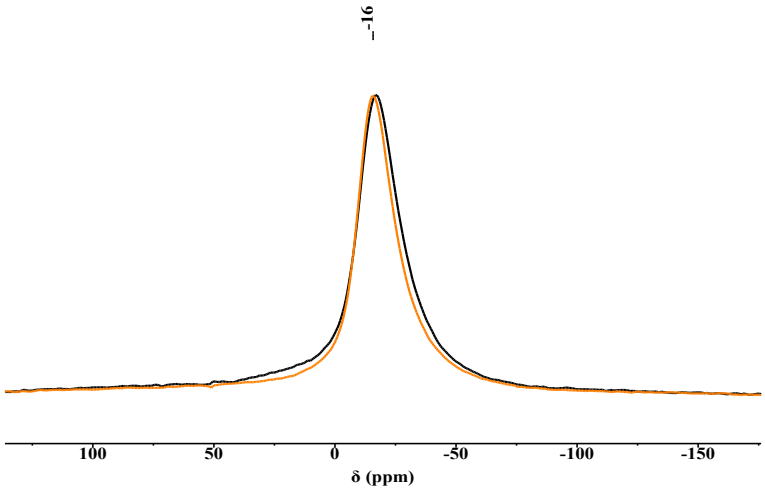

Figure 10. *^{27}Al MAS NMR spectra of ACF (black) and HF-loaded ACF (orange) taken at 27.5 kHz rotation frequency.*

b- ^{1}H MAS NMR spectroscopy

The ^{1}H MAS NMR spectrum for ACF, shown in Figure **11** (black curve, magnified by 6), reveals the presence of a few signals of relatively low intensity. The narrow signals δ = 0 ppm might correspond to "isolated OH-groups" resulting from adventitious water during the synthesis.[1] The additional signal at δ = 0.5 ppm could represent some clusters of OH-

[1] According to the synthesis, there should not be any water or air in contact with ACF; However, since glassware is used during the synthesis, it is challenging to entirely avoid the presence of water, and those signals were observed for several batches of ACF, synthesized in the same procedure.

groups. The broad signal ranging from δ = 2 ppm to δ = 9 ppm can be referred to as water, which usually appears at a signal maximum of about δ = 5 ppm. The last peak at δ = 17 ppm, is in the typical range for strongly bridged HF units.[156,323]

In the case of HF-loaded ACF, at least four signals can be distinguished (Figure **11**, orange curve). The same signal at δ = 17 ppm, as observed for ACF, is present in a considerably higher intensity, revealing the effect of the HF-loading on ACF. A second signal visible at δ = 11 ppm, which is in good agreement with values reported for $[F(HF)_n]^-$ anions, suggest the presence of such moieties at the surface of ACF.[156] Moreover, the broad signal at δ = 6 ppm includes at least two signals, due to its specific line-width and shape, and could be assigned to larger polyfluoride clusters, suggesting a possible second layer of HF.[156,323] However, despite careful handling during the sample preparation, the presence of water cannot be entirely excluded as for ACF, since the signal at δ = 6 ppm is also typical for adsorbed water molecules.[324,325] At δ = 0 ppm, an intense narrow signal is observed, which differs from the one observed on ACF. This signal is characteristic of highly mobile species and could, therefore, be attributed to physisorbed HF.

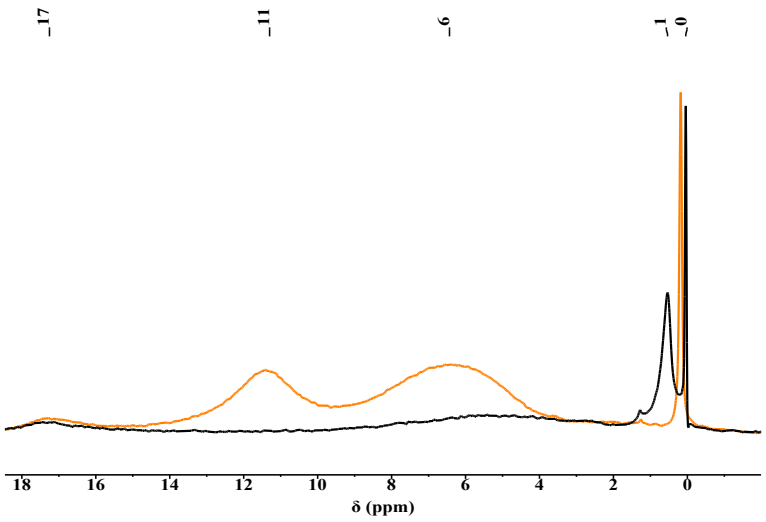

Figure 11. *^{1}H MAS NMR spectra of ACF (black, magnified by 6) and HF-loaded ACF (orange) taken at 27.5 kHz rotation frequency.*

c- ^{1}H-DQ MAS NMR spectroscopy

^{1}H-DQ MAS experiments were performed, and in the case of ACF, the absence of an off-diagonal peak reveals that all the species suggested from the ^{1}H MAS NMR spectrum of ACF are independent of each other (Figure **12**, A). The ^{1}H-DQ MAS spectrum for HF-loaded ACF, on the contrary, exhibits two off-diagonal peaks indicating correlations between the signals at δ = 6 ppm and δ = 11 ppm, which suggest a plausible presence of a second layer of HF (Figure **12**, B). Moreover, the signals at δ = 17 ppm and δ = 0 ppm do not show any cross peaks, demonstrating the isolated character of the two moieties.

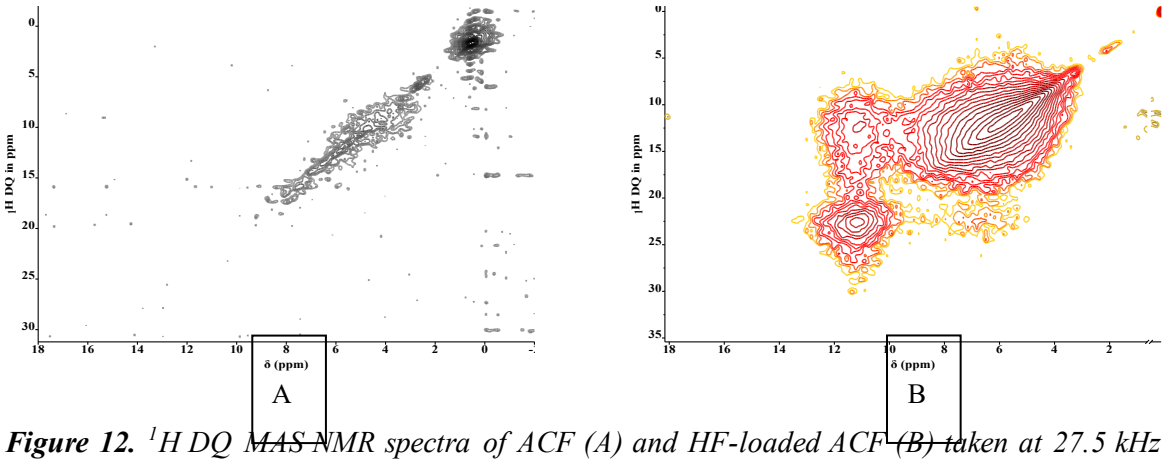

Figure 12. *^{1}H DQ MAS NMR spectra of ACF (A) and HF-loaded ACF (B) taken at 27.5 kHz rotation frequency.*

d- ^{19}F MAS NMR spectroscopy

^{19}F MAS NMR spectra of ACF and HF-loaded ACF are depicted in Figure **13**. For both samples, a broad asymmetric signal can be seen, caused by the Al-fluoride network present in the bulk of ACF.[80,324] A diminished line-width of about 3 kHz and an upfield shift of the maximum of the peak of about 2 ppm is detected for the sample loaded with HF (δ = -167 ppm) compared to the signal of ACF (δ = -165 ppm), which suggest a slight reorganization of the bulk as observed in the ^{27}Al MAS NMR spectra. Additionally, the signal for HF-loaded ACF is shifted towards the chemical shift observed for crystalline phases of AlF_3, such as for α-AlF_3 or β-AlF_3, appearing at δ = -172 ppm.[324] On the other hand, according to literature reports on liquid-state NMR of polyfluoride ions, all the fluoride signals corresponding to $[F(HF)_n]^-$ moieties are expected to be in the same range

as the signal for the fluorides in the bulk of ACF, which hinder their identification.[156,323] An additional narrow signal is observed in the spectrum of HF-loaded ACF at δ = -135 ppm, which could correspond to physisorbed HF, and therefore could be associated with the signal in the ^{1}H NMR spectrum at δ = 0 ppm.

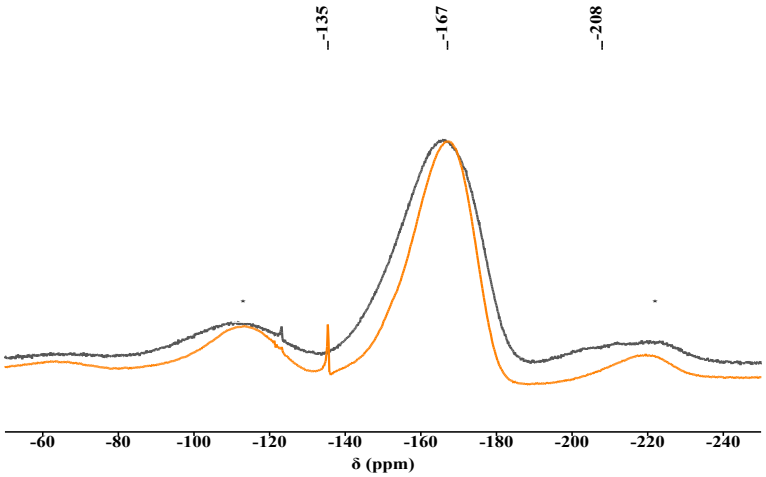

Figure 13. *^{19}F MAS NMR spectra of ACF (black) and HF-loaded ACF (orange) taken at 27.5 kHz rotation frequency. Asterisks refer to spinning bands.*

Additionally, ^{19}F MAS NMR spin echo spectra were recorded for both samples (Figure **14**). It is known that on ACF, the signal at δ = -208 ppm is attributed to terminal fluorine atoms bound at aluminum.[80] This resonance was not observed for a sample loaded with HF, as it can be seen in Figure **14**, suggesting that those terminal fluorine atoms are not present anymore.

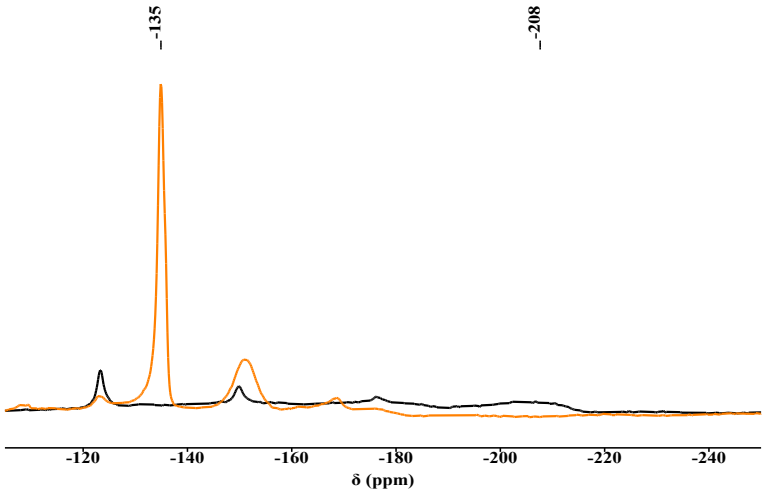

Figure 14. *^{19}F rotor synchronized spin-echo MAS NMR spectra of ACF (black) and HF-loaded ACF (orange) taken at 27.5 kHz rotation frequency.*

e- Additional 2D MAS NMR spectroscopy

A ^{1}H-^{19}F MAS NMR rotor-synchronized correlation experiment was carried out and evidenced for ACF a correlation of all the protons with the Al-fluoride network (Figure **15**, A). However, since the signal representing the Al-fluoride network is significantly broad, it is difficult to distinguish which kind of HF interaction with the surface of ACF is present. The same situation applies to the HF-loaded ACF sample (Figure **15**, B). All the proton signals exhibit cross-peaks with the fluoride signal at δ = -167, which, as mentioned before, covers all the fluoride signals of polyfluoride anions $[F(HF)_n]^-$. No correlation between the signal at δ = 0 ppm in the ^{1}H MAS NMR spectrum and the one at δ = -135 ppm in the ^{19}F MAS NMR spectrum could be observed, probably due to the high mobility of the physisorbed HF.

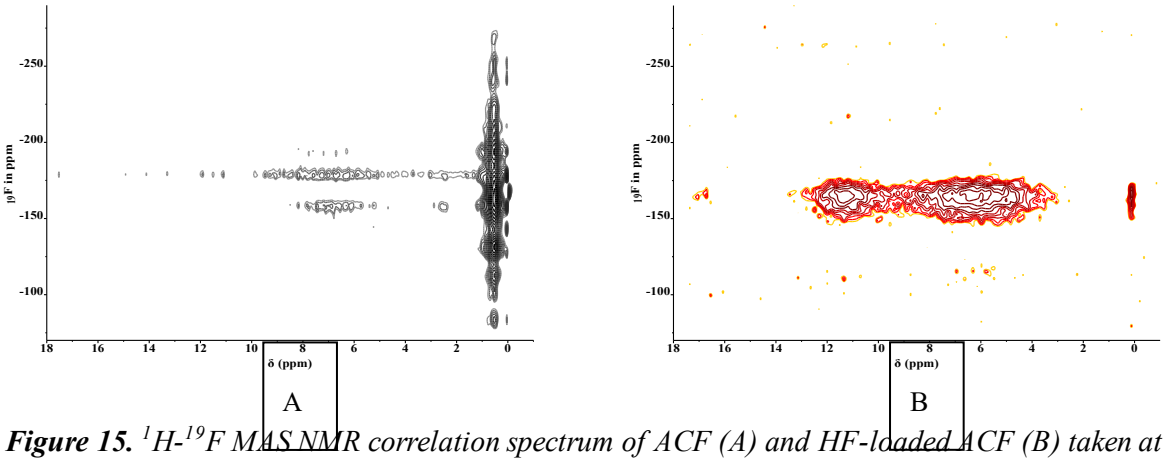

Figure 15. *^{1}H-^{19}F MAS NMR correlation spectrum of ACF (A) and HF-loaded ACF (B) taken at 27.5 kHz rotation frequency.*

Additionally, a ^{19}F-^{35}Cl TRAPDOR MAS NMR experiment was conducted to investigate the presence of chlorine atoms in both samples (Figure **16**). Applying the same experimental conditions for both samples, this experiment shows for ACF and the loaded sample with HF nearly the same peak, which suggests that the chlorine content remains unchanged after loading with HF. Notably, it is the first time that this experiment was used to evidence the presence of chlorine atoms in ACF.

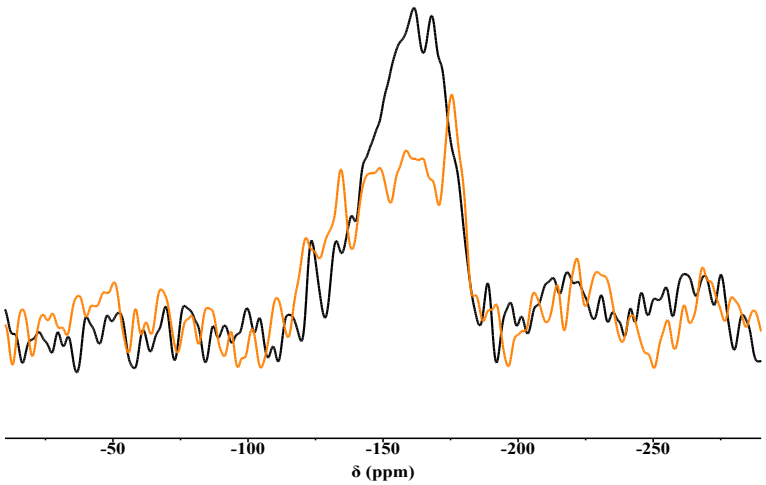

Figure 16. *^{19}F-^{35}Cl TRAPDOR MAS NMR spectra of ACF (black) and HF-loaded ACF (orange) taken at 27.5 kHz rotation frequency.*

f- Comparison between batch A and B

The second batch of HF-loaded ACF (batch B), synthesized with significantly less HF, was studied using MAS NMR spectroscopy to determine the influence of the amount of the HF loading on ACF during the synthesis. In the ^{27}Al MAS NMR spectrum, representing both batches, no distinct change could be observed (Figure **17**).

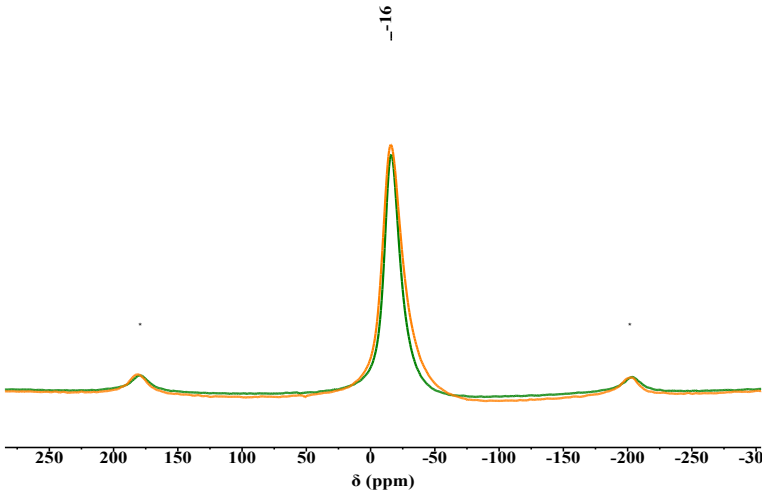

Figure 17. *^{27}Al MAS NMR spectra of batch A (orange) and batch B (green) of HF-loaded ACF taken at 20 kHz rotation frequency. Asterisks refer to spinning bands.*

For the ^{1}H MAS NMR spectrum, however, significant alterations were observed (Figure **18**). Indeed, the signal at δ = 0 ppm is considerably reduced for batch B, which supports the assignment of this signal to physisorbed HF, since less HF was loaded during the synthesis. In batch B, most of the HF will bound to terminal fluorine atom or Lewis acidic centers, and fewer HF will, therefore, be physisorbed. The three other signals at δ = 17 ppm, δ = 11 ppm, and δ = 6 ppm are very similar for both batches. However, the signal at δ = 6 ppm has a decreased intensity for batch B, indicating a less pronounced second layer when less HF was used during the synthesis.

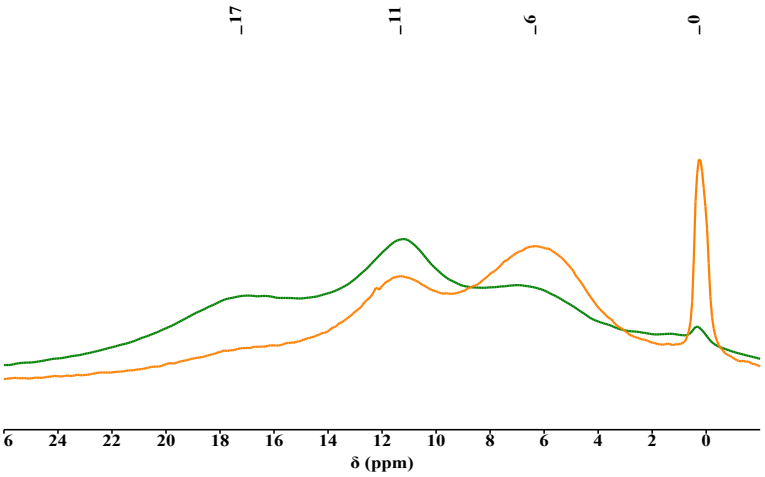

Figure 18. *^{1}H MAS NMR spectra of batch A (orange) and batch B (green) of HF-loaded ACF taken at 20 kHz rotation frequency.*

In the ^{19}F MAS NMR spectrum, for batch B, the signal at δ = -135 ppm is as well significantly reduced, in the same way as the one at δ = 0 ppm in the ^{1}H MAS NMR spectrum, which is again compatible with the presence of physisorbed HF attributed to those chemical shifts (Figure **19**). Besides, the signal at δ = -167 ppm is as well affected and exhibits a reduced intensity and line width for batch B, which reveals a lower coverage by the $[F(HF)_n]^-$ moieties compared to batch A.

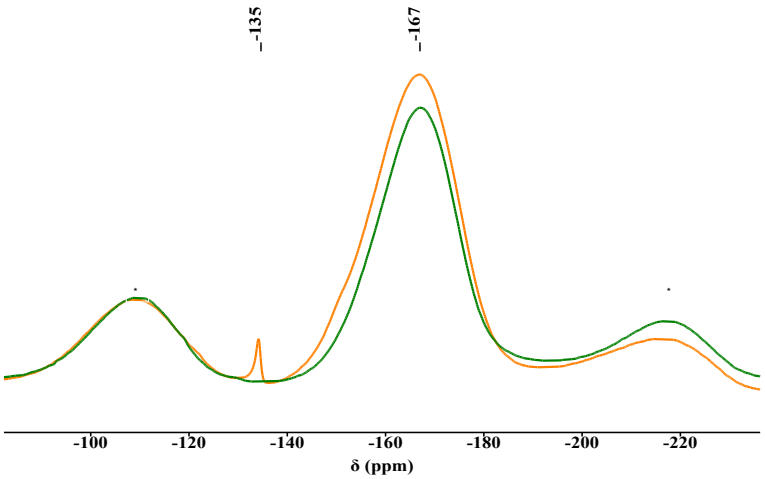

Figure 19. *^{19}F MAS NMR spectra of batch A (orange) and batch B (green) of HF-loaded ACF taken at 20 kHz rotation frequency.*

g- Study of the influence of post-vacuum treated HF-loaded ACF using MAS NMR spectroscopy.

When HF-loaded ACF (batch A) was put under vacuum for different times (30 minutes, 2 hours, and 24 hours), a decreased in the intensity of the peak at δ = 0 ppm in the ^{1}H MAS NMR spectrum was observed, supporting once more the presence of the highly physisorbed character of the HF assigned to this resonance (Figure **20**). However, an increase of the signal at δ = 6 ppm was detected, which could be due to contamination with water of the sample during the vacuum process. In the ^{19}F MAS NMR spectra, both signals at δ = -135 ppm and δ = -167 ppm decreased when increasing the vacuum time, which indicates a removal of both the physisorbed and chemisorbed HF from the polyfluoride network, superimposed by the signals from the Al-fluoride network of ACF (Figure **21**). No change could be detected in the ^{27}Al MAS NMR spectra (see Annex **S2**)

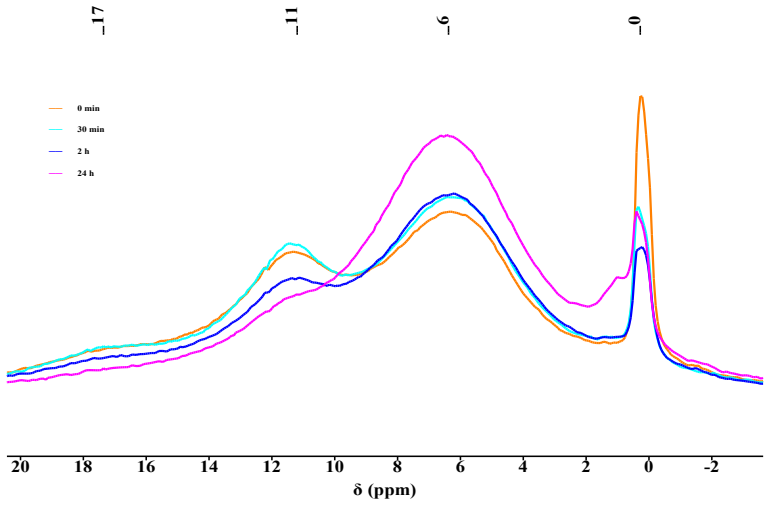

Figure 20. *^{1}H MAS NMR spectra and the influence of the vacuum time applied to HF-loaded ACF for 30 minutes (turquoise), 2 hours (blue), and 24 hours (pink) compared to the initial sample (orange) taken at 20 kHz rotation frequency.*

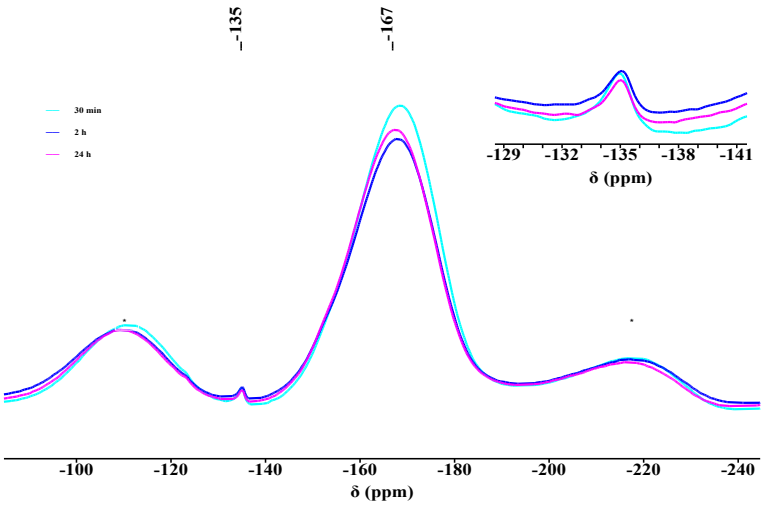

Figure 21. *^{19}F MAS NMR spectra and the influence of the vacuum time applied to HF-loaded-ACF for 30 minutes (turquoise), 2 hours (blue), and 24 hours (pink) taken at 20 kHz rotation frequency. Asterisks refer to spinning bands.*

The same trend, namely the observation of reduced signals, was observed when a thermal treatment of HF-loaded ACF at 100 °C for 24h was applied instead of vacuum treatment (see Annex **S2** and **S3**).

ii- Fourier Transform Infrared Spectroscopy and Inelastic Neutron Scattering

FTIR spectra were measured for ACF and HF-loaded ACF (batch A and B). Due to the amorphous character of ACF, no distinct bands could be detected for pure ACF, as it was described in a previous study.[80,81] For the HF-loaded ACF samples, the FTIR spectra are identical for both A and B batches; therefore, only one spectrum will be depicted (batch B). Four broad bands with maxima at 1665 cm^{-1}, 1180 cm^{-1}, 1050 cm^{-1}, and 590 cm^{-1} are visible (Figure **22**). When compared to the literature, those bands are compatible with data for $[F(HF)_n]^-$ anions in p-toluidinium hydrogen difluoride.[326] Indeed, stretching vibrations of $[F(HF)_n]^-$ anions can be associated with the band at 1665 cm^{-1}, and the bending modes of those anions are related to the bands at 1180 cm^{-1} and 1050 cm^{-1}. The band at 590 cm^{-1} corresponds to an F-Al-F vibrational mode.[327] Moreover, those values are in good agreement with a DFT study on the adsorption of HF at a β-AlF_3 surface, already mentioned

above (Table **21**).[322] They revealed in the study that depending on the binding mode of the HF at the respective under-coordinated Al centers, different frequency vibrational modes of FHF^- moieties can be found. On a T1 termination, representing under-coordinated Al moieties at a 100 surface, with a half monolayer coverage of adsorbed HF, the stretching frequency of the formed FHF^- moieties, would appear at 1654 cm^{-1}.[322] Similarly, the values for the vibrational bending mode of adsorbed HF from the study resemble the one obtained experimentaly using FTIR spectroscopy for the HF-loaded ACF samples.

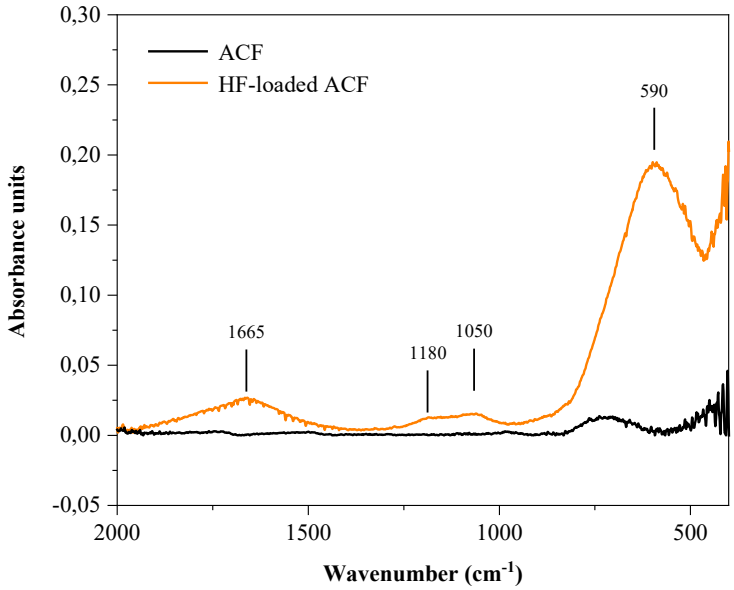

Figure 22. *FTIR spectra of ACF (black), HF-loaded ACF (orange) collected using an ATR-unit (diamond).*

Further investigations on the vibrational spectra of HF-loaded ACF were conducted by measuring inelastic neutron scattering (INS) for both pure ACF and HF-loaded ACF of batch B (Figure **23**). The experiments were performed in collaboration with the Federal Institute of Materials Research and Testing (Dr. Emmerling, Dr. Michalchuk; BAM, Berlin) and the ISIS Neutron and Muon Source (Dr. Rudić; Oxfordshire, UK). The samples were sent to the ISIS center and measured by Dr. Rudić. Owing to the large incoherent scattering cross-section of hydrogen atoms, compared to aluminum, chlorine, and fluorine atoms, hydrogen-containing vibrational modes are dominating the INS signal of the HF-loaded ACF sample. Moreover, no INS features for the pure ACF sample could be

observed, confirming the effect of the HF-loading on ACF. Six vibrational bands were detected in the INS spectrum of the HF-loaded ACF sample, summarized in Table **21**. Those vibrational frequencies are consistent with the frequencies observed by FTIR spectroscopy; however, a blue shift is noticed, which is in contradiction with the expected red-shifted vibrational frequencies for stronger H···F hydrogen bonding interactions at low temperature, upon HF cooling.[328] Nevertheless, this blue shift may originate from the chain length (n) or from the geometry of the $[F(HF)_n]^-$ clusters, which can vary with the temperature. Moreover, the $(HF)_n$ vibrational frequencies were demonstrated to vary semi-continuously with the chain length by ab initio calculation studies, and further calculations suggested that cluster geometries can also influence the vibrational frequencies significantly.[329]

The additional vibrational band at 1344 cm^{-1} observed exclusively in the INS spectrum can be related to the vibrational vertical bending mode of adsorbed HF at the surface, which was also identified by Harrison in the study on HF adsorbed on β-AlF_3 surfaces (Table **21**).[322] The band detected in the INS spectrum at 2292 cm^{-1} is compatible with combination bands observed by IR spectroscopy previously reported.[330,331]

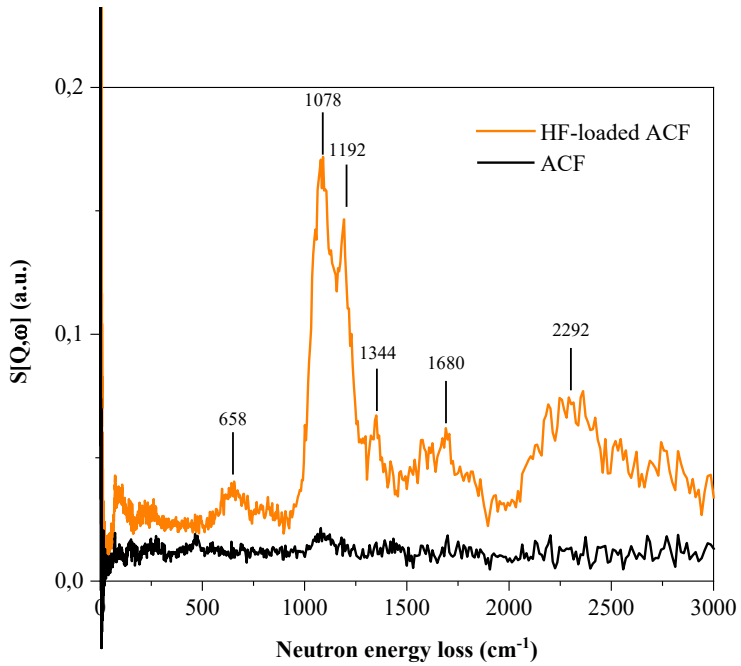

Figure 23. *INS spectra of ACF (black) and HF-loaded ACF (orange). The low frequency coherent inelastic scattering from the Al sample holder has been substracted for both samples.*

Due to the high potential for contamination with water at ACF surfaces, the INS spectra of ACF and HF-loaded ACF was compared with that of ice I_h (see Annex **S4**). In pure ACF, the absence of INS features in the spectrum strongly supports the absence of water in this sample. For the HF-loaded ACF sample, similarities can be observed between the INS spectrum of ice and the one of HF-loaded ACF. However, those similarities do not result from the presence of water after a deep analysis of the relative scattering intensities.

Table 21. *Vibrational frequencies of various FHF^- moieties:*[322]

	Stretch. [cm^{-1}]	Vert. bend. [cm^{-1}]	Horiz. Bend. [cm^{-1}]	Additional bands [cm^{-1}]
DFT T1*	1654	1347	1151	
DFT T6*	2694	1191	945	
FTIR HF-ACF	1665	1180	1050	590
INS HF-ACF	1680	1192 and 1344	1078	658 and 2292

* (100) termination, half monolayer coverage; T1: unit cell containing 26 Al ions; T6: unit cell containing 28 Al ions.

The influence of heat treatments applied after the synthesis of HF-loaded ACF was as well studied using FTIR spectroscopy. Samples from batch A were therefore heated at 200 °C or 400 °C for 4 hours. The sample heated at 200 °C exhibits the same four signals observed for the sample, which did not undergo thermal treatment (Figure **24**, red curve). Noticeably, the same wavenumbers are detected; however, the signals appear more narrow, suggesting desorption of HF by heating the sample, as it was observed in the MAS NMR study (see Annex **S3**). The sample heated at 400 °C showed the typical stretching and bending vibrational modes of F-Al-F moieties at 596 cm^{-1} and 650 cm^{-1}, respectively, of the β-AlF_3 phase, which suggests a phase transition of the sample when heated above 400 °C (Figure **24**, purple curve). Thus, a thermal analysis of HF-loaded ACF will be detailed in the next section to investigate further its thermal behavior.

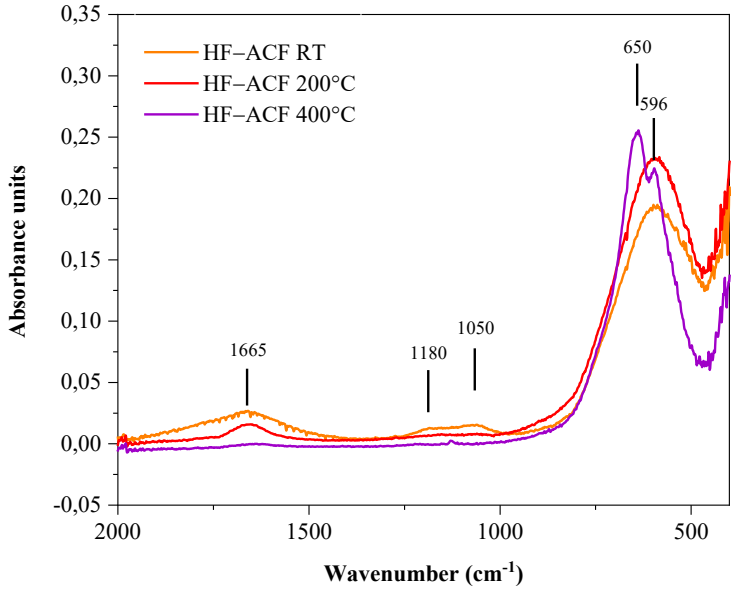

Figure 24. *FTIR spectra of HF-loaded ACF (orange), HF-loaded ACF heated at 200 °C (red), and HF-loaded ACF heated at 400 °C (purple).*

Additionally, Diffuse Reflectance Infrared Fourier Transform Spectroscopy was also used to measure the HF-loaded ACF sample. The same bands as obtained by FTIR spectroscopy and INS were obtained (see Annex **S5**).

iii- Thermoanalysis and X-ray diffraction

a- Thermoanalysis

Previous studies reported the thermal behavior of ACF.[80,81] It was established using differential thermal analysis (DTA), that around 400 °C ACF is decomposing into gaseous $AlCl_3$ and crystalline phases of AlF_3. Thermoanalysis of both batches A and B of HF-loaded ACF were carried out using thermogravimetry (TG), and DTA followed by MS (Figure **25**). No difference between the two batches A and B could be detected; thus, no mention of the batch will be made for the upcoming analysis of the results. The DTA of HF-loaded ACF shows a continuous exothermic phase transition between 50 °C and 500 °C (Figure **25**, red curve). The absence of a clear exothermic effect, as it is usually observed for ACF above 400 °C, suggests a continuous fluorination of the bulk by the HF released upon

heating of the material, as also indicated by mass spectrometry (Figure **25**, pink curve). Indeed, a broad desorption range for the HF is visible, which strongly resembles the one reported for HF-loaded *HS*-AlF_3.[75] They both display a maximum of desorption at around 200 °C, which continues up to 500 °C. As an alternative explanation, it is also known that covered surfaces with adsorbed species usually exhibit a larger slop in the DTA curve, compared to uncovered surfaces, resulting in a DTA curve extended to a wider temperature range. The thermogravimetry curve shows two mass losses around 200 °C and 400 °C, corresponding to the release of HF and some water, as shown in the mass spectrometry curves, as well as a slow fluorination and crystallization process (Figure **25**, green curve). The presence of water in the sample, whose desorption could be followed by mass spectroscopy, can arise from the sample preparation since the material has to be under air for about 30 seconds (Figure **25**, blue curve). The same situation was observed in the pure ACF (see Annex **S6**). Moreover, a total mass loss of about 17% after the thermal treatment from room temperature to 500 °C was detected, whereas, for the pure ACF, a mass loss of 9% was observed under the same conditions. Noticeably, this 9% mass loss was as well observed when *HS*-AlF_3 was heated in similar conditions.[75] Therefore, a maximum of 8% of the mass loss observed for HF-loaded ACF can be attributed to the release of HF, since 9% should arise from ACF itself.

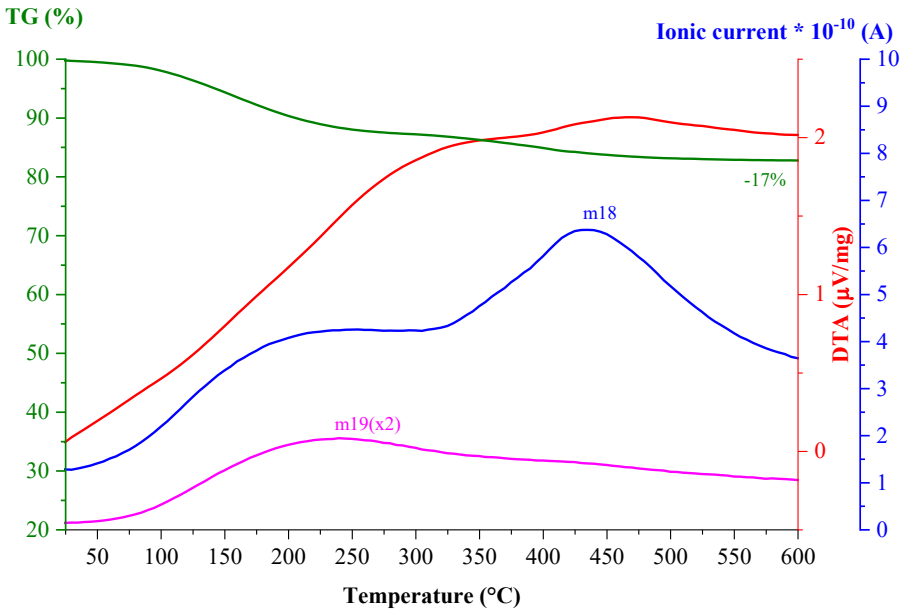

Figure 25. *TG-DTA-MS curves for HF-loaded ACF. m19 represents the mass loss of HF, and m18 represents the mass loss of water.*

b- Powder X-ray diffraction

Powder XRD data were recorded for ACF, both batches A and B of HF-loaded ACF and HF-loaded ACF (batch A), which was thermally treated at 200 °C or 400 °C for 4 hours (Figure **26**). Since ACF is an amorphous compound, no reflections could be detected. In the case of HF-loaded ACF, for both batches, no differences were observed; therefore, only one diffractogram will be displayed and discussed (Figure **26**, orange curve). The amorphicity is retained in HF-loaded ACF; however, a slight increase of the crystallinity could be observed. This result is consistent with the observation from the solid state MAS NMR, confirming a slight reorganization of the bulk towards a better-ordered aluminum fluoride after HF-loading (see above).

The sample treated at 200 °C for 4 hours did not exhibit any modification in the XRD pattern (Figure **26**, red curve). However, the sample heated at 400 °C for 4 hours showed a crystalline diffractogram, with the reflections corresponding to the β-AlF_3 phase (Figure **26**, blue and grey curves).[7,324] This observation is consistent with the results from the FTIR experiment of the same sample heated at 400 °C, which showed the vibrational frequencies of the β-AlF_3 phase (see above, Figure **24**). Additionally, samples from batch A, which have been put under vacuum for different times, did not show any crystallinity neither.

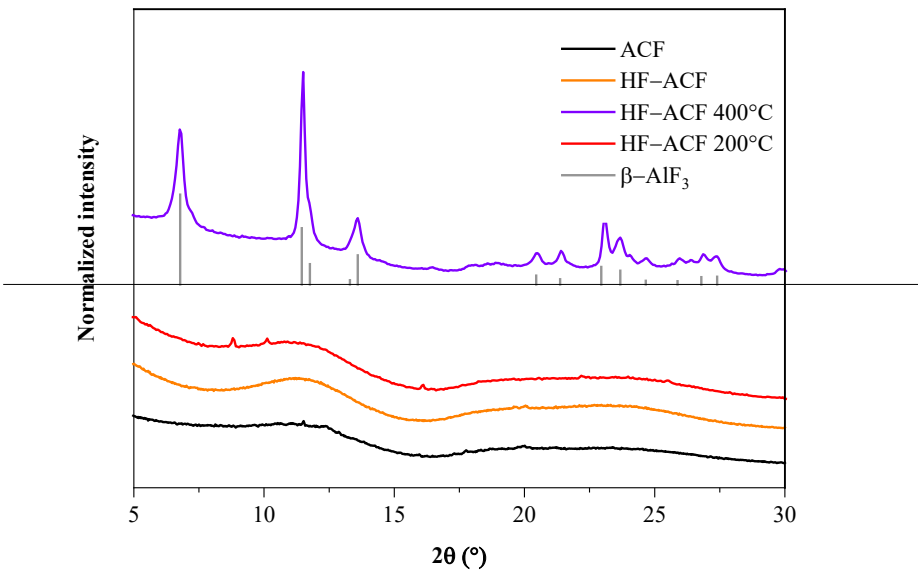

Figure 26. *Powder XRD patterns of ACF (black), HF-loaded ACF (orange), HF-loaded ACF heated at 400 °C (purple), and β-AlF_3 (grey).*

The temperature dependant phase transition in ACF was studied before.[80,81] It was shown that at 400 °C, the η–AlF_3 phase was observed when the samples were sealed in a quartz ampulla, then at 500 °C, the reflections of θ–AlF_3 were detected, and finally, at 600 °C, the β-AlF_3 phase was obtained.[80] From the results revealed by the thermoanalysis of HF-loaded ACF, it is likely that when heating HF-loaded ACF, the HF is immediately released and can further fluorinate the bulk, resulting in a faster release of HCl than it might occur on ACF; therefore, the β-AlF_3 phase could be observed at a lower temperature than for ACF (see above).

Since in the thermal analysis of HF-loaded, it was not possible to study the release of HCl with time and temperature, in situ gas phase FTIR spectra of HF-loaded ACF (batch B) and ACF were recorded while heating up to 450 °C (Figure **27**). This experiment was performed in collaboration with the group of Prof. Dr. Riedel with the help of the Ph.D. student Kurt Hoffmann at the Freie Universität Berlin. The spectrum obtained for ACF was consistent with previously reported results by Krahl *et al.* (see Annex **S7**).[80,332] The spectra for the HF-loaded ACF sample show a peak in the region of HCl; however, its shape differs slightly from the typical HCl signal, maybe due to the formation of cluster upon HF release. Noticeably, the SiF_4 signal is considerably intense compared to the other peaks, which indicate a reaction of the released HF with the glass of the experimental device. Besides, additional signals could be observed at 1190 cm^{-1}, 1102 cm^{-1}, 947 cm^{-1}, and 911 cm^{-1}, which are not visible on pure ACF, and might relate to CCl_xF_y (x=4-y, y=1,2 or 3) species (see Annex **S7**).

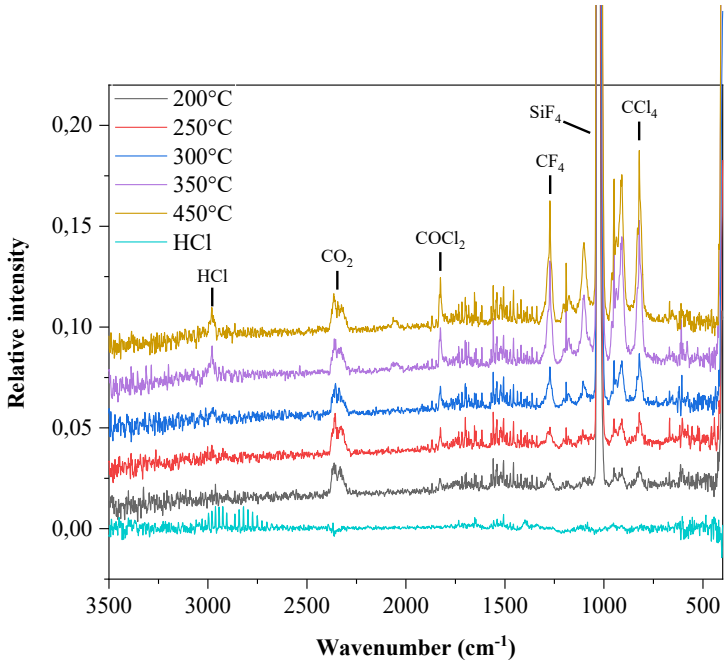

Figure 27. *In situ gas phase FTIR of HF-loaded ACF (batch B) taken at 200 °C (black), 250 °C (red), 300 °C (blue), 350 °C (purple), 450 °C (gold) compared to the HCl spectrum (turquoise).*

iv- Short summary

All those characterization methods evidenced the successful immobilization of HF at the surface of ACF, by forming polyfluorides moieties. Indeed, the IR studies show consistency with previously reported vibrational values for polyfluoride interacting with an AlF_3 surface.[322] Moreover, the loading of ACF with HF leads to a slightly better-ordered bulk, as established by the MAS NMR spectroscopy and X-ray diffraction. It was also shown that heating of the material causes the desorption of HF, which slowly fluorinate further the bulk. Up to 400 °C, the material stays amorphous and vibrational modes of polyfluorides moieties are still visible; however, when the sample is thermally treated over 400 °C, complete crystallization of the material occurs, generating the β-AlF_3 phase. Additionally, the fluorination might already occur at room temperature during the immobilization of HF a the surface of ACF, inducing a slight crystallization and, thus, a better-ordered bulk than on ACF.[333]

C- Characterization – surface studies

i- Surface area determination and pore size analysis

Investigating the porosity in microporous materials can be challenging. The Brunauer-Emmet-Teller (BET) method is the most widely spread characterization technique used to determine the surface area of a solid and derived from the gas adsorption isotherms at the boiling point of a gas (usually N_2).[334] Thus, nitrogen sorption studies were completed for ACF, and both batches of HF-loaded ACF (Figure **28**). Again, no differences could be distinguished between the batches A and B of Hf-loaded ACF; thus, only one will be displayed and discussed (batch B). The experiments were conducted without a preliminary degassing process to exclude an initial removal of the HF at the surface before the actual measurement. Indeed, it was concluded from the bulk study that when a vacuum or a thermal treatment was applied to HF-loaded ACF, some HF was released from the surface (see above). Initial degassing processes are usually performed for cleaning the surfaces of solids that can adsorb moisture; however, since the samples are kept in closed inliners in a glovebox, no pre-treatment should be necessary.

For ACF, both experiments with and without degassing were performed and gave the same results, confirming the unnecessariness for preliminary degassing of such surface; however, for better clarity, the results without degassing only will be shown (Figure **28**, black curve). According to the BET model, a type I isotherm was obtained, indicating a microporosity. Moreover, relatively fast adsorption until 0.1 in relative pressure, reaching 70 cm^3g^{-1} of adsorbed N_2, was observed, followed by a slower adsorption slope reaching a maximum value of 99 cm^3g^{-1} adsorbed N_2. The surface area for this batch of ACF reached 215 m^2g^{-1}, which is consistent with previously reported values (Table **22**).[73,80]

For the HF-loaded ACF sample, the shape and by consequent the type of isotherm is comparable to the one obtained for ACF, indicating retention of the microporosity (Figure **28**, orange curve). However, differences can be observed in the absorption values, since a maximum of only 30.5 cm^3g^{-1} of adsorbed N_2 was detected for the HF-loaded ACF sample. Moreover, the calculated surface area reached only 44 m^2g^{-1}, which is almost five times less than the surface area of ACF (Table **22**). This observation is consistent with the diminished surface area observed in the case of the HF-loaded aluminum alkoxide fluoride,

where a value of 100 m^2g^{-1} was detected, compared to the value obtained for *HS*-AlF_3 synthesized according to the conventional sol-gel route (200 m^2g^{-1}).[75]

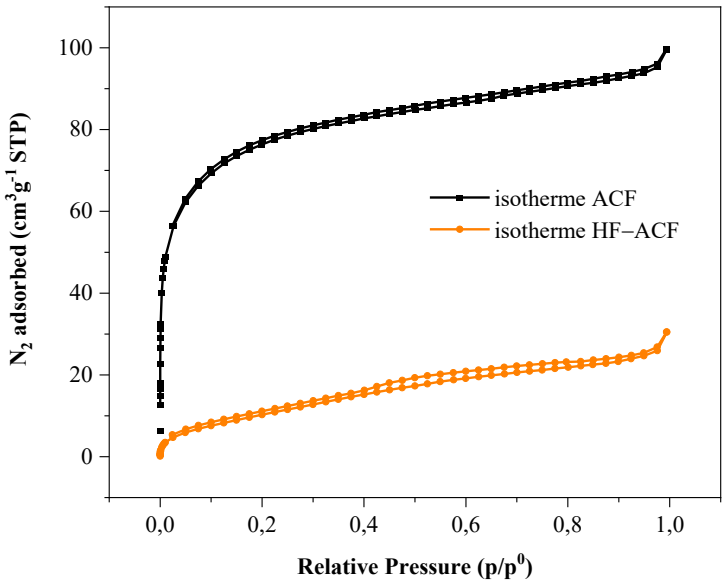

Figure 28. *N_2 sorption isotherms of ACF (black) and HF-loaded ACF (orange).*

The pore size analysis of microporous materials can be calculated based on the non local density functional theory (NLDFT). This method is based on molecular modeling, in contrast with the BJH-method, which is based on the Kelvin equation and is thus not applicable for microporous materials.[335–337] Using NLDFT, a more accurate microscopic model of adsorption, as well as a better description of the thermodynamic properties of the pore fluid, can be obtained. Therefore, the pore size analysis was re-examined using the NLDFT model for ACF. In contrast to previously reported values using the BJH model, where pores between 15 and 50 Å were detected, using the NLDFT model, two kinds of micropores could be identified on ACF, with a diameter of about 12 Å and 20 Å (Figure **29**, black curve; Table **22**).[73] When the same conditions were applied to the sample loaded with HF, one type of pores with a diameter range between 14 and 17 Å was detected (Figure **29**, orange curve; Table **22**). The disappearance of the smaller pores present on ACF (12 Å) on HF-loaded ACF suggests a complete filling of those pores by the HF moieties. In contrast, a partial filling of the larger pore on ACF (20 Å) might result in the generation of

those middle-range pores on HF-loaded ACF (14-17 Å). Additionally, X-ray data on polyfluoride anions in KHF_2 reported an F-H-F distance of about 2.277 ± 0.006 Å, whereas larger anions such as $H_4F_5^-$ were assigned an F-H-F distance of approximately 2.453 ± 0.002 Å. Those anions could, therefore, enter the pores on ACF, resulting in a reduced microporosity.

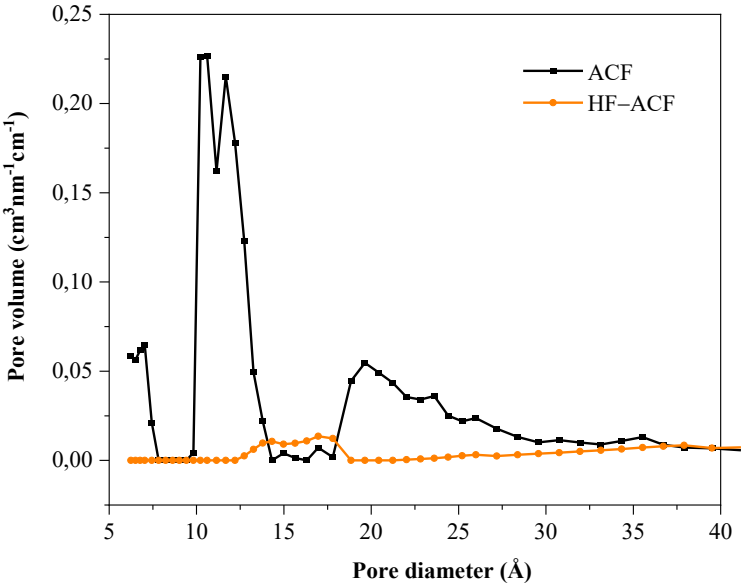

Figure 29. *Pore size analysis using non local density functional theory of ACF (black) and HF-loaded ACF (orange).*

Table 22. *Surface area and pore size distribution of ACF and HF-loaded ACF:*

Material	Surface area by BET [m^2/g]	Pore size [Å]	Pore volume [cm^3/g]
ACF	215	12 & 20	0.022 & 0.05
HF–ACF	44	14-17	0.01

Additionally, energy dispersive X-ray spectroscopy (EDX) and transmission electronic microscopy (TEM) were performed for both ACF and HF-loaded ACF (batch B) (see Annex **S8** and **T1**). By comparing the two samples, a slight change in the texture was detected, which is in good agreement with the changes in the size of the pores observed

above by NLDFT. Indeed, the rugosity on HF-loaded ACF is more pronounced than on ACF, according to the TEM images (see Annex **S8**). Both samples are polydisperse, with particles in the range of micrometers. The EDX results suggest a higher amount of fluorine on HF-loaded ACF than on ACF, with a small decrease in the chlorine and aluminum contents (see Annex **T1**).

ii- Ammonia Temperature Programmed Desorption (NH_3-TPD)

The strength of the Lewis acidic sites was intensively studied for ACF.[73,80,81] Previous reports have evidenced the presence in majority of very strong Lewis acid sites with the use of ammonia TPD.[73] When the batch A of HF-loaded ACF was tested, a clear desorption curve could be observed, having a similar shape, like the one obtained for ACF; however, it shifted to lower temperatures (Figure **30**, orange curve). This finding indicates that the acidity of the surface is retained and that enough acidic sites are present for the ammonia to adsorb onto it. However, when the second batch (B) was tested in identical conditions, despite multiple attempts, almost no desorption of ammonia could be detected (Figure **30**, green curve). One explanation for this phenomenon could be that all the acidic sites are covered by the HF, preventing any possible adsorption of the ammonia. Alternatively, the ammonia can also bind to the HF, which is at the surface of the catalyst, forming ammonium fluoride, which could not be detected by IR spectroscopy. The contrasting results obtained for both batches of HF-loaded ACF could arise from the different HF networks present at the surface of the catalyst in the two batches. In batch A, the HF might have a more physisorbed character since a large excess of HF was used during the synthesis. This would result in easier desorption of the HF when the material is pre-heated before the TPD measurement, leaving the free acidic site for the ammonia to adsorb. On the contrary, for batch B, less HF was used during the synthesis, resulting in a stronger bonding of the HF with the surface, possibly more challenging to remove by pre-heating the sample. Since this measurement was not entirely conclusive, more experiments would need to be performed to clarify the contrasting results. Thus, in an attempt to obtain more information, other probe molecules were adsorbed onto the surface of the samples, such as deuterated acetonitrile and pyridine, followed by a diffuse reflectance infrared Fourier transform spectroscopy (DRIFTS). This will be discussed in the next section.

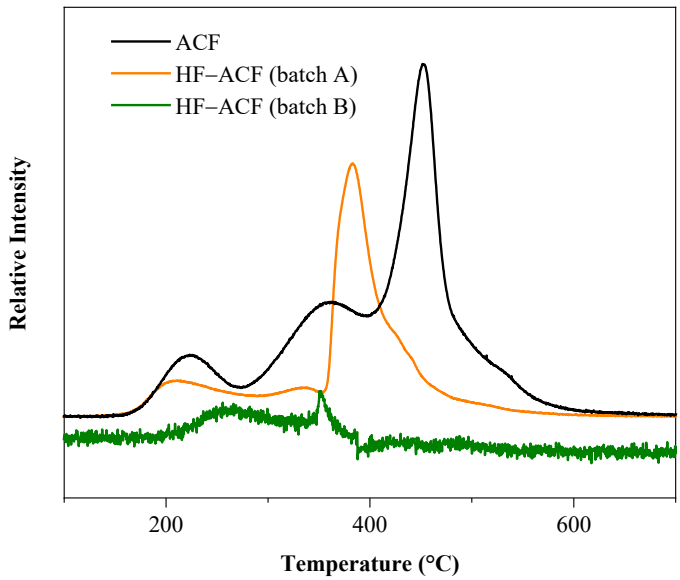

Figure 30. *NH_3-TPD of ACF (black), HF-loaded ACF batch A (orange), and HF-loaded ACF batch B (green).*

iii- Adsorption of probe molecules followed by DRIFTS

a- Deuterated-acetonitrile

Both ACF and HF-loaded ACF (batch A and B) were tested in the adsorption of deuterated acetonitrile, followed by DRIFTS. Acetonitrile is an interesting probe molecule since the lone pair of electron of the nitrogen atom can interact via σ-charge release with any surface having a Lewis acidic nature. Thus, the strength of the interaction between CD_3CN and the acidic sites can be detected by infrared spectroscopy by observing the vibration mode of the C≡N group. The more the band corresponding to the C≡N vibration is blue shifted, the more the CD_3CN is strongly binding with the surface, which is an indicator of the strength of the acidic sites. In a recent study, shifts of about 69 cm^{-1} and 95 cm^{-1} were detected for ACF compared to the free nitrile using photoacoustic spectroscopy of adsorbed deuterated acetonitrile on ACF.[73]

For an accurate comparison, adsorbed deuterated acetonitrile at ACF was also followed by DRIFTS (Figure **31**, black curve). Two bands were detected at about 2333 cm^{-1} and 2275 cm^{-1}, revealing a similar shift as obtained using photoacoustic spectroscopy (Table **23**). For

HF-loaded ACF, prepared in the same conditions, the same signals were observed, at virtually the same shift as for pure ACF, indicating a maintaining of the strong Lewis acidic sites, characteristic of ACF (Figure **31**, orange curve; Table **23**). However, the intensity of the bands is significantly reduced compared to ACF, which suggests that most of the sites are blocked by the HF, and only a few Lewis sites of the same strength as on ACF remain. No differences were observed for the two batches of HF-loaded ACF.

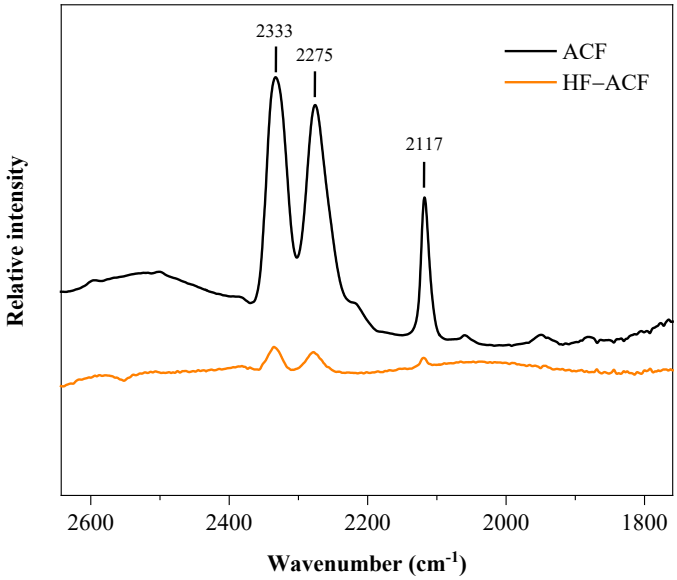

Figure 31. *DRIFTS spectra of adsorbed deuterated acetonitrile on ACF (black) and HF-loaded ACF (orange).*

Table 23. *Wavenumber of the CN vibration of CD_3CN for ACF and HF-loaded ACF:*

Material	CD_3CN (cm^{-1})	Δν
ACF	2333	65
HF-ACF	2335	67
Free $CD_3CN_{(g)}$	2268	/

*Δν represents the frequency shift observed upon adsorption of CD_3CN on the material

b- Pyridine

In order to detect the presence of possible Brønsted acid sites, pyridine was adsorbed onto ACF and HF-loaded ACF (batch A and B) followed by DRIFTS similarly as for deuterated acetonitrile (Figure **32**). For ACF, surprisingly, both bands representing the chemisorption of the pyridine on Brønsted and Lewis acidic sites were detected. The Brønsted character can be due to the remaining water present on the pyridine, which immediately reacts with the acidic sites and leads to the formation of Brønsted sites. In a previous study focusing on the surface characterization of ACF and *HS*-AlF_3, it was also shown using labeled pyridine that Brønsted acid sites are present on both catalysts.[73]

In the case of the sample loaded with HF, the band representative of the pyridine chemisorbed on Lewis acid sites at 1450 cm^{-1} was not detected, whereas a small band corresponding to the Brønsted acidic sites at 1540 cm^{-1} could be observed, together with the band at 1490 cm^{-1} representative for both types of acidic sites. Both batches exhibited the same results; hence only one will be discussed. The sample was put under a pyridine atmosphere for forty-five minutes without detecting an increase of the bands. Since the surface is already covered by the HF interacting with the aluminum centers, the pyridine likely has no remaining sites to coordinate and would, therefore, explain the low intensity of the signals. This result is comparable with the photoacoustic IR spectrum of adsorbed pyridine on HF-loaded aluminum alkoxide fluoride, where the band representative for the Lewis acidic sites could not be detected.[75]

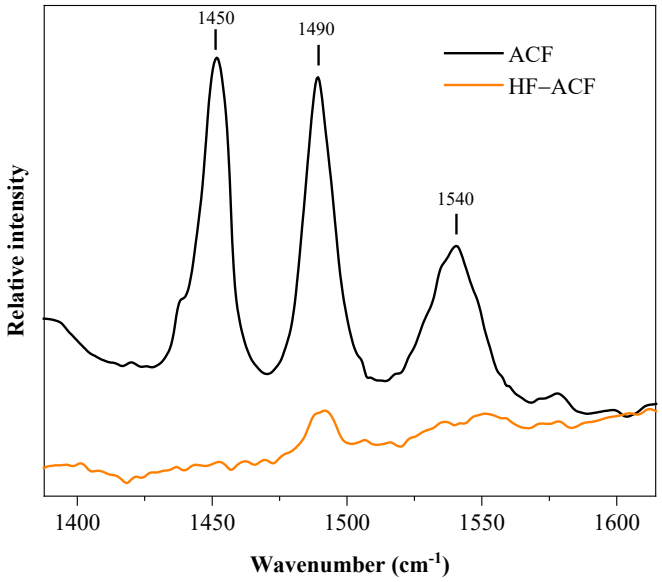

Figure 32. *DRIFTS spectra of adsorbed pyridine on ACF (black) and HF-loaded ACF (orange).*

iv- Short summary

All those surface characterizations suggest that the polyfluorides moieties formed at the surface of ACF are interacting with both the Lewis acidic centers and the terminal fluorine atoms by partially filling the micropores present on ACF. The acidity of this material seems to be reduced according to the results from the adsorption of probe molecules, although a certain small amount of sites remains. Unlike the HF/SbF_5 system, no superacid material was generated by loading HF onto ACF.[39] It was strongly suggested that the HF is blocking the acidic sites, which hinders certain probe molecules from interacting with the acidic sites. The results obtained are comparable to the study on HF-loaded *HS*-AlF_3, where the material exhibited as well a reduced acidity due to the blocking of the acidic sites by HF.

3- Reactivity

A- Isomerization reaction

The isomerization reaction used for testing the strength of freshly synthesized ACF was performed using HF-loaded ACF for both batches. In both cases, no conversion from 1,2-dibromohexafluoropropane to 2,2-dibromohexafluoropropane could be observed (Scheme **52**). As described in the introduction, ACF performs this reaction at room temperature within 2 hours to reach more than 90% of conversion.[81]

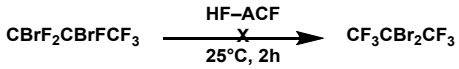

Scheme 52. *Isomerization reaction of 1,2-dibromohexafluoropropane using HF-loaded ACF.*

This observation is consistent with the results obtained from the surface study, strongly supporting a probable blocking of the acidic sites by the HF, which are needed to conduct the isomerization reaction of 1,2-dibromohexafluoropropane into 2,2-dibromohexafluoropropane. Moreover, when the HF-loaded aluminum alkoxide fluoride was tested in the same isomerization reaction, no conversion could be observed neither, and the authors concluded that the HF was strongly adsorbed at the Lewis acidic sites, blocking their access for further catalytic reactions.[75]

Nevertheless, various substrates showing potential for hydrofluorination reactions were tested and will be described in the next section. Both batches were used as catalysts for each reaction; however, since the batch B showed slightly improved conversion in most of the reactions, the results presented here will refer to HF-loaded ACF bach B as the catalyst. Batch B was synthesized with distinctively less HF than batch A (See Annex).

B- Hydrofluorination of alkynes

Fluorinated olefins are of high interest in a variety of fields. As described above, several research groups have used alkynes to synthesized fluorinated olefins via different synthetic methods.[257,309,310,312,313,338–340] To the best of our knowledge, a nanoscopic Lewis acid

coupled with HF was never used as a material for hydrofluorination reactions. Therefore, the HF-loaded ACF was tested for several alkynes (**21a**, **21b**, **21c**, and **21d**) (Scheme **53**). For all the alkynes tested, the hydrofluorination of the triple bond was achieved, giving the corresponding Markovnikov products (**22a**, **22b**, **22c**, and **22d**). Moreover, for 4-ethynyltoluene (**21a**) and ethynylbenzene (**21b**), difluorination products (**22a** and **22a'** from **21a**; **22b** and **22b'** from **21b**) were observed, where the second hydrofluorination reactions take place at the already fluorinated carbon. Notably, the conversions were low, even though the reaction tubes were monitored over 7 days and kept at 70 °C. It is likely, that not enough HF was present at the surface of ACF to allow higher conversions.

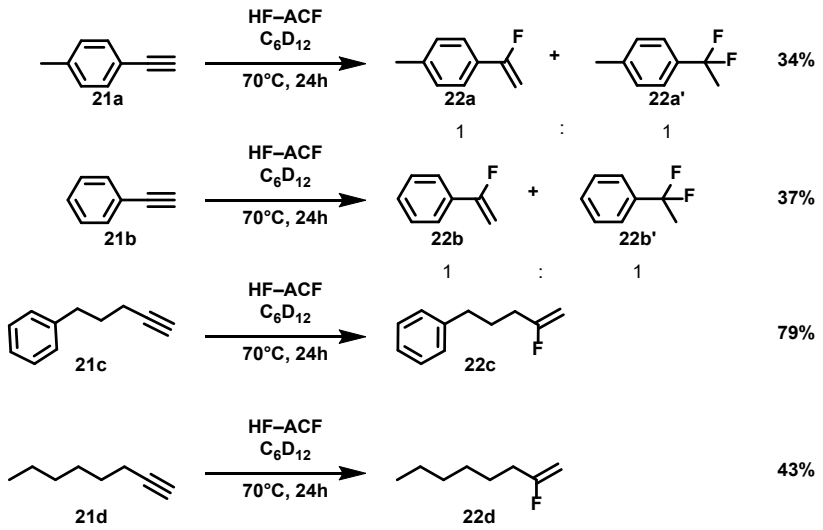

Scheme 53. *Hydrofluorination reactions of various four in the presence of HF-loaded ACF (batch B) and C_6D_{12} as the solvent.*

C- Hydrofluorination of ynamides

Ynamides are regarded as special alkynes, connected to a nitrogen atom bearing an electron-withdrawing group, which result in enhanced stability and unique reactivity.[341] Transformations of ynamides are widely known; however, due to the low regio- and stereoselectivity of those reactions, hydrofluorination reactions are rather scarcely reported.[341–345] When four different ynamides (**23a**, **23b**, **23c**, and **23d**) were treated at 70 °C in the presence of HF-loaded ACF and C_6D_{12} as a solvent, hydrofluorination of the C≡C was observed (Scheme **54**). Generation of the corresponding regioselective (E)-α-fluoroenamides (**24a**, **24b**, **24c**, and **24d**) was detected for all the four substrates in majority

after monitoring the reaction over 7 days. Despite the extended reaction time, only low conversions were observed, as in the hydrofluorination reactions of alkynes (see above). Similarly, it can also be expected that not enough HF was present, therefore allowing only low conversion. Nevertheless, the reactions were highly regio and stereoselective and could be further optimized to generate an attractive synthetic route to (E)-α-fluoroenamides.

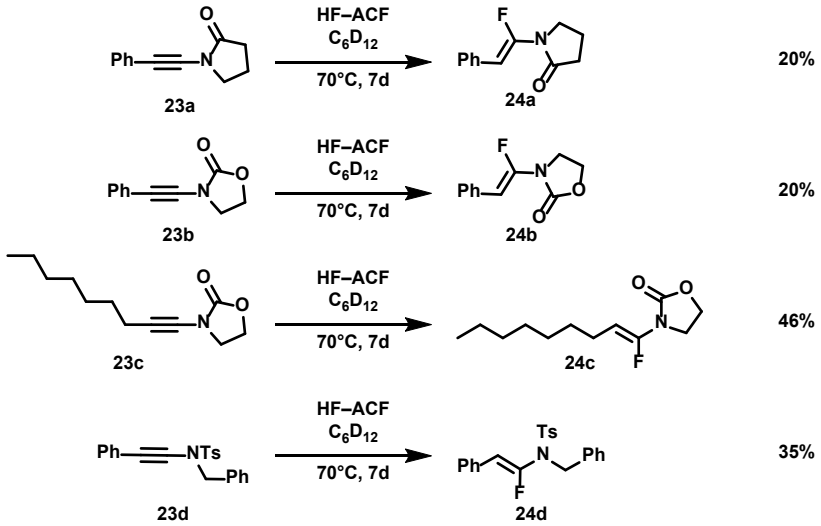

Scheme 54. *Hydrofluorination reactions of four ynamides in the presence of HF-loaded ACF (batch B) and C_6D_{12} as the solvent.*

D- Hydrofluorination of alkenes

i- Non functionalized alkenes

Direct hydrofluorination of alkenes was recently achieved using a nucleophilic fluorination reagent based on $KHSO_4$-13HF, or ion-exchange resin-supported hydrogen fluoride.[260,319] Treatment of 2-pentene *cis* (**25a**) and *trans* (**25b**) isomers or 1-phenyl-1-cyclohexene (**25c**) in the presence of HF-loaded ACF gave only traces of their corresponding hydrofluorination products **26a**, **26b**, and **26c** respectively (Scheme **55**). Therefore, deep studies were not conducted on alkenes.

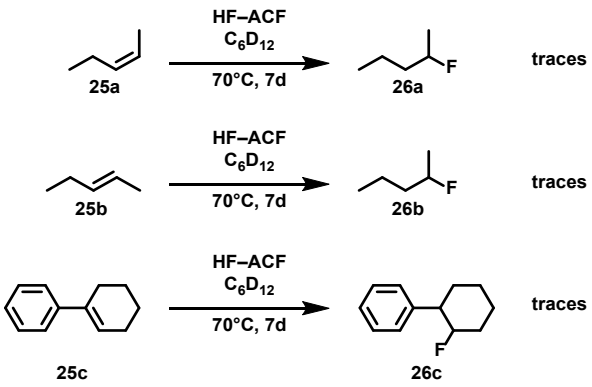

Scheme 55. *Hydrofluorination reactions of three alkenes in the presence of HF-loaded ACF (batch B) and C_6D_{12} as the solvent.*

ii- Fluorinated alkenes

The reactivity of some fluorinated olefins was already studied using pure ACF as a catalyst.[97] It was, therefore, of interest to investigate the reactivity of the novel HF-loaded ACF towards the same tetrafluoroolefins and the influence of the HF loading on the reactivity. When (Z)-1,3,3,3-tetrafluoropropene (**19a**) was put in the presence of HF-loaded ACF and C_6D_{12} as the solvent, the isomerization product (E)-1,3,3,3-tetrafluoropropene (**19b**), as well as the hydrofluorination product 1,1,1,3,3-pentafluoropropane (**10a**) were detected in a 3:1 ratio respectively (Scheme **56**, top). Isomerization reaction was again observed when (E)-1,3,3,3-tetrafluoropropene (**19b**) was used as a substrate in the presence of HF-loaded ACF in the same condition (Scheme **56**, bottom). Indeed, the isomerization of (E)-1,3,3,3-tetrafluoropropene (**19b**) into (Z)-1,3,3,3-tetrafluoropropene (**19a**) was detected, together with the formation of 1,1,1,3,3-pentafluoropropane (**10a**) in a ratio 12:1 respectively. Several patents describe the isomerization reaction between the *cis* and *trans*-1,3,3,3-tetrafluoropropenes in the presence of HF and a catalyst.[346–348] When the reactions were performed using the pure ACF, the isomerization products could be as well observed; however, without the formation of the 1,1,1,3,3-pentafluoropropane product. This finding suggests that the acidic sites on ACF responsible for the isomerization reaction of tetrafluoropropenes are still present on HF-loaded ACF. Moreover, the isomerization reaction of tetrafluoropropenes could be coupled with a hydrofluorination reaction when HF-loaded ACF is present in the reaction mixture, emphasizing the bifunctional potential of this material. Noticeably, when the 3,3,3,2-tetrafluoropropene was tested in the same

conditions as its 1,3,3,3-tetrafluoropropene isomers, only traces of the 1,1,1,2,2-pentafluoropropane were detected.

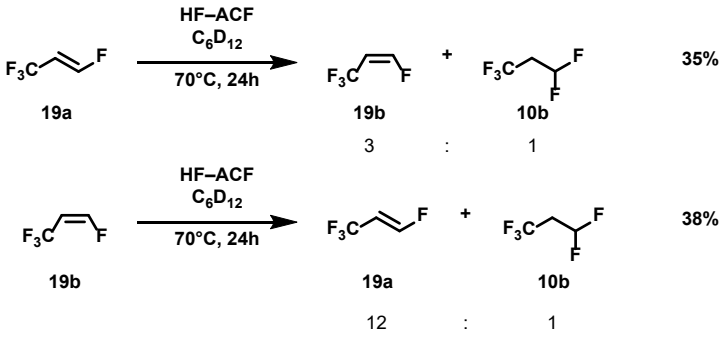

Scheme 56. *Reactivity **19a** and **19b** in the presence of HF-loaded ACF (batch B) and C_6D_{12} as the solvent.*

E- Ring-opening of epoxides and aziridines

i- Epoxides

Fluorohydrins are of recent interest due to their potential to act as a precursor in the synthesis of steroids, amino acids, or carbohydrates.[222,349,350] Various methods exist to access fluorohydrins, and among them, the ring-opening of epoxides with a fluorinating reagent is one of the most extensively used.[350] Various fluorinating reagents were found to be effective in the ring-opening of epoxides, such as KHF_2, SiF_4, $BF_3{\cdot}OEt_2$, pyridine·HF, or $Et_3N{\cdot}3HF$ only to cite a few examples. Depending on the substituents, the acidity, and the nucleophilicity of the reagents, the selectivity of the reactions differ. Indeed, an S_N1 reaction will be favored by carbenium-ion stabilizing substituents, whereas an S_N2 reaction will occur in the presence of destabilizing substituents. Moreover, the HF concentration in the media can also have a great influence on the selectivity and the conversion.[351,352] When 1,1-dimethyloxirane (**27a**) was treated in the presence of HF-loaded ACF and C_6D_{12} as the solvent, selective formation of 2-fluoro-2-methyl-propan-1-ol (**28a**) in 25% yield, derived from the most stable cation intermediate was detected (Scheme **57**, top). A second epoxide, cyclopentene oxide (**27b**), was tested in the same conditions, namely in the same solvent and same amount of HF-loaded ACF (Scheme **57**, bottom). Generation of trans-2-fluorocyclopentanol (**28b**) was observed, reaching 64% yield after 4 days. For comparison, **27b** could be converted at 90% within 3 days into the corresponding fluorohydrins at 50 °C using Jacobsen's catalyst in combination with 100% of AgF in CH_3N.[350]

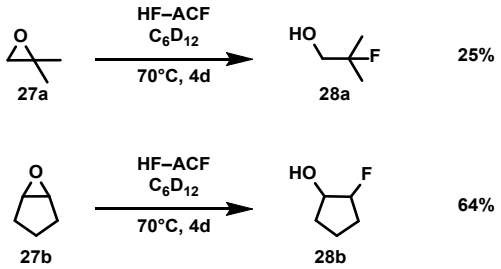

Scheme 57. *Ring-opening of 1,1-dimethyloxirane (**27a**, top) and cyclopentene oxide (**27b**, bottom) in the presence of HF-loaded ACF (batch B) and C_6D_{12} as the solvent.*

ii- Aziridines

The ring-opening of aziridines can also give access to attracting vicinal di-functionalized compounds.[100] In particular, β-fluoroamines are of great significance since they are increasingly incorporated in drugs due to their improved stability.[353] However, the acid-mediated ring-opening of aziridines generally suffers from a lack of selectivity and conversion.[354–356] HF-based reagents were deeply tested, and as in the ring-opening of epoxides, depending on the reagent used, side products and various yield can be obtained.[29,260,354,357–359] For instance, when (S)-2-Benzyl-1-tosylaziridine (**29**) was treated in the presence of the A26 resin HF developed by Hammond, hydrofluorination reaction occurred within 3 hours, reaching 64% yield. Treatment of (S)-2-Benzyl-1-tosylaziridine (**29**) in the presence of HF-loaded ACF and C_6D_{12} as solvent gave the N-(2-fluoro-3-phenylpropyl)-4-methylbenzenesulfonamide (**30**) after 2 days in 30% yield (Scheme **58**).

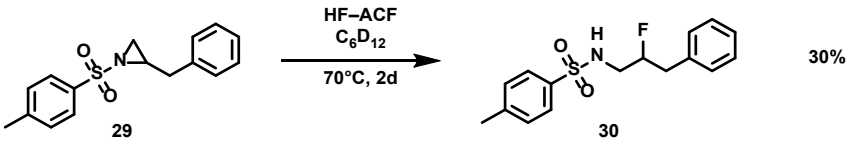

Scheme 58. *Ring-opening of (S)-2-Benzyl-1-tosylaziridine (11a) in the presence of HF-loaded ACF (batch B) and C_6D_{12} as the solvent.*

F- Short summary

Fluorination reactions were successful in the presence of HF-loaded ACF for a variety of substrates. Even though only a few substrates were tested for each kind of reaction (hydrofluorination of alkynes, ynamides, and alkenes as well as in the ring-opening of

epoxides and aziridines), the corresponding fluorinated products were observed, suggesting a wide variety of application for this material. However, the yields were relatively low, supporting the results obtained in the surface study of the material, which indicated a reduced acidity of the system. Therefore, optimization for fluorination reactions is needed. Moreover, the isomerization reaction of the 1,3,3,3-tetrafluoropropene suggests the preservation of some of the Lewis acidic sites, responsible for the isomerization of the latter. This is consistent with the results observed in the adsorption of deuterated acetonitrile, which has revealed the presence of Lewis acidic sites, however, in a decreased intensity. Overall, HF-loaded ACF has some potential for hydrofluorination reactions, with the advantages of combining Lewis acidic sites and an HF reservoir.

Chapter 5 Conclusion

This research aimed to study the solid Lewis acid Aluminum chlorofluoride as a catalyst for the formation of industry-relevant fluorinated compounds. To achieve this goal, on the one hand, derivatization of polyfluorinated substrates such as hydrochlorofluorocarbons and hydrofluorocarbons via C−F bond activations was investigated using ACF as a catalyst in various conditions. On the other hand, hydrofluorination reactions of alkynes, alkenes, ynamides, epoxides, and aziridines were studied using a modified ACF loaded with HF. Additionally, this HF-loaded ACF was fully characterized using various bulk and surface technics to understand the effect of the HF loading on ACF. The outcomes of those studies revealed the considerable potential of using ACF for diverse types of reactions, as well as its simple functionalization in order to expand its reactivity towards yet untested substrates.

Using the first approach, 2-chloro-1,1,1,2-tetrafluoropropane (HCFC-244bb) was effectively activated via dehydrofluorination under mild conditions, which underlines the effectiveness in performing C−F bond activation using ACF as a catalyst. It was evidenced that in the case of HCFC-244bb, no hydrogen sources were needed to convert it into the dehydrofluorination product 2-chloro-3,3,3-trifluoropropene (HFO-1233xf), allowing a straightforward recovery of the product and the catalyst (Scheme **59**, right). The C−F bond in the CFCl group in HCFC-244bb was activated exclusively, leaving the CF_3 group intact. Similarly, the C−F bond in the CH_2F group in 1,1,1,2,3-pentafluoropropane (HFC-245eb) could be activated by ACF, without the use of a hydrogen source, giving the dehydrofluorination and refluorination products under mild conditions (Scheme **59**, left). The studies have demonstrated that a single C−F bond can be activated by ACF without the use of a hydrogen source, under mild conditions.

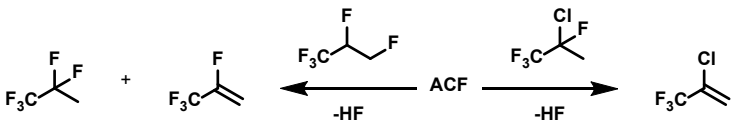

Scheme 59. *Single C−F bond activation of HCFC-244bb (right) and HFC-245eb (left) in the presence of ACF as the catalyst.*

Furthermore, when a hydrogen source was introduced in the above-mentioned reactions, further activation products were generated, involving an alternative mechanism, based on the formation of silylium-ions at the surface of ACF previously described in the literature (Scheme **60**). In an initial step, the proton from the hydrogen source can interact with the Lewis acidic centers at the surface of the catalyst, generating silylium-like species. A subsequent C−F bond activation at the substrate can generate $FSiEt_3$, the corresponding carbenium-like species, and a surface-bound hydride, followed by the generation of hydrodefluorination products or dehydrofluorination products in combination with H_2 as it was depicted in Chapter 2. Alternatively, an abstraction of a fluoride could also be the initial step, followed by an interaction of the silane with the surface-fluoride generating fluorosilane and the hydrodefluorination products as it was described in the mechanistic studies of the substrates. In this Ph.D. work, it was also demonstrated that in the presence of silane, the CF_3 group in both substrates (HCFC-244bb and HFC-245eb) was activated via allylic monohydrodefluorination, which could not be observed in the absence of silane (Scheme **60**). Therefore, it can be suggested that the silane promotes allylic monohydrodefluorination reaction at CF_3 groups in the presence of ACF.

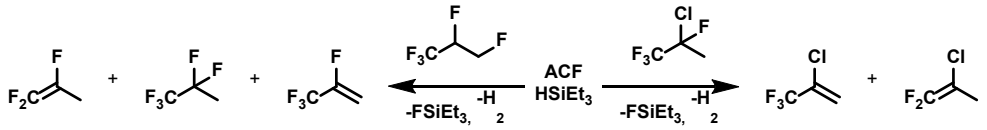

Scheme 60. *Reactivity of HCFC-244bb (right) and HFC-245eb (left) in the presence of $HSiEt_3$ and ACF as the catalyst.*

The reactivity studies of the hydrofluorocarbons 1,1,1,3,3-pentafluoropropane (HFC-245fa) and 1,1,1,2,2-pentafluoropropane (HFC-245cb) revealed the necessity of a hydrogen source in the reaction mixture to observe the conversion of those substrates (Scheme **61**). This observation indicates the difficulty of activating CF_2 and CF_3 groups using ACF, which can be promoted by the formation of thermodynamically stable F−Si bonds in the presence of $HSiEt_3$. Besides, the CHF_2 group in HFC-245fa could be converted in higher yield than the CF_2 group in HFC-245cb, which is consistent with the observation made in the case of HFC-245eb, where the C−F bond in the CH_2F was favorably activated as compared to the secondary carbon also bearing a fluorine atom (CHF group).

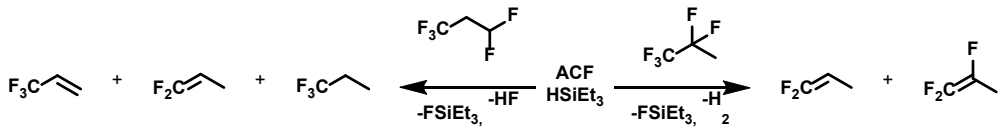

Scheme 61. *Reactivity of HFC-245cb (right) and HFC-245fa (left) in the presence of $HSiEt_3$ and ACF as the catalyst.*

Additionally, it was observed that by using an aromatic solvent such as C_6D_6, Friedel Crafts type reactions, as well as hydroarylation reactions, were promoted, allowing easy access to various interesting compounds for all the substrates studied in this work.

Overall, this research study evidenced that by varying the conditions, such as the presence and the amount of silane and the type of solvent, different products can be generated. It was hence possible to control the formation of desirable products such as the industry-relevant olefins HFO-1234yf and HFO-1234ze, by choosing the adapted conditions. These findings open new routes to generate highly demanded fluorinated compounds useful in a variety of application fields such as pharmaceuticals, agrochemicals, and material science. Moreover, in future work, other fluorinated alkanes with longer alkyl chains such as polyfluorinated butanes and pentanes or even fully fluorinated substrates could be interesting to study using ACF as the catalyst to elucidate the full potential of this nanoscopic Lewis acid. Additionally, it was shown that $HSiEt_3$ is an excellent hydrogen source in combination with ACF, allowing hydrodefluorination, dehydrofluorination, and refluorination reactions. Thus, varying the hydrogen source, as it was already tested previously by using germanes, could lead to different reactivities of the substrates and may give more insight into the different mechanisms taking place depending on the hydrogen source used.

As refluorination reactions were observed at ACF when HF was present in the reaction mixture, the second goal of this Ph.D. thesis was to develop and investigate a material based on the immobilization of HF at the surface of ACF and to test it towards hydrofluorination reactions. Therefore, a synthetic method was designed by pre-drying gaseous HF and condensing it on ACF (Scheme **62**).

Scheme 62. *Synthesis of HF-loaded ACF.*

Based on the variety of characterizations performed on this material, such as MAS NMR spectroscopy, vibrational spectroscopy (FTIR, Inelastic Neutron Scattering, Diffuse Reflectance Infrared Fourier Transform, in situ gas phase FTIR), thermoanalysis, X-ray diffraction, pore size analysis, surface area determination, NH_3-TPD, and adsorption of probe molecules, the formation of polyfluoride moieties at the surface of ACF was evidenced, interacting with both the Lewis acidic centers and the terminal fluorine atoms present on ACF. It appears that the loading of HF on ACF induce a slightly better-ordered bulk and a reduced acidity. Indeed, the HF seems to block the access of the acidic site at the surface of ACF, hindering the adsorption of molecules on those sites. The reactivity study of HF-loaded ACF towards various substrates showed promising results since most of the reactions showed successful hydrofluorination (Scheme **63**). However, the yields obtained were relatively low, which is in accordance with the observation of a reduced acidity using surface characterization methods. Therefore, as an outlook, the optimization of some of the reactions might improve the yields, for instance, by having a larger amount of HF present in the reaction mixture. Additionally, further substrates could be in a future work tested to study the ability of HF-loaded ACF thoroughly.

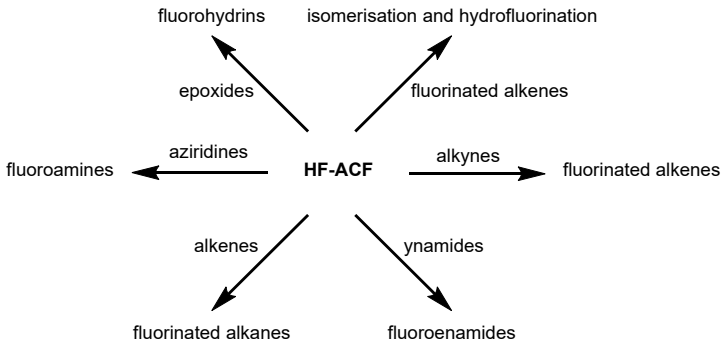

Scheme 63. *Summary of hydrofluorination reactions of various types of substrates performed by HF-loaded ACF.*

Chapter 6 Experimental section

1- Materials and general techniques

The solvents C_6D_6 and C_6D_{12} were purchased from Eurisotop. C_6D_6 was dried over K-Solvona and distilled prior to use. C_6D_{12} was purged by bubbling argon and kept over molecular sieves. All the reagents were acquired from commercial suppliers (Sigma Aldrich, abcr, Alfa Aeasar, Solvay Fluor GmbH, and Arkema). HF was a gift from Solvay Fluor GmbH and was purified using $KNiF_6$ prior usage.

Due to the air and moisture sensitivity of the materials, standard Schlenk techniques under argon atmosphere and an MBraun glove box were used for carrying out all the experiments.

2- Synthesis of the catalysts

A- Synthesis of ACF

Aluminum chlorofluoride ($AlCl_xF_{3-x,}$ x = 0.05-0.3; ACF) was synthesized according to the literature.[81] Namely, under dry conditions, a chlorine-fluorine exchange is induced by slowly adding the fluorinating agent CCl_3F to $AlCl_3$ in the presence of CCl_4, which acts as a solvent. During the synthesis, a dry ice condenser was used as well as an ice bath. At the end of the addition of the fluorinating agent, the solvent was removed under reduced pressure, and the flask containing ACF was stored in a glovebox. The number of active sites was found to be roughly 1 mmol acidic sites per gram of catalyst, according to NH_3-TPD measurement.

In addition, the isomerization reaction of 1,2-dibromohexafluoropropane into 2,2-dibromohexafluoropropane is used as a benchmark reaction for very strong Lewis acid. In a pear-shape flask, 25 mg of the catalysts (ACF or HF-loaded ACF) were suspended in 250 µL of 1,2-dibromohexafluoropropane. The reaction mixture was stirred for 2h at room temperature. The reaction was stopped after 2h by adding deuterated chloroform. The organic phase containing the dissolved product was separated and analyzed by ^{19}F NMR.

The conversions were calculated by integration of the signals of both the substrate and the product.

B- Synthesis of different batches of HF-loaded ACF

Figure S1. *Picture of the experimental set up for the synthesis of HF-loaded ACF.*

Since an argon flow was needed to carry the HF outside the bottle onto the inliners, a distinct determination of the exact amount of HF condensed on ACF was unfeasible; therefore, an estimated large excess was condensed having the ACF fully immersed in HF (batch A). In an attempt to relatively evaluate the influence of the amount of HF condensed onto the surface of ACF, a second batch was synthesized according to the same procedure, only this time, a reduced amount of dried HF was condensed, to only have a moistened ACF, in contrast to a fully immersed one (batch B).

3- Analytical methods

A- NMR

NMR spectra were recorded on a Bruker DPX 300 at room temperature. ^{1}H NMR chemical shifts were referenced to residual C_6D_5H (δ = 7.16 ppm) or $C_6D_{11}H$ (δ = 1.38 ppm). The ^{19}F NMR spectra were referenced to $PhCF_3$ (δ = -63.5 ppm).

B- GC MS

An Agilent 6890 N gas-phase chromatograph (Agilent 19091S-433 Hewlett-Packard) with an Agilent 5973 Network mass selective detector at 70 eV and an HP-5 ms column was used for GC-MS experiment.

C- MAS NMR spectroscopy

The MAS NMR spectra were recorded on a Bruker AVANCE 600 spectrometer (B_0 = 14.1 T) at room temperature using a 2.5 mm magic angle sample spinning (MAS) probe, and the MAS frequency was 27.5 kHz. The spectra shown in Figures **17**, **18**, **19**, **20**, and **21** were recorded on a Bruker AVANCE 400 spectrometer (B_0 = 9.4 T) at room temperature, using the same 2.5 mm rotor. The rotation frequency used was 20 kHz. The chemical shifts are given with respect to (i) the $CFCl_3$ standard for ^{19}F, (ii) TMS for ^{1}H, and (iii) and aqueous solution of $AlCl_3$ for ^{27}Al. Data analysis was performed with the software TopSpin 2.1.

D- X-Ray diffraction

X-ray powder diffraction measurements were performed on an STOE Stadi MP diffractometer equipped with a Dectris Mythen 1K linear silicon strip detector and Ge(111) double-crystal monochromator (Mo-Kα_1 radiation) in transmission geometry.

E- DTA-TG MS

The thermal behavior of the solids was studied by conventional thermal analysis (TA) in an argon atmosphere. A NETZSCH Thermo analyzer STA409C Skimmer, being additionally equipped with a conventional high-temperature SiC oven, was used to record the thermoanalytical curves. An online-coupled BALZERS QMG 421 enabled MS-analysis of evolved gases. A DTA-TG sample carrier system with platinum crucibles (beaker, 0.8

mL) and Pt/PtRh10 thermocouples were used. Measurements were performed under an argon atmosphere by applying a heating rate of 10 K min^{-1}.

F- FTIR & INS

All FT-IR spectra were acquired with a Bruker Vertex 70 spectrometer equipped with an ATR unit (diamond). Inelastic neutron scattering spectra were collected on the indirect geometry instrument TOSCA at the ISIS Neutron and Muon Facility. Samples (0.928 g HF-loaded ACF) were loaded under an argon atmosphere into Al sachets and sealed into Al sample holders before loading onto the instrument. The samples were cooled to < 20 K before data collection in order to minimize Debye-Waller dampening. Data were collected in the forward and backward scattering geometries and summed.

G- N_2 adsorption and Pore size analysis

The porosity of materials was measured by nitrogen adsorption/desorption using an Autosorb iQ instrument with Helium mode. Brunauer-Emmett-Teller (BET) surface area (SBET) was calculated in relative pressure range (p/p0) from 0.05 to 0.35. Pore size distribution was calculated using the NLDFT Model.

H- TEM and EDX

Transmission electron microscopy (TEM) images were recorded on a Philips CM 200 microscope equipped with a LaB_6 cathode and operated at 200 kV. Energy-dispersive X-ray spectroscopy (EDX) analysis was performed using an EDAX SDD detector (EDAX Inc., Mahwah, NJ, USA) coupled to the TEM.

I- NH_3-TPD

For TPD experiments, about 30 mg of the samples filled with around 100 mg of quartz glass beads (to avoid clocking of the reactor) was added in a quartz flow reactor and heated at 523 K under nitrogen flow for 1 hour, unless otherwise indicated. Afterward, ammonia was adsorbed onto the surface of the samples at 393 K. After flushing the excess NH_3 with N_2 for 1 h and cooling to 353 K, the TPD program was started (10K/min up to 773 K, then holding until no more NH_3 is desorbed). Desorbed ammonia was continuously monitored by IR spectroscopy (FT-IR System 2000, Perkin-Elmer) following the band at 930 cm^{-1}. For quantification, the total amount of desorbed ammonia was reacted with a diluted solution of sulfuric acid and then titrated with sodium hydroxide solution.

J- CD_3CN and pyridine adsorption followed by DRIFTS

Diffuse reflectance infrared Fourier transform spectra (DRIFTS) of adsorbed deuterated acetonitrile (CD_3CN) were measured using a PIKE Technologies DiffusIR Environmental chamber (HTV) and DiffusIR diffuse reflectance accessory. Prior to the measurements, the samples were kept under vacuum for 2 h, then contacted with 90 mbar of CD_3CN or pyridine, and afterward degassed for 30 min at room temperature. All spectra were recorded on a Thermo Fischer Scientific Nicolet iS50 spectrometer equipped with an MCT detector at 2 cm^{-1} spectral resolution over the range 4000–600 cm^{-1}.

4- General procedures

A- Procedures for the reactions with HCFC-244bb (1) and HFO-1233xf (2)

25 mg of ACF was introduced in a JYoung NMR tube inside a glovebox. Using Schlenk techniques, 0.5 mL of the solvent (either C_6D_6 or C_6D_{12}) was added. In the experiment involving $HSiEt_3$, 60 µL (or in neat $HSiEt_3$: 0.5 mL) was introduced under dry conditions. Then, HCFC-244bb (**1**) or HFO-1233xf (**2**) was condensed into the JYoung NMR tube from a small glass bulb filled with 0.5 atm (0.21 mmol) of the gaseous substrate. The tubes

were warmed up to 70 °C and monitored over time by ^{1}H and ^{19}F NMR spectroscopy. An external standard ($PhCF_3$) was used to calculate the conversion by the integration of the consumed substrate in the ^{19}F NMR spectra. Using the same procedure, blank test reactions were performed without adding the catalyst. Additionally, the catalyst (ACF) was replaced by $AlCl_3$ or *HS*-AlF_3 under the same conditions and using the same procedures as described above. Turnover numbers were calculated, assuming 1 mmol of active sites/g at the catalyst.

B- Procedures for the gas reactions

The reactions were carried out using Schlenk techniques and JYoung NMR tubes. A Jyoung NMR tube was loaded with 25 mg of ACF inside a glovebox. 0.5 mL of the solvent (either C_6D_6 or C_6D_{12}) was added to the tubes under Schlenk conditions. When $HSiEt_3$ was needed, the corresponding amount was introduced (60 µL, 30 µL, or in neat $HSiEt_3$: 0.5 mL). The gaseous substrates were then condensed using a small glass bulb filled with 0.5 atm into the reactions mixture. The tubes were kept at 70 °C and monitored over 7 days. $PhCF_3$ or C_6F_6 was used as an external standard in a closed capillary to calculate the conversion based on the consumed substrates by the integration of the ^{19}F NMR spectra. Blank test reactions were conducted using the same procedure without the presence of a catalyst.

5- Analytical NMR data

Table S1. *NMR resonances of reactants and products:*

Compound	δ ^{1}H NMR (ppm)	δ ^{19}F NMR (ppm)	δ ^{13}C NMR (ppm)
Et_3SiH	0.98 (t, 9H, CH_3, $^{3}J_{H,H}$ =7.9 Hz)	-	8.4 (s, CH_3), 2.8 (s, CH_2)
Et_3SiF	0.92 (t, 9H, CH_3,$^{3}J_{H,H}$ =8.0 Hz)	-176.5 (m)	6.3 (d, CH_3, $^{3}J_{C,F}$ =1.8 Hz), 5.2 (d, CH_2, $^{2}J_{C,F}$ =14.3 Hz)
Et_2SiF_2	0.80 (t, 6H, CH_3,$^{3}J_{H,H}$ =8.0 Hz)	-144.3 (m)	4.0 (t, CH_2, $^{2}J_{C,F}$=15.0 Hz)

Analytical data of $CF_3CClFCH_3$ (1):

δ ^{1}H NMR (300 MHz, C_6D_6): 1.35 (d, *J* = 19.3 Hz, 1H) ppm

δ ^{19}F NMR (282 MHz, C_6D_6): -85.1 (d, *J* = 4 Hz, 3F, CF_3); -120.2 (m, 1F, CF) ppm

δ ^{19}F{^{1}H} NMR (282 MHz, C_6D_6): -85.1 (s, 3F, CF_3); -120.2 (s, 1F, CF) ppm

Analytical data of $CF_3CCl=CH_2$ (2):

δ ^{1}H NMR (300 MHz, C_6D_{12}): 5.92 (d, *J* = 2.4 Hz, 1H); 5.61 (m, 1H) ppm

δ ^{19}F NMR (282 MHz, C_6D_{12}): -72.4 (s, 1F, CF_3) ppm

δ ^{19}F{^{1}H} NMR (282 MHz, C_6D_{12}): -72.4 (s, 1F, CF_3) ppm

Analytical data of $CF_3CClDCH_2C_6D_5$ (3):

δ ^{1}H NMR (300 MHz, C_6D_6): 2.90 (d, *J* = 14.5 Hz, 1H); 2.60 (d, *J* = 14.5 Hz, 1H) ppm

δ ^{19}F NMR (282 MHz, C_6D_6): -75.7 (s, 1F, CF_3) ppm

δ ^{19}F{^{1}H} NMR (282 MHz, C_6D_6): -75.7 (s, 1F, CF_3) ppm

GC/MS: *m/z* = 214

Analytical data of $CF_2=CClCH_3$ (4):

δ ^{19}F NMR (282 MHz, C_6D_{12}): -91.9 (d, *J* = 49 Hz, 1F, CF); -98.2 (d, *J* = 49 Hz, 1F, CF) ppm

δ ^{19}F{^{1}H} NMR (282 MHz, C_6D_{12}): -92.0 (d, *J* = 49 Hz, 1F, CF); -98.2 (d, *J* = 49 Hz, 1F, CF) ppm

GC/MS: *m/z* = 111

Analytical data of $CF_2=CClCH_2C_6D_5$ (5):

δ ^{1}H NMR (300 MHz, C_6D_6): 3.13 (m, CH_2) ppm

δ ^{19}F NMR (282 MHz, C_6D_6): -91.3 (d, br, *J* = 45 Hz, 1F, CF); -96.8 (dt, *J* = 45 Hz, *J* = 3 Hz, 1F, CF) ppm

δ ^{19}F{^{1}H} NMR (282 MHz, C_6D_6): -91.3 (d, *J* = 45 Hz, 1F, CF); -96.8 (d, *J* = 45 Hz, 1F, CF) ppm

GC/MS: *m/z* = 193

Analytical data of $CF_3CF=CH_2$ (6):

δ ^{1}H NMR (300 MHz, C_6D_{12}): 4.46 (dd, *J* = 13.2 Hz, *J* = 4.9 Hz, 1H, CH_2); 4.32 (ddq, *J* = 14.8 Hz, *J* = 4.9 Hz, *J* = 1.6 Hz, 1H, CH_2) ppm

δ ^{19}F NMR (282 MHz, C_6D_{12}): -74.4 (dd, *J* = 11 Hz, *J* = 1.6 Hz, 3F, CF_3); -125.2 (ddq, *J* = 44 Hz, *J* = 14.8, *J* = 11 Hz, 1F, CF) ppm

δ ^{19}F{^{1}H} NMR (282 MHz, C_6D_{12}): -74.4 (d, *J* = 11 Hz, 3F, CF_3); -125.2 (q, *J* = 11 Hz, 1F, CF) ppm

Analytical data of $CF_2=CFCH_3$ (7):

δ ^{1}H NMR (300 MHz, C_6D_6): 3.87 (dt, *J* = 17 Hz, *J* = 4.2 Hz, 3H, CH_3) ppm

δ ^{19}F NMR (282 MHz, C_6D_6): -107.4 (ddq, *J* = 91 Hz, *J* = 32 Hz, *J* = 4.2 Hz, 1F, CF_2); -127.2 (ddq, *J* = 114 Hz, *J* =91 Hz, *J* = 4.2 Hz, 1F, CF_2); -168.2 (ddq, *J* = 114 Hz, *J* = 32 Hz, *J* = 17 Hz, 1F, CF) ppm

δ ^{19}F{^{1}H} NMR (282 MHz, C_6D_6): -107.4 (dd, *J* = 91 Hz, *J* = 32 Hz, 1F, CF_2); -127.2 (dd, *J* = 114 Hz, *J* = 91 Hz, 1F, CF_2); -168.2 (dd, *J* = 114 Hz, *J* = 32 Hz, 1F, CF) ppm

Analytical data of $CF_2CFCH_2C_6D_5$ (8):

δ ^{1}H NMR (300 MHz, C_6D_6): 3.1 (ddd, *J* = 23 Hz, *J* = 4 Hz, *J* = 3 Hz, 3H, CH_3) ppm

δ ^{19}F NMR (282 MHz, C_6D_6): -107 (ddt, *J* = 87 Hz, *J* = 32 Hz, *J* = 3 Hz, 1F, CF_2); -125.7 (ddt, *J* = 114.7 Hz, *J* = 86.4 Hz, *J* = 4.4 Hz, 1F, CF_2); -173 (ddt, *J* = 114.7 Hz, *J* = 32 Hz, *J* = 23 Hz, 1F, CF) ppm

δ ^{19}F{^{1}H} NMR (282 MHz, C_6D_6): -107 (dd, *J* = 87 Hz, *J* = 32 Hz, 1F, CF_2); -125.7 (dd, *J* = 114.7 Hz, *J* = 86.4 Hz, 1F, CF_2); -173 (ddt, *J* = 114.7 Hz, *J* = 32 Hz, *J* = 23 Hz, 1F, CF) ppm

Analytical data of $CF_3CCl_2CH_3$ (9):

δ ^{1}H NMR (300 MHz, C_6D_6): 1.53 (s, 3H, CH_3) ppm

δ ^{19}F NMR (282 MHz, C_6D_6): -87.9 (d, *J* = 5 Hz, 3F, CF_3) ppm

δ ^{19}F{^{1}H} NMR (282 MHz, C_6D_6): -87.9 (s, 3F, CF_3) ppm

Analytical data of CF_3CHFCH_2F (10a):

δ ^{1}H NMR (300 MHz, C_6D_6): 4.84 (m, 1H, CHF); 4.66 (m, 1H, CH_2F); 4.76 ppm (m, 1H, CH_2F) ppm

δ ^{19}F NMR (282 MHz, C_6D_6): -79.6 (q, J = 6 Hz, J = 11 Hz, J = 25 Hz, 3F, CF_3); -208.3 (m, 1F, CHF); -237.3 (m, 1F, CH_2F) ppm

δ ^{19}F{^{1}H} NMR (282 MHz, C_6D_6): -79.6 (q, J = 6 Hz, J = 11 Hz, J = 16 Hz, 3F, CF_3); -208.3 (qt, J = 6 Hz, J = 11 Hz, J = 16 Hz, 1F, CHF); -237.3 (m, 1F, CH_2F) ppm

Analytical data of $CF_3CH_2CHF_2$ (10b):

δ ^{1}H NMR (300 MHz, C_6D_6): 2.66 (m, J = 4.7 Hz, 3H, CH_2); 5.97 (tt, J = 4.7 Hz, J = 54 Hz, 1H, CHF_2) ppm

δ ^{19}F NMR (282 MHz, C_6D_6): -63.1 (tm, J = 8 Hz, 3F, CF_3); -116 (dm, J = 8 Hz, J = 57 Hz, 2F, CHF_2) ppm

δ ^{19}F{^{1}H} NMR (282 MHz, C_6D_6): -63.1 (t, J = 8 Hz, 3F, CF_3); -116 (m, J = 8 Hz, 2F, CHF_2) ppm

Analytical data of $CF_3CF_2CH_3$ (10c):

δ ^{1}H NMR (300 MHz, C_6D_6): 1.7 (tt, J = 1.2 Hz, J = 18 Hz, 3H, CH_3) ppm

δ ^{19}F NMR (282 MHz, C_6D_6): -88.3 (s, 3F, CF_3); -112.8 (q, J = 18 Hz, 2F, CF_2) ppm

δ ^{19}F{^{1}H} NMR (282 MHz, C_6D_6): -88.3 (s, 3F, CF_3); -112.8 (s, J = 18 Hz, 2F, CF_2) ppm

Analytical data of $CF_3CHFCH_2C_6D_5$ (11):

δ ^{1}H NMR (300 MHz, C_6D_6): 2.25 (d, J = 6 Hz, 2H, CH_2); 3.94 (t, J = 6 Hz, 1H, CH) ppm

δ ^{19}F NMR (282 MHz, C_6D_6): -79.4 (dd, J = 6 Hz, J = 11 Hz, 3F, CF_3); -202 (m, J = 18, 1F, CF) ppm

δ ^{19}F{^{1}H} NMR (282 MHz, C_6D_6): -79.4 (d, J = 11, 3F, CF_3); -202 (q, J = 11, 1F, CF) ppm

Analytical data of $CF_3CDFCH_2C_6D_5$ (12):

δ ^{1}H NMR (300 MHz, C_6D_6): 2.28 (d, J = 6 Hz, 2H, CH_2) ppm

δ ^{19}F NMR (282 MHz, C_6D_6): -80.7 (dd, J = 6 Hz, J = 11 Hz, 3F, CF_3); -200 (m, J = 18, 1F, CF) ppm

δ ^{19}F{^{1}H} NMR (282 MHz, C_6D_6): -80.7 (d, J = 11, 3F, CF_3); -200 (q, J = 11, 1F, CF) ppm

Analytical data of CF_3CHFCH_3 (13):

δ ^{1}H NMR (300 MHz, C_6D_6): 1.5 (dd, J = 25 Hz, J = 6 Hz, 3H, CH_3); 4.8 (dm, J = 46 Hz, J = 6 Hz, 1H, CH) ppm

δ ^{19}F NMR (282 MHz, C_6D_6): -83.5 (dd, J = 11 Hz, J = 6 Hz, 3F, CF_3); -195.8 (m, J = 10 Hz, 1F, CF) ppm

δ ^{19}F{^{1}H} NMR (282 MHz, C_6D_6): -82.3 (d, J = 11 Hz, 3F, CF_3); -194.5 (q, J = 10 Hz, 1F, CF) ppm

Analytical data of CF_2CHCH_3 (14):

δ ^{1}H NMR (300 MHz, C_6D_6): 4 (dqd, J = 25 Hz, J = 7 Hz, J = 2 Hz, 1H, CH); 1.48 (dt, J = 7 Hz, J = 3 Hz, 3H, CH_3) ppm

δ ^{19}F NMR (282 MHz, C_6D_6): -90.4 (m, 1F, CF_2); -94.1 (ddq, J = 48 Hz, J = 25 Hz, J = 3 Hz, 1F, CF_2) ppm

δ ^{19}F{^{1}H} NMR (282 MHz, C_6D_6): -90.4 (d, J = 48 Hz, 1F, CF_2); -94.1 (d, J = 48 Hz, 1F, CF_2) ppm

Analytical data of $CF_3CH_2CH_3$ (15):

δ ^{1}H NMR (300 MHz, C_6D_6): 1.95 (m, 2H, CH_2); 1.06 (t, J = 8 Hz, 3H, CH_3) ppm

δ ^{19}F NMR (282 MHz, C_6D_6): -70.5 (t, J = 10 Hz, 3F, CF_3) ppm

δ ^{19}F{^{1}H} NMR (282 MHz, C_6D_6): -70.5 (s, 3F, CF_3) ppm

Analytical data of $CF_3CH=CH_2$ (16):

δ ^{1}H NMR (300 MHz, C_6D_6): 5.39 - 5.33 (m, 2H, CH_2); 4.88 - 4.75 (m, 1H, CH) ppm

δ ^{19}F NMR (282 MHz, C_6D_6): -67.4 (d, J = 4 Hz, 3F, CF_3) ppm

δ ^{19}F{^{1}H} NMR (282 MHz, C_6D_6): -67.4 (s, 3F, CF_3) ppm

Analytical data of $CF_2=CHCH_2C_6D_5$ (17):

δ ^{1}H NMR (300 MHz, C_6D_6): 3.99 (dtd, J = 22.4 Hz, J = 8 Hz, J = 2.1 Hz, 1H, CH); 2.94 (dt, J = 22.4 Hz, J = 8 Hz, 2H, CH_2) ppm

δ ^{19}F NMR (282 MHz, C_6D_6): -90.3 (d, J = 46 Hz, 1F, CF_2); -93.1 - -93.7 (m, 1F, CF_2) ppm

δ ^{19}F{^{1}H} NMR (282 MHz, C_6D_6): -90.3 (d, J = 46 Hz, 1F, CF_2); -93.1 - -93.7 (d, J = 46 Hz, 1F, CF_2) ppm

Analytical data of $CF_3CHClCH_3$ (18):

δ ^{1}H NMR (300 MHz, C_6D_6): 4.04 (q, J = 6 Hz, 1H, CH); 1.37 (d, J = 6 Hz, 3H, CH_3) ppm

δ ^{19}F NMR (282 MHz, C_6D_6): -74.2 (d, J = 10 Hz, 3F, CF_3)

δ ^{19}F{^{1}H} NMR (282 MHz, C_6D_6): -74.2 (s, 3F, CF_3)

Analytical data of $CF_3CH=CHF$ (19a):

δ ^{1}H NMR (300 MHz, C_6D_{12}): 5.42 (dd, J = 77 Hz, J = 5 Hz, 1H, CH); 4.26 (dqd, J = 37 Hz, J = 7.7 Hz, J = 5 Hz, 1H, CH) ppm

δ ^{19}F NMR (282 MHz, C_6D_{12}): -58.7 (dd, J = 7 Hz, J = 17 Hz, 3F, CF_3); -110 (dm, J = 77, J = 17 Hz, 1F, CF) ppm

δ ^{19}F{^{1}H} NMR (282 MHz, C_6D_{12}): -58.7 (d, J = 17 Hz, 3F, CF_3), -110.3 (q, J = 17, 1F, CF) ppm

Analytical data of $CF_3CH=CHF$ (19b):

δ ^{1}H NMR (300 MHz, C_6D_{12}): 6.24 (ddq, *J* = 77 Hz, *J* = 11 Hz, *J* = 2 Hz, 1H, CH); 4.88 (dqd, *J* = 15 Hz, *J* = 11 Hz, *J* = 7 Hz, 1H, CH) ppm

δ ^{19}F NMR (282 MHz, C_6D_{12}): -62.3 (tt, *J* = 8 Hz, *J* = 2 Hz, 3F, CF_3); -119.3 (dm, *J* = 77, *J* = 8 Hz, 1F, CF) ppm

δ ^{19}F{^{1}H} NMR (282 MHz, C_6D_{12}): -61.5 (d, *J* = 8 Hz, 3F, CF_3); -119.3 (q, *J* = 8 Hz, 1F, CF) ppm

Analytical data of $CF_3CHCH_2C_6D_5$ (20):

δ ^{1}H NMR (300 MHz, C_6D_6): 6.1 (dq, *J* = 14 Hz, *J* = 2 Hz, 1H, CHPh); 5.4 (dq, *J* = 14 Hz, *J* = 6 Hz, 1H, CH) ppm

δ ^{19}F NMR (282 MHz, C_6D_6): -65 (dd, *J* = 6 Hz, *J* = 2 Hz, 3F, CF_3) ppm

δ ^{19}F{^{1}H} NMR (282 MHz, C_6D_6): -65 (s, 3F, CF_3) ppm

6- Supplementary information of Chapter 3

A- MAS NMR spectroscopy

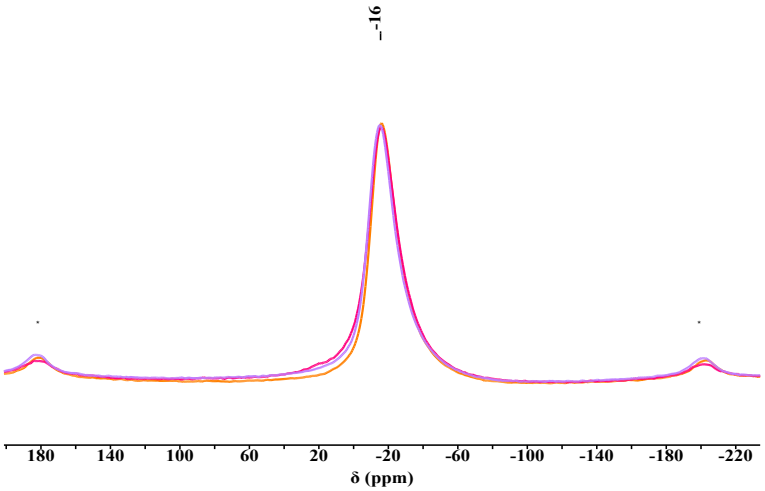

Figure S2. *^{27}Al MAS NMR spectra of HF-loaded ACF (orange), HF-loaded ACF after 24h vacuum (pink), and HF-loaded ACF after 24h at 100 °C (violet) taken at 20 kHz rotation frequency. Asterisks refer to spinning bands.*

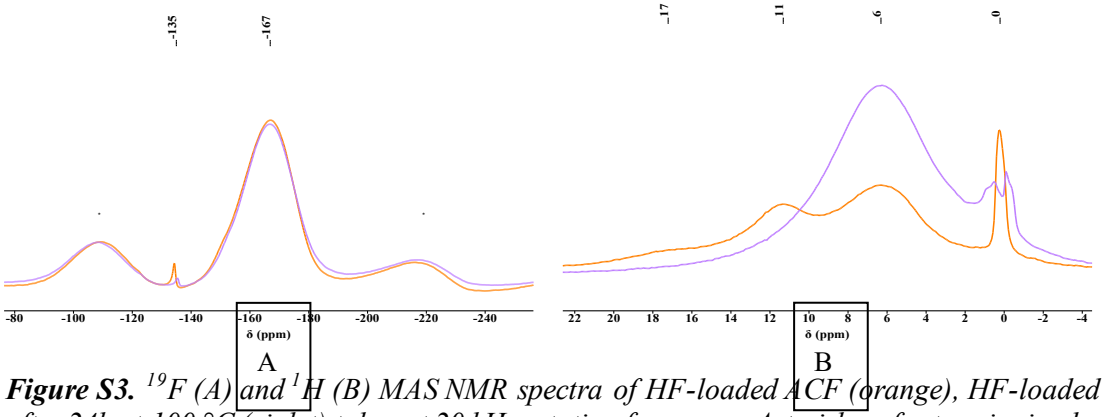

Figure S3. *^{19}F (A) and ^{1}H (B) MAS NMR spectra of HF-loaded ACF (orange), HF-loaded ACF after 24h at 100 °C (violet) taken at 20 kHz rotation frequency. Asterisks refer to spinning bands.*

B- FTIR & INS

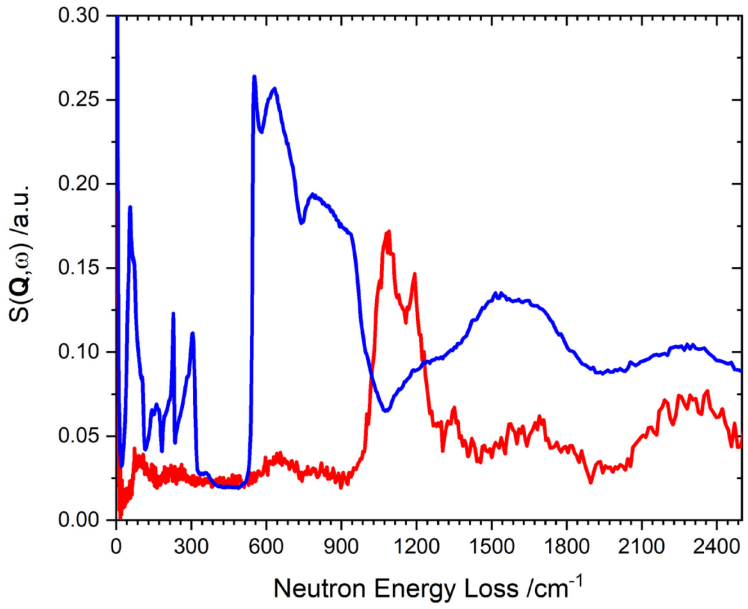

Figure S4. *INS of Ice (blue) and HF-loaded ACF (red). The low frequency coherent inelastic scattering from the Al sample holder has been substracted for both samples.*

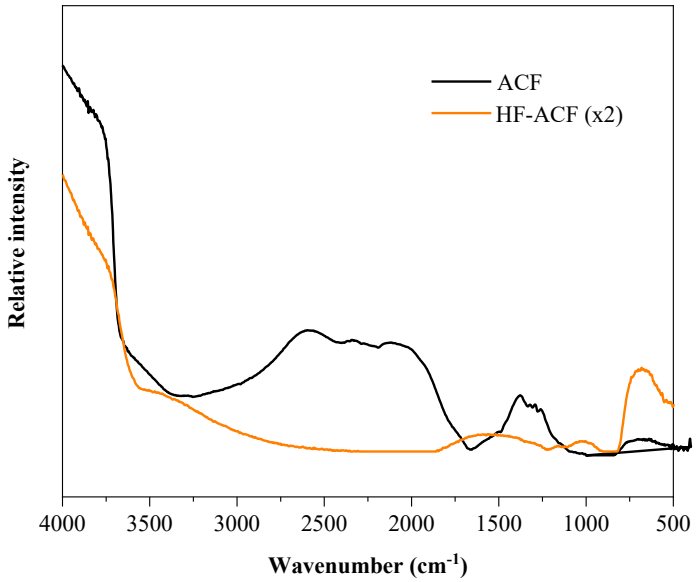

Figure S5. *Diffuse reflectance infrared Fourier transform spectra of ACF (black) and HF-loaded ACF (batch B).*

C- Thermoanalysis

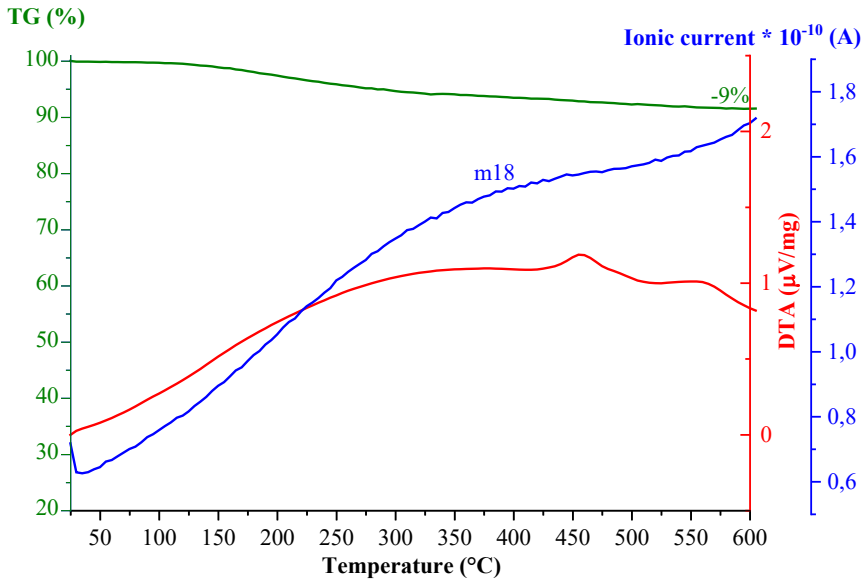

Figure S6. *TG-DTA MS of ACF. m18 represents the mass loss of water.*

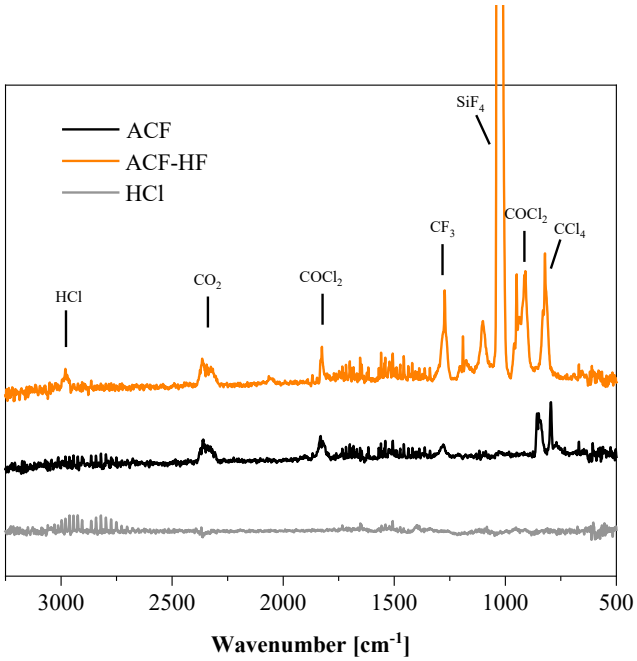

Figure S7. *In situ gas phase FTIR of ACF (black), HF-loaded ACF (orange), taken at 450 °C compared to the HCl spectrum (grey).*

D- Energy Dispersive X-ray spectroscopy and Transmission electronic microscopy

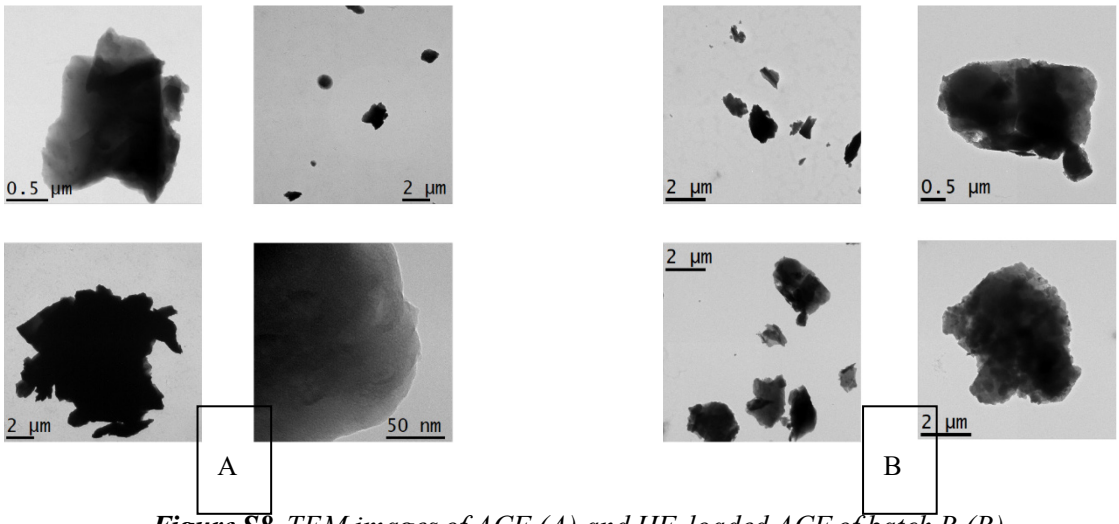

Figure S8. *TEM images of ACF (A) and HF-loaded ACF of batch B (B).*

Table S2. *Atomic percentage of fluorine, chlorine and aluminum in ACF and HF-loaded ACF using EDX:*

Atom/Material	ACF	HF-loaded ACF
Fluorine	78 %	83 %
Chlorine	4 %	1 %
Aluminum	19 %	16 %

E- NMR spectra for the reactivity

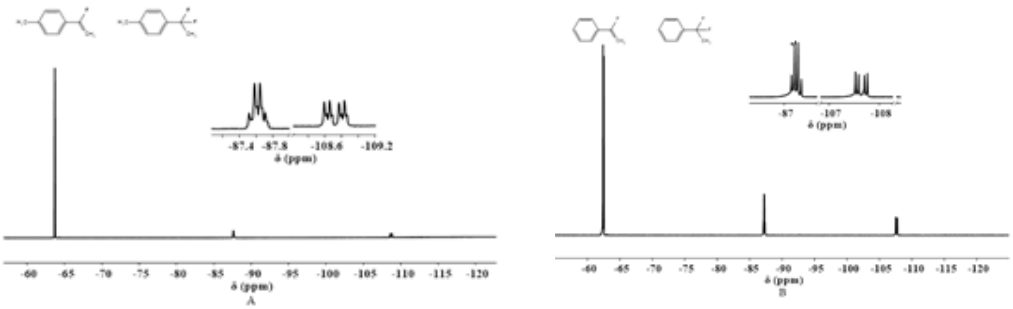

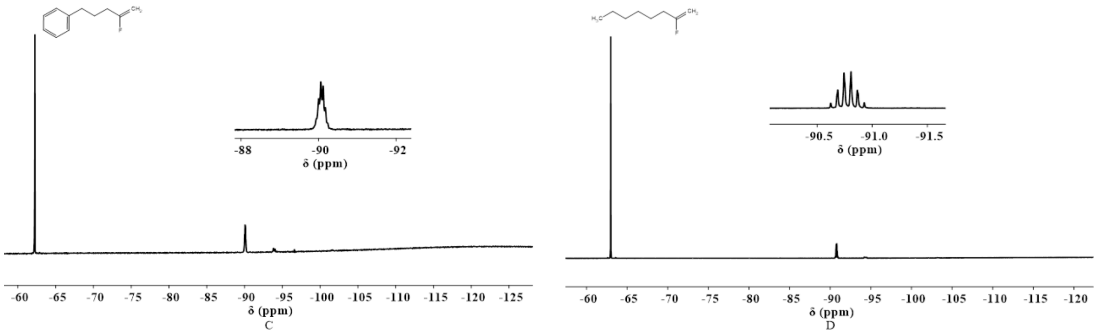

Figure S9. *^{19}F NMR spectra of the hydrofluorination of alkynes into **22a** and **22a'** (A), **22b** and **22b'** (B), **22c** (C) and **22d** (D) in the presence of HF-loaded ACF after 24 hours of reaction time.*

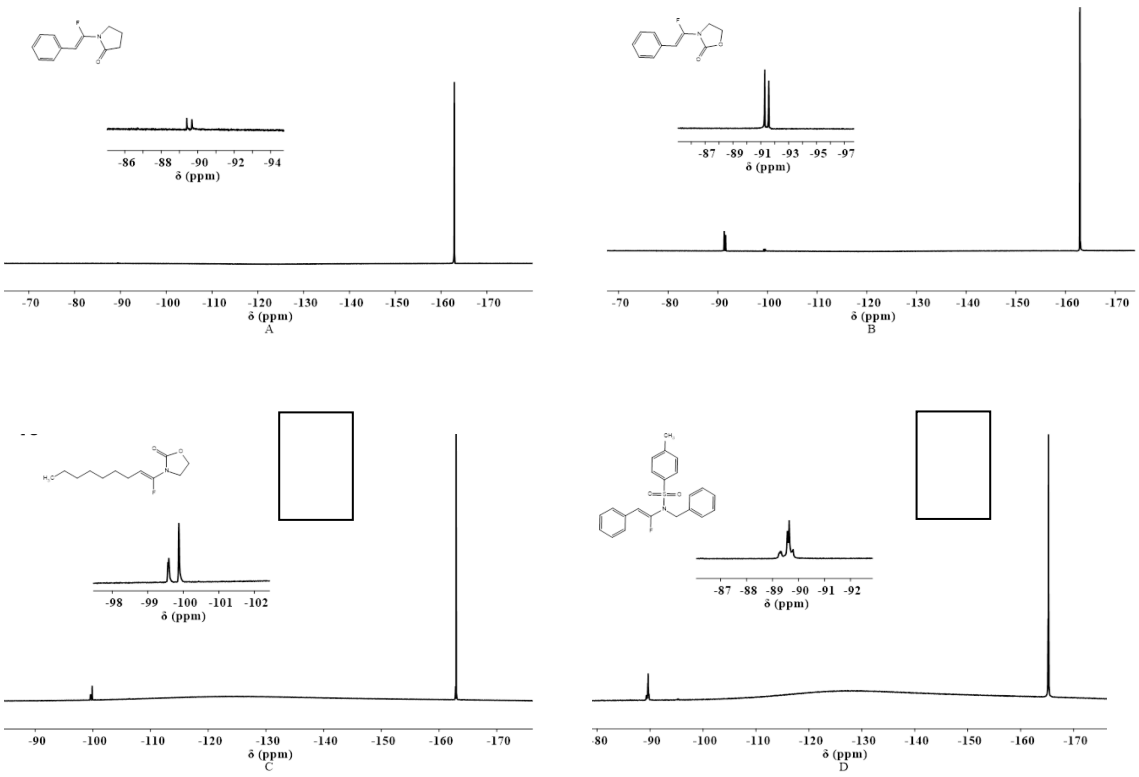

Figure S10. *^{19}F NMR spectra of the hydrofluorination of ynamides into **24a** (A), **24b** (B), **24c** (C) and **24d** (D) in the presence of HF-loaded ACF after 7 days of reaction time.*

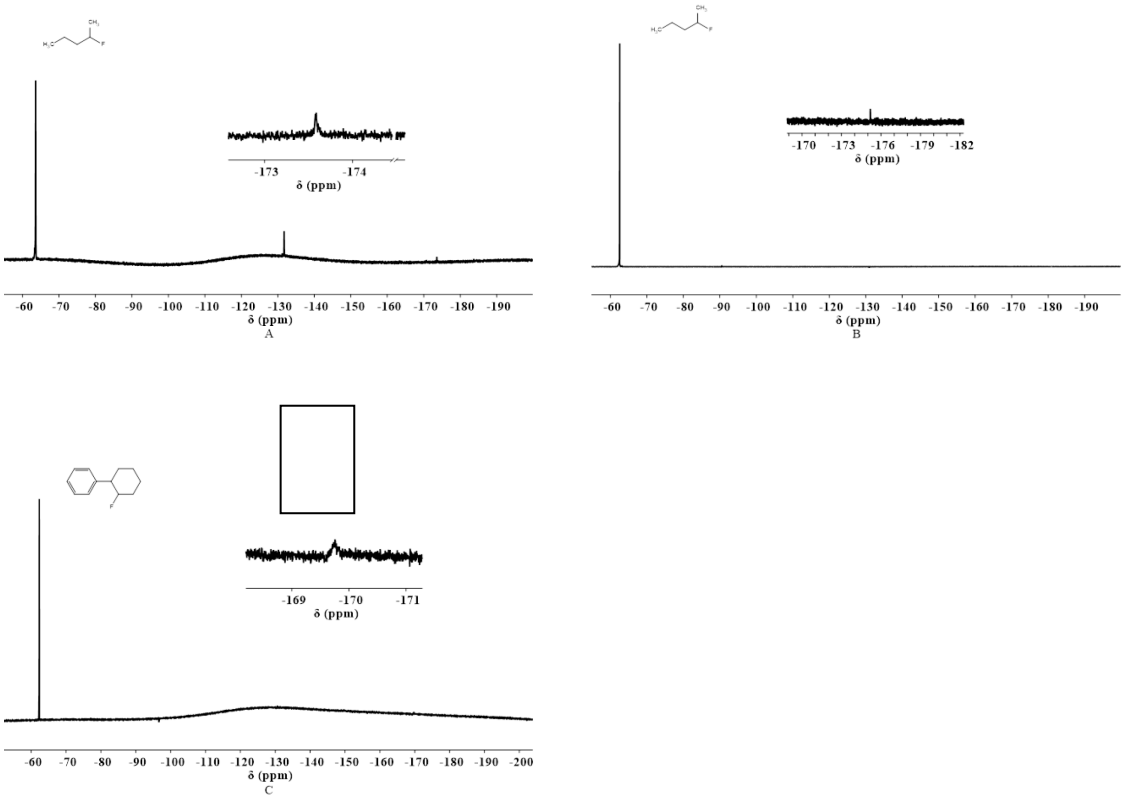

Figure S11. *^{19}F NMR spectra of the hydrofluorination of alkenes into **26a** (A), **26b** (B), and **26c** (C) in the presence of HF-loaded ACF after 7 days of reaction time.*

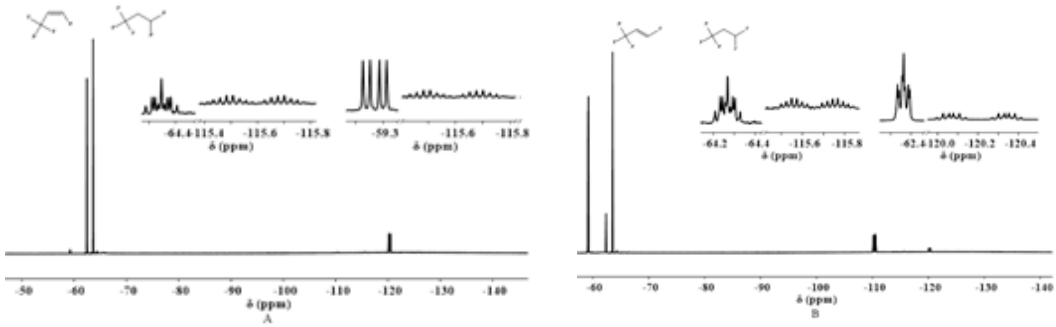

Figure S12. *^{19}F NMR spectra of the hydrofluorination of 1,3,3,3-tetrafluoropropenes Z (**27a**) into **27b** and **28a** (A) and E (**27b**) into **27a** and **28a** (B) in the presence of HF-loaded ACF after 24 hours of reaction time*

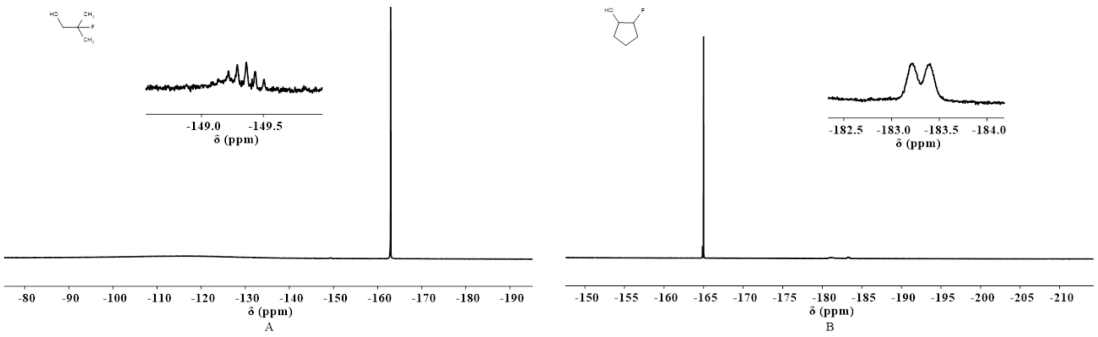

Figure S13. *^{19}F NMR spectra of the ring-opening of 1,1-dimethyloxirane (**29a**) into **30a** (A) and cyclopentene oxide (**29b**) into **30b** (B) in the presence of HF-loaded ACF after 4 days of reaction time.*

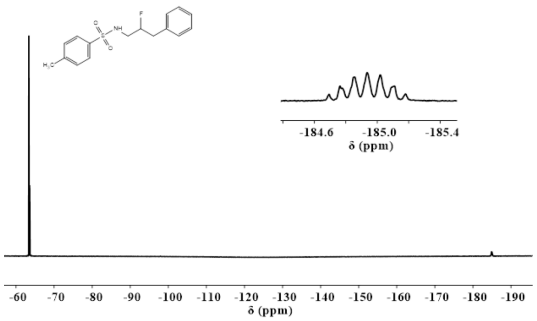

Figure S14. *^{19}F NMR spectra of the ring-opening of (S)-2-Benzyl-1-tosylaziridine (**31**) into **32** in the presence of HF-loaded ACF after 4 days of reaction time.*

Chapter 7 References

[1] B. Lindström, L. J. Pettersson, *CATTECH* **2003**, *7*, 130–138.
[2] J. Berzelius, *Ann. Chim. Phys.* **1836**, *61*, 146–151.
[3] "IUPAC Compendium of Chemical Terminology," DOI 10.1351/goldbook, **2009**.
[4] J. Greeley, *Annu. Rev. Chem. Biomol. Eng.* **2016**, *7*, 605–635.
[5] F. Zaera, *Catal. Letters* **2012**, *142*, 501–516.
[6] W. Huang, W. X. Li, *Phys. Chem. Chem. Phys.* **2019**, *21*, 523–536.
[7] N. Herron, W. E. Farneth, *Adv. Mater.* **1996**, *8*, 959–968.
[8] J. M. Thomas, *J. Chem. Phys.* **2008**, *128*, 182502.
[9] H. H. Kung, M. C. Kung, *Top. Catal.* **2005**, *34*, 77–83.
[10] J. J. Bravo-Suárez, R. V. Chaudhari, B. Subramaniam, *ACS Symp. Ser.* **2013**, *1132*, 3–68.
[11] K. Wilson, A. F. Lee, *Catal. Sci. Technol.* **2012**, *2*, 884–897.
[12] J. Wisniak, *Educ. Química* **2010**, *21*, 60–69.
[13] M. E. Dry, *Appl. Catal. A Gen.* **1996**, *138*, 319–344.
[14] M. E. Dry, *Catal. Today* **2002**, *71*, 227–241.
[15] A. M. Squires, *Circ. Fluid. Bed Technol.* **1986**, 1–19.
[16] A. A. Avidan, M. Edwards, H. Owen, *Rev. Chem. Eng.* **1990**, *6*, 1–72.
[17] K. Tanabe, *Appl. Catal. A Gen.* **1999**, *181*, 399–434.
[18] C. H. Bartholomew, R. J. Farrauto, *Fundamentals of Industrial Catalytic Processes: Second Edition*, John Wiley & Sons, Inc., Hoboken, NJ, USA, **2010**.
[19] J. Hagen, *Industrial Catalysis: A Practical Approach*, **2015**.
[20] A. Corma, *Curr. Opin. Solid State Mater. Sci.* **1997**, *2*, 63–75.
[21] J. H. Clark, *Green Chem.* **1999**, *1*, 1–8.
[22] J. C. Védrine, *Res. Chem. Intermed.* **2015**, *41*, 9387–9423.
[23] P. Gupta, S. Paul, *Catal. Today* **2014**, *236*, 153–170.
[24] S. Kobayashi, K. Manabe, *Pure Appl. Chem.* **2000**, *72*, 1373–1380.
[25] A. Corma, H. García, *Chem. Rev.* **2003**, *103*, 4307–4366.
[26] G. N. Lewis, J. N. Murrell, *Phys. Teach.* **1968**, *6*, 46–47.
[27] G. N. Lewis, *J. Franklin Inst.* **1938**, *226*, 293–313.
[28] G. A. Olah, in *Accross Conv. Lines*, **2003**, pp. 109–118.
[29] G. M. Alvernhe, C. M. Ennakoua, S. M. Lacombe, A. J. Laurent, *J. Org. Chem.* **1981**, *46*, 4938–4948.
[30] J. -F Scuotto, D. Mathieu, R. Gallo, R. Phan-Tan-Luu, J. Metzger, M. Desbois, *Bull. des Sociétés Chim. Belges* **1985**, *94*, 897–907.
[31] S. Fukuzumi, *Bull. Chem. Soc. Jpn.* **1997**, *70*, 1–28.
[32] Z. Liu, J. H. Q. Lee, R. Ganguly, D. Vidović, *Chem. - A Eur. J.* **2015**, *21*, 11344–11348.
[33] N. J. Saettel, O. Wiest, D. A. Singleton, M. P. Meyer, *J. Am. Chem. Soc.* **2002**, *124*, 11552–11559.
[34] G. A. Olah, G. K. Surya Prakash, R. Molnr, J. Sommer, *Superacid Chemistry*,

Wiley, **2009**.
[35] L. Paquette, D. Crich, P. Fuchs, G. Molander, A. Van Dyke, T. Jamison, *Chem. Biochem. Fac. B. Gall.* **2009**.
[36] L. Greb, *Chem. – A Eur. J.* **2018**, *24*, 17881–17896.
[37] L. O. Müller, D. Himmel, J. Stauffer, G. Steinfeld, J. Slattery, G. Santiso-Quiñones, V. Brecht, I. Krossing, *Angew. Chemie - Int. Ed.* **2008**, *47*, 7659–7663.
[38] F. Liu, A. Martin-Mingot, M.-P. Jouannetaud, F. Zunino, S. Thibaudeau, *Org. Lett.* **2010**, *12*, 868–871.
[39] A. Martin-Mingot, G. Compain, F. Liu, M.-P. Jouannetaud, C. Bachmann, G. Frapper, S. Thibaudeau, *J. Fluor. Chem.* **2012**, *134*, 56–62.
[40] M. Rohde, L. O. Müller, D. Himmel, H. Scherer, I. Krossing, *Chem. - A Eur. J.* **2014**, *20*, 1218–1222.
[41] J. C. Haartz, D. H. McDaniel, *J. Am. Chem. Soc.* **1973**, *95*, 8562–8565.
[42] R. G. Pearson, *J. Am. Chem. Soc.* **1963**, *85*, 3533–3539.
[43] T.-L. Ho, *Chem. Rev.* **1975**, *75*, 1–20.
[44] R. G. Pearson, *J. Am. Chem. Soc.* **1963**, *85*, 3533–3539.
[45] R. G. Pearson, *Acc. Chem. Res.* **1993**, *26*, 250–255.
[46] G. Klopman, *J. Am. Chem. Soc.* **1968**, *90*, 223–234.
[47] E.-C. Koch, *Propellants, Explos. Pyrotech.* **2005**, *30*, 5–16.
[48] S. Nagendran, H. W. Roesky, *Organometallics* **2008**, *27*, 457–492.
[49] M. R. Mason, in *Encycl. Inorg. Bioinorg. Chem.*, John Wiley & Sons, Ltd, Chichester, UK, **2015**, pp. 1–22.
[50] J. Metson, in *Fundam. Alum. Metall. Prod. Process. Appl.*, **2010**, pp. 23–48.
[51] A. M. Abyzov, *Refract. Ind. Ceram.* **2019**, *60*, 24–32.
[52] A. Pearson, J. R. Wall, *Production of Aluminum Compound Abstract*, **1985**.
[53] G. Bárdossy, *Comptes Rendus l'Academie Sci. - Ser. IIa Sci. la Terre des Planetes* **1997**, *324*, 1031–1040.
[54] F. Habashi, Q. City, *Bull. Hist. Chem.* **1995**, *18*, 15–19.
[55] K. Wefers, C. Misra, *Alcoa Tech. Pap.* **1987**, *19*, 1–100.
[56] K. J. Bayer, *Process of Obtaining Alumina*, **1888**.
[57] G. Busca, *Chem. Rev.* **2007**, *107*, 5366–5410.
[58] G. Busca, in *Adv. Catal.*, Academic Press Inc., **2014**, pp. 319–404.
[59] M. Trueba, S. P. Trasatti, *Eur. J. Inorg. Chem.* **2005**, *2005*, 3393–3403.
[60] B. C. Lippens, J. H. de Boer, *Acta Crystallogr.* **1964**, *17*, 1312–1321.
[61] K. Sohlberg, S. J. Pennycook, S. T. Pantelides, *Chem. Eng. Commun.* **2000**, *181*, 107–135.
[62] R. -S Zhou, R. L. Snyder, *Acta Crystallogr. Sect. B* **1991**, *47*, 617–630.
[63] F. R. Chen, J. G. Davis, J. J. Fripiat, *J. Catal.* **1992**, *133*, 263–278.
[64] S. Soled, *J. Catal.* **1983**, *81*, 252–257.
[65] A. A. Tsyganenko, K. S. Smirnov, A. M. Rzhevskij, P. P. Mardilovich, *Mater. Chem. Phys.* **1990**, *26*, 35–46.
[66] X. Krokidis, P. Raybaud, A. E. Gobichon, B. Rebours, P. Euzen, H. Toulhoat, *J. Phys. Chem. B* **2001**, *105*, 5121–5130.
[67] T. Krahl, E. Kemnitz, *Catal. Sci. Technol.* **2017**, *7*, 773–796.

[68] E. Kemnitz, U. Groß, S. Rüdiger, C. S. Shekar, *Angew. Chemie Int. Ed.* **2003**, *42*, 4251–4254.
[69] E. Kemnitz, D.-H. H. Menz, *Prog. Solid State Chem.* **1998**, *26*, 97–153.
[70] R. Köster, *Justus Liebigs Ann. Chem.* **1958**, *618*, 31–43.
[71] K. Ziegler, R. Köster, *Justus Liebigs Ann. Chem.* **1957**, *608*, 1–7.
[72] S. Rüdiger, E. Kemnitz, *Dalton Trans.* **2008**, *0*, 1117.
[73] B. Calvo, C. P. Marshall, T. Krahl, J. Kröhnert, A. Trunschke, G. Scholz, T. Braun, E. Kemnitz, *Dalton Trans.* **2018**, *47*, 16461–16473.
[74] D. M. Byler, D. F. Shriver, *Inorg. Chem.* **1973**, *12*, 1412–1416.
[75] S. K. Ruediger, U. Groß, M. Feist, H. A. Prescott, S. C. Shekar, S. I. Troyanov, E. Kemnitz, *J. Mater. Chem.* **2005**, *15*, 588–597.
[76] R. König, G. Scholz, E. Kemnitz, *J. Sol-Gel Sci. Technol.* **2010**, *56*, 145–156.
[77] K. Okuhara, *J. Org. Chem.* **1978**, *43*, 2745–2749.
[78] V. A. Petrov, C. G. Krespan, B. E. Smart, *J. Fluor. Chem.* **1998**, *89*, 125–130.
[79] A. C. Sievert, C. G. Krespan, F. J. Weigert, *Process for Chlorofluoropropanes*, **1992**, US5157171A.
[80] T. Krahl, R. Stösser, E. Kemnitz, G. Scholz, M. Feist, G. Silly, J. Y. Buzaré, *Inorg. Chem.* **2003**, *42*, 6474–6483.
[81] T. Krahl, E. Kemnitz, *J. Fluor. Chem.* **2006**, *127*, 663–678.
[82] C. G. Krespan, D. A. Dixon, *J. Fluor. Chem.* **1996**, *77*, 117–126.
[83] C. G. Krespan, V. a. Petrov, *Chem. Rev.* **1996**, *96*, 3269–3302.
[84] V. A. A. Petrov, C. G. G. Krespan, B. E. E. Smart, *J. Fluor. Chem.* **1996**, *77*, 139–142.
[85] V. A. Petrov, C. G. Krespan, *J. Fluor. Chem.* **2000**, *102*, 199–204.
[86] M.-C. Kervarec, C. P. Marshall, T. Braun, E. Kemnitz, *J. Fluor. Chem.* **2019**, *221*, 61–65.
[87] J. K. Murthy, U. Gross, S. Rüdiger, V. V. Rao, V. V. Kumar, A. Wander, C. L. Bailey, N. M. Harrison, E. Kemnitz, *J. Phys. Chem. B* **2006**, *110*, 8314–8319.
[88] C. G. Krespan, *Process for Production of Polyfluoroolefins*, **1991**, US5162594A.
[89] V. A. Petrov, F. Davidson, B. E. Smart, *J. Org. Chem.* **1995**, *60*, 3419–3422.
[90] M. H. G. Prechtl, M. Teltewskoi, A. Dimitrov, E. Kemnitz, T. Braun, *Chem. - A Eur. J.* **2011**, *17*, 14385–14388.
[91] B. Calvo, J. Wuttke, T. Braun, E. Kemnitz, *ChemCatChem* **2016**, *8*, 1945–1950.
[92] D. O'Hagan, *Chem. Soc. Rev.* **2008**, *37*, 308–319.
[93] M. Ahrens, G. Scholz, T. Braun, E. Kemnitz, *Angew. Chemie Int. Ed.* **2013**, *52*, 5328–5332.
[94] A. K. Siwek, M. Ahrens, M. Feist, T. Braun, E. Kemnitz, *ChemCatChem* **2017**, *9*, 839–845.
[95] G. Meißner, M. Feist, T. Braun, E. Kemnitz, *J. Organomet. Chem.* **2017**, *847*, 234–241.
[96] G. Meißner, D. Dirican, C. Jäger, T. Braun, E. Kemnitz, *Catal. Sci. Technol.* **2017**, *7*, 3348–3354.
[97] G. Meißner, K. Kretschmar, T. Braun, E. Kemnitz, *Angew. Chem. Int. Ed.* **2017**, *56*,

16338–16341.
[98] T. Okazoe, *Proc. Japan Acad. Ser. B Phys. Biol. Sci.* **2009**, *85*, 276–289.
[99] E. P. Gillis, K. J. Eastman, M. D. Hill, D. J. Donnelly, N. A. Meanwell, *J. Med. Chem.* **2015**, *58*, 8315–8359.
[100] S. Purser, P. R. Moore, S. Swallow, V. Gouverneur, *Chem. Soc. Rev.* **2008**, *37*, 320–330.
[101] G. Haufe, *Angew. Chemie Int. Ed.* **2008**, *47*, 4051–4051.
[102] L. McKeen, in *Introd. to Fluoropolymers*, Elsevier, **2013**, pp. 5–15.
[103] W. R. Dolbier, *J. Fluor. Chem.* **2005**, *126*, 157–163.
[104] J. T. Welch, S. Eswarakrishnan, *Fluorine in Bioorganic Chemistry*, Wiley, **1991**.
[105] J. Wang, M. Sánchez-Roselló, J. L. Aceña, C. del Pozo, A. E. Sorochinsky, S. Fustero, V. A. Soloshonok, H. Liu, *Chem. Rev.* **2014**, *114*, 2432–2506.
[106] M. Braun, J. Eicher, in *Mod. Synth. Process. React. Fluorinated Compd.*, Elsevier, **2017**, pp. 7–25.
[107] P. Jeschke, *ChemBioChem* **2004**, *5*, 570–589.
[108] K. Müller, C. Faeh, F. Diederich, *Science* **2007**, *317*, 1881–6.
[109] T. Nakajima, H. Groult, *Fluorinated Materials for Energy Conversion*, Elsevier, **2005**.
[110] H. Moissan, *Comptes Rendus* **1886**, *102*, 1543–1544.
[111] A. Tressaud, *Angew. Chemie - Int. Ed.* **2006**, *45*, 6792–6796.
[112] H. Moissan, *Nature* **1900**, *62*, 291–292.
[113] R. E. Banks, *J. Fluor. Chem.* **1986**, *33*, 3–26.
[114] T. Midgley, A. L. Henne, *Ind. Eng. Chem.* **1930**, *22*, 542–545.
[115] H. Goldwhite, *J. Fluor. Chem.* **1986**, *33*, 109–132.
[116] J. H. Simons, L. P. Block Vol, *J. Am. Chem. Soc.* **1932**, *61*, 2962–2966.
[117] L. Hunter, *Beilstein J. Org. Chem.* **2010**, *6*, 38.
[118] A. Dreveton, *Procedia Eng.* **2016**, *138*, 240–247.
[119] G. Haufe, *Adv. Synth. Catal.* **2001**, *343*, 311–311.
[120] M. Shimizu, T. Hiyama, *Angew. Chemie Int. Ed.* **2005**, *44*, 214–231.
[121] V. P. Reddy, *Organofluorine Compounds in Biology and Medicine*, Elsevier, **2015**.
[122] K. L. Kirk, *Org. Process Res. Dev.* **2008**, *12*, 305–321.
[123] I. Ojima, *Fluorine in Medicinal Chemistry and Chemical Biology*, John Wiley And Sons, Chichester, UK, **2009**.
[124] J. Fried, E. F. Sabo, *J. Am. Chem. Soc.* **1954**, *76*, 1455–1456.
[125] J. Ruiz-Cabello, B. P. Barnett, P. A. Bottomley, J. W. M. Bulte, *NMR Biomed.* **2011**, *24*, 114–129.
[126] M. R. Kilbourn, J. R. Huizenga, *Fluorine-18 Labeling of Radiopharmaceuticals*, **1990**.
[127] V. Gouverneur, *Fluorine in Pharmaceutical and Medicinal Chemistry: From Biophysical Aspects to Clinical Applications*, **2012**.
[128] M. Blau, W. Nagler, M. Bender, *J. Nucl. Med.* **1962**, *3*.
[129] P. W. Miller, N. J. Long, R. Vilar, A. D. Gee, *Angew. Chemie - Int. Ed.* **2008**, *47*, 8998–9033.
[130] M. Piel, I. Vernaleken, F. Rösch, *J. Med. Chem.* **2014**, *57*, 9232–9258.
[131] T. J. Wallington, O. J. Nielsen, in *Organofluorines*, Springer-Verlag, Berlin/Heidelberg, **2006**, pp. 85–102.

[132] P. Maienfisch, R. G. Hall, *Chim. Int. J. Chem.* **2004**, *58*, 93–99.
[133] "World Enzymes - Demand and Sales Forecasts, Market Share, Market Size, Market Leaders," can be found under https://www.freedoniagroup.com/World-Fluorochemicals.html.
[134] R. E. Banks, J. C. Tatlow, *J. Fluor. Chem.* **1986**, *33*, 71–108.
[135] H. W. Daudt, M. A. Youker, *Organic Fluorine Compound*, **1935**.
[136] R. J. Plunkett, *Tetrafluoroethylene Polymers*, **1939**.
[137] G. D. Hayman, R. G. Derwent, *Environ. Sci. Technol.* **1997**, *31*, 327–336.
[138] K. H. Kim, Z. H. Shon, H. T. Nguyen, E. C. Jeon, *Atmos. Environ.* **2011**, *45*, 1369–1382.
[139] R. Ciconkov, *Int. J. Refrig.* **2018**, *86*, 441–448.
[140] M. J. Molina, F. S. Rowland, *Nature* **1974**, *249*, 810–812.
[141] F. S. Rowland, M. J. Molina, *Rev. Geophys.* **1975**, *13*, 1.
[142] P. G. Simmonds, M. Rigby, A. Mcculloch, S. O'doherty, D. Young, J. Mühle, P. B. Krummel, P. Steele, P. J. Fraser, A. J. Manning, et al., *Atmos. Chem. Phys* **2017**, *17*, 4641–4655.
[143] J. M. Calm, *Int. J. Refrig.* **2008**, *31*, 1123–1133.
[144] G. J. M. Velders, D. W. Fahey, J. S. Daniel, M. McFarland, S. O. Andersen, *Proc. Natl. Acad. Sci.* **2009**, *106*, 10949–10954.
[145] E. G. Locke, W. R. Erode, A. L. Henne, *J. Am. Chem. Soc.* **1934**, *56*, 1726–1728.
[146] A. L. Henne, E. C. Ladd, *J. Am. Chem. Soc.* **1936**, *58*, 402–403.
[147] H. S. Booth, W. L. Mong, P. E. Burchfield, *Ind. Eng. Chem.* **1932**, *24*, 328–331.
[148] T. Fujiwara, D. O'Hagan, *J. Fluor. Chem.* **2014**, *167*, 16–29.
[149] G. Theodoridis, *Adv. Fluor. Sci.* **2006**, *2*, 121–175.
[150] P. Jeschke, *Pest Manag. Sci.* **2010**, *66*, 10–27.
[151] G. Haufe, F. R. Leroux, *Fluorine in Life Sciences: Pharmaceuticals, Medicinal Diagnostics, and Agrochemicals: Progress in Fluorine Science Series*, Elsevier, **2018**.
[152] K. Naumann, *Pestic. Sci.* **1998**, *52*, 3–20.
[153] D. O'Hagan, D. B. Harper, *J. Fluor. Chem.* **1999**, *100*, 127–133.
[154] N. A. Meanwell, *J. Med. Chem.* **2018**, *61*, 5822–5880.
[155] A. Bondi, *J. Phys. Chem.* **1964**, *68*, 441–451.
[156] I. G. Shenderovich, S. N. Smirnov, G. S. Denisov, V. A. Gindin, N. S. Golubev, A. Dunger, R. Reibke, S. Kirpekar, O. L. Malkina, H.-H. Limbach, *Berichte der Bunsengesellschaft für Phys. Chemie* **1998**, *102*, 422–428.
[157] B. K. Park, N. R. Kitteringham, *Drug Metab. Rev.* **1994**, *26*, 605–643.
[158] C. D. Murphy, G. Sandford, *Expert Opin. Drug Metab. Toxicol.* **2015**, *11*, 589–599.
[159] L. Pauling, *J. Am. Chem. Soc.* **1932**, *54*, 3570–3582.
[160] L. Pauling, G. W. Wheland, *J. Chem. Phys.* **1934**, *2*, 482.
[161] M. B. Van Niel, I. Collins, M. S. Beer, H. B. Broughton, S. K. F. Cheng, S. C. Goodacre, A. Heald, K. L. Locker, A. M. MacLeod, D. Morrison, et al., *J. Med. Chem.* **1999**, *42*, 2087–2104.
[162] Peer Kirsch, *Modern Fluoroorganic Chemistry. Synthesis, Reactivity, Applications*, John Wiley & Sons, Ltd, **2013**.

[163] B. E. Smart, *J. Fluor. Chem.* **2001**, *109*, 3–11.
[164] C. Thiehoff, Y. P. Rey, R. Gilmour, *Isr. J. Chem.* **2017**, *57*, 92–100.
[165] D. Y. Buissonneaud, T. van Mourik, D. O'Hagan, *Tetrahedron* **2010**, *66*, 2196–2202.
[166] K. B. Wiberg, *Acc. Chem. Res.* **1996**, *29*, 229–234.
[167] J. R. Durig, J. Liu, T. S. Little, V. F. Kalasinsky, *J. Phys. Chem.* **1992**, *96*, 8224–8233.
[168] K. B. Wiberg, P. R. Rablen, *J. Am. Chem. Soc.* **1993**, *115*, 614–625.
[169] T. Stahl, H. F. T. Klare, M. Oestreich, *ACS Catal.* **2013**, *3*, 1578–1587.
[170] H. Amii, K. Uneyama, *Chem. Rev.* **2009**, *109*, 2119–2183.
[171] U. Mazurek, H. Schwarz, *Chem. Commun.* **2003**, *0*, 1321–1326.
[172] M. F. Kuehnel, D. Lentz, T. Braun, *Angew. Chemie Int. Ed.* **2013**, *52*, 3328–3348.
[173] T. Braun, R. P. Hughes, *Organometallic Fluorine Chemistry*, Springer International Publishing, Cham, **2015**.
[174] R. P. Hughes, *Eur. J. Inorg. Chem.* **2009**, *2009*, 4591–4606.
[175] H. Torrens, in *Coord. Chem. Rev.*, Elsevier, **2005**, pp. 1957–1985.
[176] T. Braun, R. N. Perutz, *Chem. Commun.* **2002**, *0*, 2749–2757.
[177] J. L. Kiplinger, T. G. Richmond, C. E. Osterberg, *Chem. Rev.* **1994**, *94*, 373–431.
[178] K. Uneyama, H. Amii, *J. Fluor. Chem.* **2002**, *114*, 127–131.
[179] C. Saboureau, M. Troupel, S. Sibille, J. Périchon, *J. Chem. Soc. Chem. Commun.* **1989**, 1138–1139.
[180] P. Clavel, G. Lessene, C. Biran, M. Bordeau, N. Roques, S. Trévin, D. de Montauzon, *J. Fluor. Chem.* **2001**, *107*, 301–310.
[181] C. B. Caputo, D. W. Stephan, *Organometallics* **2012**, *31*, 27–30.
[182] H. F. T. Klare, M. Oestreich, *Dalton Trans.* **2010**, *39*, 9176–9184.
[183] C. Douvris, C. M. Nagaraja, C.-H. Chen, B. M. Foxman, O. V. Ozerov, *J. Am. Chem. Soc.* **2010**, *132*, 4946–4953.
[184] K. K. K. Goh, A. Sinha, C. Fraser, R. D. Young, *RSC Adv.* **2016**, *6*, 42708–42712.
[185] V. J. Scott, R. Çelenligil-Çetin, O. V. Ozerov, *J. Am. Chem. Soc.* **2005**, *127*, 2852–2853.
[186] C. Douvris, O. V Ozerov, F. Diederich, Y. Choliy, T. J. Emge, K. Krogh-Jespersen, A. S. Goldman, *Science* **2008**, *321*, 1188–90.
[187] W. Gu, M. R. Haneline, C. Douvris, O. V. Ozerov, *J. Am. Chem. Soc.* **2009**, *131*, 11203–11212.
[188] M. Klahn, C. Fischer, A. Spannenberg, U. Rosenthal, I. Krossing, *Tetrahedron Lett.* **2007**, *48*, 8900–8903.
[189] J. J. Wu, J. H. Cheng, J. Zhang, L. Shen, X. H. Qian, S. Cao, *Tetrahedron* **2011**, *67*, 285–288.
[190] J. Terao, S. A. Begum, Y. Shinohara, M. Tomita, Y. Naitoh, N. Kambe, *Chem. Commun.* **2007**, 855–857.
[191] M. E. Vol'pin, N. V. Shevchenko, G. I. Bolestova, Y. V. Zeifman, Y. A. Fialkov, Z. N. Parnes, *Mendeleev Commun.* **1991**, *1*, 118–119.
[192] A. L. Henne, M. S. Newman, *J. Am. Chem. Soc.* **1938**, *60*, 1697–1698.
[193] M. P. Doyle, C. C. McOsker, C. T. West, *J. Org. Chem.* **1976**, *41*, 1393–1396.
[194] J. A. Nicasio, S. Steinberg, B. Inés, M. Alcarazo, *Chem. - A Eur. J.* **2013**, *19*, 11016–11020.
[195] C. B. Caputo, D. W. Stephan, *Organometallics* **2012**, *31*, 27–30.

[196] N. Lühmann, R. Panisch, T. Müller, *Appl. Organomet. Chem.* **2010**, *24*, 533–537.
[197] T. Ooi, D. Uraguchi, N. Kagoshima, K. Maruoka, *Tetrahedron Lett.* **1997**, *38*, 5679–5682.
[198] R. K. Ramchandani, R. D. Wakharkar, A. Sudalai, *Tetrahedron Lett.* **1996**, *37*, 4063–4064.
[199] K. Hirano, K. Fujita, H. Yorimitsu, H. Shinokubo, K. Oshima, *Tetrahedron Lett.* **2004**, *45*, 2555–2557.
[200] D. R. Kronenthal, R. H. Mueller, P. L. Kuester, T. P. Kissick, E. J. Johnson, *Tetrahedron Lett.* **1990**, *31*, 1241–1244.
[201] G. L. Li, T. Ishihara, H. Nishiguchi, Y. Moro-Oka, Y. Takita, *Chem. Lett.* **1996**, *25*, 507–508.
[202] M. Van Der Puy, *Fluorinated Propenes from Pentafluoropropane*, **1998**, US 5,986,151.
[203] G.-L. Li, H. Nishiguchi, T. Ishihara, Y. Moro-oka, Y. Takita, *Appl. Catal. B Environ.* **1998**, *16*, 309–317.
[204] A. C. Sivert, N. A. Carlson, *Preparation of Hydrofluoroolefins by Dehydrofluorination*, **2009**, US8552227B2.
[205] H. Wang, H. S. Tung, *Process for the Production of HFO Trans-1234ze from HFC-245fa*, **2011**, US 8,067,650 B2.
[206] V. N. mallikarjuna Rao, M. J. Nappa, A. C. Sievert, R. N. Miller, *Tetrafluoropropene Production Processes*, **2013**, US7722781B2.
[207] H. Wang, H. S. Tung, R. R. Singh, I. Shankland, *Process for Producing 2,3,3,3-Tetrafluoropropene*, **2014**, US 8,766,020 B2.
[208] S. Pen, M. J. Nappa, *Dehydrofluorination of 245fa to 1234ze*, **2016**, US930296B2.
[209] Y. Luo, *Comprehensive Handbook of Chemical Bond Energies*, CRC Press, Boca Raton, **2007**.
[210] B. F. Skiles, *Dehydrofluorination of 1, 1-Difluoroethane*, **1952**, US2674632A.
[211] L. E. Gardner, *Hydrofluorination and Dehydrofluorination and Catalysts Therefor*, **1968**, US3607955A.
[212] L. E. Gardner, *Dehydrofluorination Process and Products*, **1965**, US3432562A.
[213] K. Teinz, S. Wuttke, F. Börno, J. Eicher, E. Kemnitz, *J. Catal.* **2011**, *282*, 175–182.
[214] K. Teinz, S. R. Manuel, B. Bin Chen, A. Pigamo, N. Doucet, E. Kemnitz, *Appl. Catal. B Environ.* **2015**, *165*, 200–208.
[215] W. Mao, Y. Bai, B. Wang, W. Wang, H. Ma, Y. Qin, C. Li, J. Lu, Z. Liu, *Appl. Catal. B Environ.* **2017**, *206*, 65–73.
[216] W. Mao, Y. Bai, Z. Jia, Z. Yang, Z. Hao, J. Lu, *Appl. Catal. A Gen.* **2018**, *564*, 147–156.
[217] F. Wang, W. Zhang, Y. Liang, Y. Wang, J. Lu, M. Luo, *Chem. Res. Chinese Univ.* **2015**, *31*, 1003–1006.
[218] X.-X. Fang, Y. Wang, W.-Z. Jia, J.-D. Song, Y.-J. Wang, M.-F. Luo, J.-Q. Lu, *Appl. Catal. A Gen.* **2019**, *576*, 39–46.
[219] W. Jia, M. Liu, X. Lang, C. Hu, J. Li, Z. Zhu, *Catal. Sci. Technol.* **2015**, *5*, 3103–3107.

[220] S. D. Taylor, C. C. Kotoris, G. Hum, *Tetrahedron* **1999**, *55*, 12431–12477.
[221] C. Chatalova-Sazepin, R. Hemelaere, J. F. Paquin, G. M. Sammis, *Synth.* **2015**, *47*, 2554–2569.
[222] J. A. Wilkinson, *Chem. Rev.* **1992**, *92*, 505–519.
[223] S. T. Purrington, B. S. Kagen, T. B. Patrick, *Chem. Rev.* **1986**, *86*, 997–1018.
[224] R. F. Merritt, *J. Org. Chem.* **1966**, *31*, 3871–3873.
[225] J. S. Moilliet, in *J. Fluor. Chem.*, Elsevier, **2001**, pp. 13–17.
[226] G. Sandford, *J. Fluor. Chem.* **2007**, *128*, 90–104.
[227] R. H. Hesse, *Isr. J. Chem.* **1978**, *17*, 60–70.
[228] T. Umemoto, M. Nagayoshi, K. Adachi, G. Tomizawa, *J. Org. Chem.* **1998**, *63*, 3379–3385.
[229] S. Singh, D. D. DesMarteau, S. S. Zuberi, M. Witz, H. N. Huang, *J. Am. Chem. Soc.* **1987**, *109*, 7194–7196.
[230] W. E. Barnette, *J. Am. Chem. Soc.* **1984**, *106*, 452–454.
[231] T. Umemoto, S. Fukami, G. Tomizawa, K. Harasawa, K. Kawada, K. Tomita1, *J. Am. Chem. Soc.* **1990**, *112*, 8563–8575.
[232] T. Umemoto, K. Kawada, K. Tomita, *Tetrahedron Lett.* **1986**, *27*, 4465–4468.
[233] G. Sankar Lal, * and Guido P. Pez, R. G. Syvret, G. S. Lal, G. P. Pez, R. G. Syvret, *Chem. Rev.* **1996**, *96*, 1737–1755.
[234] R. E. Banks, *J. Fluor. Chem.* **1998**, *87*, 1–17.
[235] G. S. Lal, G. P. Fez, R. J. Pesaresi, F. M. Prozonic, *Chem. Commun.* **1999**, 215–216.
[236] W. J. Middleton, *J. Org. Chem.* **1975**, *40*, 574–578.
[237] H. Sun, S. G. DiMagno, *J. Am. Chem. Soc.* **2005**, *127*, 2050–2051.
[238] M. R. C. Gerstenberger, A. Haas, *Angew. Chemie Int. Ed. English* **1981**, *20*, 647–667.
[239] J. W. Lee, M. T. Oliveira, H. Bin Jang, S. Lee, D. Y. Chi, D. W. Kim, C. E. Song, *Chem. Soc. Rev.* **2016**, *45*, 4638–4650.
[240] E. Fritz-Langhals, *Tetrahedron: Asymmetry* **1994**, *5*, 981–986.
[241] H. Sun, S. G. DiMagno, *Angew. Chemie Int. Ed.* **2006**, *45*, 2720–2725.
[242] H. Sun, S. G. DiMagno, *Chem. Commun.* **2007**, 528–529.
[243] O. Farooq, *New J. Chem.* **2000**, *24*, 81–84.
[244] J. H. Clark, *Chem. Rev.* **1980**, *80*, 429–452.
[245] J. Yin, D. S. Zarkowsky, D. W. Thomas, M. M. Zhao, M. A. Huffman, *Org. Lett.* **2004**, *6*, 1465–1468.
[246] V. A. Petrov, S. Swearingen, W. Hong, W. Chris Petersen, *J. Fluor. Chem.* **2001**, *109*, 25–31.
[247] A. Takaoka, H. Iwakiri, N. Ishikawa, *Bull. Chem. Soc. Jpn.* **1979**, *52*, 3377–3380.
[248] T. Umemoto, R. P. Singh, Y. Xu, N. Saito, *J. Am. Chem. Soc.* **2010**, *132*, 18199–18205.
[249] S. Bresciani, A. M. Z. Slawin, D. O'Hagan, *J. Fluor. Chem.* **2009**, *130*, 537–543.
[250] J. Jacquesy, C. Berrier, … M. J.-, undefined 2002, *Wiley Online Libr.* **n.d.**
[251] M. T. Rogers, J. J. Katz, *J. Am. Chem. Soc.* **1952**, *74*, 1375–1377.
[252] N. Yoneda, *Tetrahedron* **1991**, *47*, 5329–5365.
[253] K. M. Dawood, *Tetrahedron* **2004**, *60*, 1435–1451.
[254] R. F. Hirschmann, R. Miller, J. Wood, R. E. Jones, *J. Am. Chem. Soc.* **1956**, *78*, 4956–

4959.
[255] G. A. Olah, X.-Y. Li, *Synlett* **1990**, *1990*, 267–269.
[256] G. A. Olah, J. T. Welch, Y. D. Vankar, M. Nojima, I. Kerekes, J. A. Olah, *J. Org. Chem.* **1979**, *44*, 3872–3881.
[257] O. E. Okoromoba, J. Han, G. B. Hammond, B. Xu, *J. Am. Chem. Soc.* **2014**, *136*, 14381–14384.
[258] S. Liang, G. B. Hammond, B. Xu, *Chem. - A Eur. J.* **2017**, *23*, 17850–17861.
[259] C. Laurence, K. A. Brameld, J. Graton, J. Y. Le Questel, E. Renault, *J. Med. Chem.* **2009**, *52*, 4073–4086.
[260] Z. Lu, B. S. Bajwa, O. E. Otome, G. B. Hammond, B. Xu, *Green Chem.* **2019**, *21*, 2224–2228.
[261] A. R. Ravishankara, A. A. Turnipseed, N. R. Jensen, S. Barone, M. Mills, C. J. Howard, S. Solomon, *Science (80-.).* **1994**, *263*, 71–75.
[262] S. A. Montzka, B. D. Hall, J. W. Elkins, *Geophys. Res. Lett.* **2009**, *36*, n/a-n/a.
[263] T. J. Wallington, W. F. Schneider, J. Sehested, O. J. Nielsen, *Faraday Discuss.* **1995**, *100*, 55–64.
[264] United Nations Environment Programme, *The Montreal Protocol on Substances That Deplete the Ozone Layer*, **2018**.
[265] J. S. Daniel, G. J. M. Velders, S. Solomon, M. McFarland, S. A. Montzka, *J. Geophys. Res. Atmos.* **2007**, *112*, DOI 10.1029/2006JD007275.
[266] G. J. M. Velders, S. O. Andersen, J. S. Daniel, D. W. Fahey, M. McFarland, *Proc. Natl. Acad. Sci. U. S. A.* **2007**, *104*, 4814–9.
[267] S. A. Montzka, M. McFarland, S. O. Andersen, B. R. Miller, D. W. Fahey, B. D. Hall, L. Hu, C. Siso, J. W. Elkins, *J. Phys. Chem. A* **2015**, *119*, 4439–4449.
[268] W.-T. Tsai, *Chemosphere* **2005**, *61*, 1539–1547.
[269] United Nations Environment Programme, *Ratification of the Kigali Amendment*, **2017**.
[270] United Nations Environment Programme, *The Kigali Amendment to the Montreal Protocol: HFC Phase-Down*, **2016**.
[271] United Nations Environment Programme, *Amendment to the Montreal Protocol on Substances That Deplete the Ozone Layer*, **2016**.
[272] T. Gehring, S. Oberthur, *The Copenhagen Meeting*, **1993**.
[273] L. J. M. Kuijpers, *Int. J. Refrig.* **1993**, *16*, 210–220.
[274] P. Arora, G. Seshadri, A. K. Tyagi, *Curr. Sci.* **2018**, *115*, 1497–1503.
[275] W. A. Fouad, L. F. Vega, *AIChE J.* **2018**, *64*, 250–262.
[276] K. Taddonio, N. Sherman, S. O. Andersen, *Next Generation Refrigerant Transition: Lessons Learned from Automotive Industry Experiences with CFC-12, HFC-134a and HFO-1234yf*, **2019**.
[277] A. G. Devecioğlu, V. Oruç, *Energy Procedia* **2015**, *75*, 1452–1457.
[278] M. Van Der Puy, *Process for the Preparation of 2,3,3,3-Tetrafluoropropene (HFO-1234yf)*, **2011**, US8071826B2.
[279] Y. L. Yagupolskii, N. V. V. Pavlenko, S. V. V. Shelyazhenko, A. A. A. Filatov, M. M. M. Kremlev, A. I. I. Mushta, I. I. I. Gerus, S. Peng, V. A. A. Petrov, M. Nappa, *J. Fluor.*

Chem. **2015**, *179*, 134–141.
[280] B. A. Light, S. D. Phillips, Fleming Kim M., S. A. Ferguson, J. J. Ma, C. L. Bortz, M. Van Der Puy, D. C. Merkel, H. S. Tung, S. Mukhopadhyay, *Method for Producing Fluorinated Organic Compounds*, **2007**, US9102579B2.
[281] R. Akasaka, *Int. J. Refrig.* **2010**, *33*, 907–914.
[282] M. Ali, L.-P. Liu, G. B. Hammond, B. Xu, *Tetrahedron Lett.* **2009**, *50*, 4078–4080.
[283] J. Burdeniuc, B. Jedicka, R. H. Crabtree, *Chem. Ber.* **1997**, *130*, 145–154.
[284] M. J. Nappa, R. D. Lousenberg, A. Jackson, *Synthesis of 1234yf by Selective Dehydrochlorination of 244bb*, **2009**, US 8,263,817 B2.
[285] H. T. Pham, R. R. Singh, H. Tung, K. A. Pokrovski, D. C. Merkel, *Azeotrope-like Composition of 2-Chloro-1,1,1,2-Tetrafluoropropane (HCFC-244bb) and Hydrogen Fluoride (HF)*, **2009**, US 8,070,975 B2.
[286] W. Mao, Y. Bai, W. Wang, B. Wang, Q. Xu, L. Shi, C. Li, J. Lu, *ChemCatChem* **2017**, *9*, 824–832.
[287] S. Lim, M. S. Kim, J. W. Choi, H. Kim, B. S. Ahn, S. D. Lee, H. Lee, C. S. Kim, D. J. Suh, J. M. Ha, et al., *Catal. Today* **2017**, *293–294*, 42–48.
[288] H. Wang, W. Han, X. Li, B. Liu, H. Tang, Y. Li, H. Wang, W. Han, X. Li, B. Liu, et al., *Molecules* **2019**, *24*, 361.
[289] C. L. Parker, *Ind. Eng. Chem.* **1911**, *3*, 622.
[290] J.-D. Song, T.-Y. Song, T.-T. Zhang, Y. Wang, M.-F. Luo, J.-Q. Lu, *J. Catal.* **2018**, *364*, 271–281.
[291] M. Feist, M. Ahrens, A. Siwek, T. Braun, E. Kemnitz, *J. Therm. Anal. Calorim.* **2015**, *121*, 929–935.
[292] C. D. Drake, R. D. Cramer, C. O. Wilfred, *Dehydrofluorination of Polyfluoroalkanes*, **1946**, US2442993A.
[293] A. Dimitrov, D. Heidemann, E. Kemnitz, *Inorg. Chem.* **2006**, *45*, 10807–10814.
[294] C. Guillon, P. Vierling, *J. Fluor. Chem.* **1992**, *59*, 297–300.
[295] G. Groppello, M. Vecchio, V. Fattore, L. Lodi, R. Covibi, *Aluminum Fluoride-Based Catalyst for the Gas-Phase Fluorination of Hydrocarbons*, **1971**, US3793229A.
[296] M. J. Nappa, A. C. Sivert, *Perhalofluorinated Butanes and Hexanes*, **2000**, US6066768A.
[297] D. C. Merkel, K. A. Pokrovski, H. Tung, H. T. Pham, R. R. Singh, *Azeotropic Compositions of 2-Chloro-3,3,3-Trifluoropropene (HCFC-1233xf), 2-Chloro-1,1,1,2-Tetrafluoropropane (HCFC-244bb), and Hydrogen Fluoride (HF)*, **2011**, 8,034,251 B2.
[298] D. C. . Merkel, H. S. . Tung, *Method for Producing 2-Chloro-3,3,3,-Trifluoropropene (HCFC-1233xf)*, **2008**, US7,795,480B2.
[299] W. Zhang, Z. Yang, J. Lu, J. Lu, *J. Chem. Eng. Data* **2013**, *58*, 2307–2310.
[300] L. Wendlinger, A. Pigamo, P. Bonnet, *Process for the Manufacture of 2-Chloro-3,3,3-Trifluoropropene (HCFO 1233xf) by Liquid Phase Fluorination of Pentachloropropane*, **2010**, US 2014/0155659 A1.
[301] T. Braun, F. Wehmeier, K. Altenhöner, *Angew. Chemie Int. Ed.* **2007**, *46*, 5321–5324.
[302] F. Wang, Y. Liang, W.-X. Zhang, Y.-J. Wang, J.-Q. Lu, & Meng-, F. Luo, *Indian J. Chem.* **2015**, *54*, 1192–1197.
[303] T. Liang, C. N. Neumann, T. Ritter, *Angew. Chemie - Int. Ed.* **2013**, *52*, 8214–8264.

[304] Z. Li, G. B. Hammond, B. Xu, *J. Fluor. Chem.* **2016**, *184*, 72–74.
[305] C. Hollingworth, V. Gouverneur, *Chem. Commun.* **2012**, *48*, 2929.
[306] P. A. Champagne, J. Desroches, J.-D. Hamel, M. Vandamme, J.-F. Paquin, *Chem. Rev.* **2015**, *115*, 9073–9174.
[307] Q. Zhang, D. P. Stockdale, J. C. Mixdorf, J. J. Topczewski, H. M. Nguyen, *J. Am. Chem. Soc.* **2015**, *137*, 11912–11915.
[308] M. G. Braun, A. G. Doyle, *J. Am. Chem. Soc.* **2013**, *135*, 12990–12993.
[309] J. A. Akana, K. X. Bhattacharyya, P. Müller, J. P. Sadighi, *J. Am. Chem. Soc.* **2007**, *129*, 7736–7737.
[310] F. Nahra, S. R. Patrick, D. Bello, M. Brill, A. Obled, D. B. Cordes, A. M. Z. Slawin, D. O'Hagan, S. P. Nolan, *ChemCatChem* **2015**, *7*, 240–244.
[311] X. Zeng, S. Liu, G. B. Hammond, B. Xu, *Chem. - A Eur. J.* **2017**, *23*, 11977–11981.
[312] B. C. Gorske, C. T. Mbofana, S. J. Miller, *Org. Lett.* **2009**, *11*, 4318–4321.
[313] T. J. O'Connor, F. D. Toste, *ACS Catal.* **2018**, *8*, 5947–5951.
[314] J. Limanto, A. Shafiee, P. N. Devine, V. Upadhyay, R. A. Desmond, B. R. Foster, D. R. Gauthier, R. A. Reamer, R. P. Volante, *J. Org. Chem.* **2005**, *70*, 2372–2375.
[315] D. M. Sedgwick, I. López, R. Román, N. Kobayashi, O. E. Okoromoba, B. Xu, G. B. Hammond, P. Barrio, S. Fustero, *Org. Lett.* **2018**, *20*, 2338–2341.
[316] D. Bello, D. O'Hagan, *Beilstein J. Org. Chem.* **2015**, *11*, 1902–1909.
[317] S. Thibaudeau, H. Carreyre, A. Mingot, in *Mod. Synth. Process. React. Fluorinated Compd. Prog. Fluor. Sci.*, Elsevier, **2017**, pp. 349–388.
[318] S. Thibaudeau, A. Martin-Mingot, M.-P. Jouannetaud, O. Karam, F. Zunino, *Chem. Commun.* **2007**, *0*, 3198.
[319] Z. Lu, X. Zeng, G. B. Hammond, B. Xu, *J. Am. Chem. Soc.* **2017**, *139*, 18202–18205.
[320] M. Di Serio, R. Tesser, L. Pengmei, E. Santacesaria, *Energy & Fuels* **2008**, *22*, 207–217.
[321] T. Krahl, A. Vimont, G. Eltanany, M. Daturi, E. Kemnitz, *J. Phys. Chem. C* **2007**, *111*, 18317–18325.
[322] C. L. Bailey, A. Wander, S. Mukhopadhyay, B. G. Searle, N. M. Harrison, *Phys. Chem. Chem. Phys.* **2008**, *10*, 2918.
[323] L. Gouin, J. Cousseau, J. A. S. Smith, *J. Chem. Soc. Faraday Trans. 2 Mol. Chem. Phys.* **1977**, *73*, 1878–1883.
[324] R. König, G. Scholz, K. Scheurell, D. Heidemann, I. Buchem, W. E. S. Unger, E. Kemnitz, *J. Fluor. Chem.* **2010**, *131*, 91–97.
[325] R. König, G. Scholz, A. Pawlik, C. Jäger, B. van Rossum, H. Oschkinat, E. Kemnitz, *J. Phys. Chem. C* **2008**, *112*, 15708–15720.
[326] K. M. Harmon, R. R. Lovelace, *J. Phys. Chem.* **1982**, *86*, 900–903.
[327] U. Gross, S. Rüdiger, E. Kemnitz, K. W. Brzezinka, S. Mukhopadhyay, C. Bailey, A. Wander, N. Harrison, *J. Phys. Chem. A* **2007**, *111*, 5813–5819.
[328] B. Desbat, P. V. Huong, *J. Chem. Phys.* **1983**, *78*, 6377–6383.
[329] S. Hirata, S. Iwata, *J. Phys. Chem. A* **1998**, *102*, 8426–8436.
[330] A. Ažman, A. Ocvirk, D. Hadži, P. A. Giguère, M. Schneider, *Can. J. Chem.* **1967**,

45, 1347–1350.

[331] T. von Rosenvinge, M. Parrinello, M. L. Klein, *J. Chem. Phys.* **1997**, *107*, 8012–8019.

[332] T. Krahl, Amorphes Aluminiumchlorofluorid Und -Bromofluorid — Die Stärksten Bekannten Festen Lewis-Säuren, Humboldt-Universit¨at zu Berlin, **2005**.

[333] M. C. Kervarec, E. Kemnitz, G. Scholz, S. Rudić, T. Braun, C. Jäger, A. A. L. Michalchuk, F. Emmerling, *Chem. - A Eur. J.* **2020**, *26*, 7314–7322.

[334] A. Lecloux, J. . Pirard, *J. Colloid Interface Sci.* **1979**, *70*, 265–281.

[335] M. Luisa Ojeda, J. Marcos Esparza, A. Campero, S. Cordero, I. Kornhauser, F. Rojas, *Phys. Chem. Chem. Phys.* **2003**, *5*, 1859.

[336] J. Landers, G. Y. Gor, A. V. Neimark, *Colloids Surfaces A Physicochem. Eng. Asp.* **2013**, *437*, 3–32.

[337] G. Kupgan, T. P. Liyana-Arachchi, C. M. Colina, *Langmuir* **2017**, *33*, 11138–11145.

[338] R. Gauthier, M. Mamone, J. F. Paquin, *Org. Lett.* **2019**, *21*, 9024–9027.

[339] A. Gómez-Herrera, F. Nahra, M. Brill, S. P. Nolan, C. S. J. Cazin, *ChemCatChem* **2016**, *8*, 3381–3388.

[340] A. Gorgues, D. Stéphan, J. Cousseau, *J. Chem. Soc., Chem. Commun.* **1989**, *0*, 1493–1494.

[341] G. Evano, A. Coste, K. Jouvin, *Angew. Chemie Int. Ed.* **2010**, *49*, 2840–2859.

[342] G. He, S. Qiu, H. Huang, G. Zhu, D. Zhang, R. Zhang, H. Zhu, *Org. Lett.* **2016**, *18*, 1856–1859.

[343] G. Compain, K. Jouvin, A. Martin-Mingot, G. Evano, J. Marrot, S. Thibaudeau, *Chem. Commun.* **2012**, *48*, 5196.

[344] J. Che, Y. Li, F. Zhang, R. Zheng, Y. Bai, G. Zhu, *Tetrahedron Lett.* **2014**, *55*, 6240–6242.

[345] G. Zhu, S. Qiu, Y. Xi, Y. Ding, D. Zhang, R. Zhang, G. He, H. Zhu, *Org. Biomol. Chem.* **2016**, *14*, 7746–7753.

[346] S. Okamoto, N. Takada, F. Sakyu, T. Kitamoto, T. Tonomura, M. Kanai, *Method for Producing Cis-1,3,3,3-Tetrafluoropropene*, **2016**, US9365472B2.

[347] Sakyu. Fuyuhiko, S. Okamoto, Y. Hibino, *Method for Producing Trans-1,3,3,3-Tetrafluoropropene*, **2013**, US 8,513.473 B2.

[348] H. Wang, H. Sung Tung, Y. Chiu, G. Cerri, S. A. Cottrell, *Integrated HFC Trans-1234ze Manufacture Process*, **2007**, US7485760B2.

[349] V. A. Soloshonok, *Enantiocontrolled Synthesis of Fluoro-Organic Compounds: Stereochemical Challenges and Biomedical Targets*, Wiley, **1999**.

[350] G. Haufe, *J. Fluor. Chem.* **2004**, *125*, 875–894.

[351] G. A. Olah, R. D. Chambers, G. K. S. Prakash, in *Accross Conv. Lines*, World Scientific, **2003**, pp. 1034–1038.

[352] A. Sattler, G. Haufe, *J. Fluor. Chem.* **1994**, *69*, 185–190.

[353] W. K. Hagmann, *J. Med. Chem.* **2008**, *51*, 4359–4369.

[354] R. H. Fan, Y. G. Zhou, W. X. Zhang, X. L. Hou, L. X. Dai, *J. Org. Chem.* **2004**, *69*, 335–338.

[355] W. X. Zhang, L. Su, W. G. Hu, J. Zhou, *Synlett* **2012**, *23*, 2413–2415.

[356] J. A. Kalow, A. G. Doyle, *Tetrahedron* **2013**, *69*, 5702–5709.

[357] T. N. Wade, *J. Org. Chem.* **1980**, *45*, 5328–5333.

[358] R. T. Coutts, A. Benderly, A. L. C. Mak, *J. Fluor. Chem.* **1980**, *16*, 277–283.
[359] O. E. Okoromoba, Z. Li, N. Robertson, M. S. Mashuta, U. R. Couto, C. F. Tormena, B. Xu, G. B. Hammond, *Chem. Commun.* **2016**, *52*, 13353–13356.

Chapter 8 Appendix

1- Abbreviations

ACF	Aluminum Chlorofluoride
BET	Brunauer–Emmett–Teller
CFC	Chlorofluorocarbon
CP	Cross Polarization
DAST	Diethylaminosulfur Trifluoride
DFT	Density Functional Theory
DMPU-HF	1,3-dimethyl-3,4,5,6-tetrahydro-2(1H)-pyrimidinone-HF
DQ	Double Quantum
DRIFTS	Diffuse Reflectance Infrared Fourier-Transform Spectroscopy
DTA	Differential Thermal Analysis
Ea	Activation Energy
EDX	Energy Dispersive X-Ray Analysis
FIA	Fluoride Ion Affinity
FTIR	Fourier-Transform Infrared Spectroscopy
GC	Gas Chromatography
GWP	Global Warming Potential
HCFC	Hydrochlorofluorocarbon
HF	Hydrogen Fluoride
HFC	Hydrofluorocarbon
HFO	Hydrofluoroolefin
HOMO	Highest Occupied Molecular Orbital
HSAB	Hard and Soft Acids and Bases
HS-AlF_3	*High Surface* Aluminum Fluoride

INS	Inelastic Neutron Scattering
IUPAC	International Union of Pure and Applied Chemistry
KNF	Hexafluoronickelate
LUMO	Lowest Unoccupied Molecular Orbital
MAS NMR	Magic-Angle-Spinning Nuclear Magnetic Resonance
MS	Mass Spectroscopy
NLDFT	Non local Density Functional Theory
NMR	Nuclear Magnetic Resonance
ODP	Ozone Depletion Potential
ODS	Ozone Depletion Substances
PCTFE	Polychlorotrifluoroethylene
PET	Positron Emission Tomography
Powder XRD	Powder X-ray Diffraction
PTFE	Polytetrafluoroethylene
Pulse TA	Pulse Thermal Analysis
STP	Standard Temperature and Pressure
TBAF	Tetra-n-butylammonium fluoride
TEM	Transmission Electron Microscopy
TFE	Tetrafluoroethene
TG	Thermogravimetry
TON	Turnover Number
TPD	Temperature Programme Desorption
TRAPDOR	Transfer of Population in Double Resonance
XANES	X-ray Absorption Near Edge Structure

2- List of Figures

3- List of Schemes

4- List of Tables

5- Selbstständigkeitserklärung

„Ich erkläre, dass ich die Dissertation selbständig und nur unter Verwendung der von mir, gemäß § 7 Abs. 3 der Promotionsordnung der Mathematisch-Naturwissenschaftlichen Fakultät, veröffentlicht im Amtlichen Mitteilungsblatt der Humboldt-Universität zu Berlin, Nr. 42/2018 am 11.07.2018, angegebenen Hilfsmittel angefertigt habe."

"I declare that I have completed the thesis independently using only the aids and tools specified. I have not applied for a doctor's degree in the doctoral subject elsewhere and do not hold a corresponding doctor's degree. I have taken due note of the Faculty of Mathematics and Natural Sciences PhD Regulations, published in the Official Gazette of Humboldt-Universität zu Berlin no. 42/2018 on 11/07/2018."

Berlin, den 05.09.2020